Paleotopography and Sea-level Controls on Facies Distribution and Stratal Architecture in the Westerville Limestone Member (Upper Pennsylvanian) NE Kansas and NW Missouri

by

Justin M. Fairchild
B.S., University of Wisconsin, 2006

Submitted to the Department of Geology
and the Faculty of the Graduate School of
The University of Kansas in partial
fulfillment of the requirements for the
degree of Master of Science
2012

Advisory Committee:

_____
Evan K. Franseen (Co-Chair)

_____
Robert H. Goldstein (Co-Chair)

_____
George P. Tsoflias

Date Defended: December, 17th 2012

The Thesis Committee for Justin M Fairchild certifies that this is the approved version of the following thesis:

Paleotopography and Sea-level Controls on Facies Distribution and Stratal Architecture in the Westerville Limestone Member (Upper Pennsylvanian) NE Kansas and NW Missouri

Co-Chairs:

_____

Evan K. Franseen

_____

Robert H. Goldstein

Date Approved: December, 10th 2012

Abstract

Justin M. Fairchild
Department of Geology, June 2012
The University of Kansas

Oolitic grainstone facies form important reservoirs in the subsurface around the world. The Westerville Limestone Member (Pennsylvanian) is an oolitic grainstone-rich reservoir analog deposited during high-amplitude glacioeustatic fluctuations and exposed in a 510 $km^2$ area near Kansas City in Kansas and Missouri. The Westerville Limestone Member consists of eight lithofacies: bioclastic packstone; bioclastic grainstone; oolitic grainstone; oncolitic packstone; fossiliferous siliciclastic-mudstone; peloidal packstone; microbial boundstone; and coarse-grained packstone. Interpreted deposition of the Westerville Limestone Member (2–6 m thick) is divided into three intervals, W1, W2, and W3, each separated by a marine or subaerial truncation surface. Interval W1 is composed mostly of bioclastic packstone of relatively uniform thickness (~1 m) throughout the field area. Deposition occurred in normal marine water during a relative rise in sea level and did not fill accommodation. A marine truncation surface altered local paleotopography and created subtle (dm-scale) relief during a relative fall in sea level and prior to deposition of Interval W2. Interval W2 is composed of grainstones (oolitic and bioclastic) that were deposited during a relative fall in sea level. The oolitic grainstone facies are preserved within paleotopographic low areas. A subaerial exposure surface truncates the unit, and the tracing of this surface and interpretation of depositional depths for facies are used to calculate a relative fall in sea level of at least 15.5 meters. After exposure, a relative rise of at least 11.5 meters is interpreted before Interval W3. Initial W3 deposits are composed of oolitic grainstone facies that locally build constructional relief on the flank of a regional paleotopographic high and

represent deposition during highstand at an intermediate ramp position. During a relative fall in sea level of at least 8.2 meters, accommodation became limited, oolitic grainstone is deposited on the flanks of local paleohighs, a thin layer of microbial boundstone drapes paleotopography, and oncolitic packstone and fossiliferous siliciclastic-mudstone onlap paleotopography and fill local paleolows. Deposition of stratigraphically higher supratidal peloidal packstone fills accommodation, and unit thickness requires a relative rise in sea level of at least 3 meters. Exposure features are present along the uppermost surface of the Westerville Limestone Member and indicate a period of subaerial exposure after a relative fall in sea level of at least 2.3 meters. Results of this study indicate that fluctuations in relative sea level interacting with subtle paleotopography can result in significant facies heterogeneity. Oolitic grainstones are typically thought to form constructional relief on high areas in shallow water. This study indicates, however, that oolitic grainstone deposits may accumulate in paleotopographic lows, especially during falling stages of sea level. The interpreted depositional history of the Westerville Limestone Member and associated units demonstrates that smaller scale variations in the rate and direction of fluctuations in sea level can have a significant effect on sequence heterogeneity during a large scale fall in sea level.

TABLE OF CONTENTS

List of Figures and Tables:

# ACKNOWLEDGEMENTS

First and foremost I need to acknowledge my family. I owe all that I am to them. Without their unwavering support this thesis would have been left unfinished years ago.

I would like to express my sincere gratitude to my co-advisors, Dr. Evan Franseen and Dr. Bob Goldstein for their guidance and patience. I know that their advice will serve me well, not only in geology, but in whatever this life has to offer. I would like to thank the faculty of the geology department for the many thought provoking classes and fieldtrips. A special thanks to Dr. Steve Hasiotis for first, convincing me to turn a class project into a GSA presentation and PALAIOS publication, and then having the patience to help me see it through. I am grateful to the staff at the Kansas Geological Survey and the Department of Geology, especially Ian Rowell and Yolanda Balderas, for their assistance. The student staff at the KU Writing Center are a great resource and expedited the review of this manuscript.

I would like to thank Karl Bethke, retired educator, from Madison Area Technical College for changing the way in which I view the world. I would also like to thank the faculty at the Department of Geology and Geophysics at the University of Wisconsin-Madison, especially Toni Simo for taking me into the field and encouraging me to apply to KU.

# INTRODUCTION

Recent studies have shown that there are complex three-dimensional (3-D) facies relationships at outcrop scale within Pennsylvanian limestone deposits in Kansas caused by interactions between paleotopography and relative sea-level change (Handford and Loucks, 1993; McKirahan et al., 2003; Washburn, 2004; Emry, 2005). Few studies, however, have effectively evaluated the internal facies variations within oolitic, grainstone-rich, deposits to assess the relationship between carbonate production, relative sea level, and paleotopography. The goal of this study is to evaluate controls on the 3-D facies relationships and geometries of an ooid-bearing grainstone-rich deposit by studying the Westerville Limestone Member in detail.

Relatively thin (m-scale) laterally continuous carbonate deposits are part of the classic stacked Pennsylvanian Midcontinent cyclothem deposits (Heckel, 1977). Oolitic portions of Pennsylvanian carbonates have been productive reservoirs in the subsurface along the Central Kansas Uplift, producing six billion barrels of oil to date; they continue to be targets for enhanced oil recovery (Raef et al., 2005). Lateral and vertical heterogeneities of reservoir and nonreservoir facies within thin carbonate units cause production anomalies. A better understanding of controls on heterogeneity of thin oolitic deposits is especially important because heterogeneities are below the resolution of conventional seismic surveys (Raef et al., 2005). Studies of modern carbonate depositional systems have illustrated the potential complexities of reservoir and nonreservoir facies with oolitic deposits (e.g. Wilson and Jordan, 1983; Harris, 1984; Handford, 1988; Gonzalez and Eberli, 1997; Rankey et al., 2006; Reeder and Rankey, 2008; Rankey and Reeder, 2011). Whereas rock-based studies have shown that

grainstone facies can build depositional relief preferentially on paleotopographic highs, or can fill depositional relief preferentially in paleotopographic lows (Weber et al., 1995; Franseen and Goldstein, 2004; Washburn, 2004). Franseen and Goldstein (2004) and Franseen et al. (2007) investigated the influence of sedimentary processes, relative fluctuations in sea level, and paleotopographic relief on the formation of reservoir-analog mixed carbonate-siliciclastic systems that form in a mid-ramp setting during high-amplitude relative sea-level fluctuations. Their results show oolitic facies preserved both on topographic highs and in topographic lows. Their model defines a build-and-fill zone (e.g. mid-ramp setting) in which carbonate facies either build or fill topographic relief as fluctuations in sea level interact with paleotopography. Build-and-fill sequences are laterally uniform in thickness, but are internally heterogeneous. Thickness of individual sequences is less than the available accommodation. This record of unfilled accommodation can be explained by a carbonate system that is stressed and not accumulating at maximum modern rates (Franseen and Goldstein, 2004; Franseen et al., 2007).

The focus of this study is the Westerville Limestone Member (Westerville) of the Cherryvale Formation, Kansas City Group (Missourian, Pennsylvanian). The Westerville was chosen because of the abundance of oolitic and other grainy facies. The project focuses on a ~510 $km^2$ area, which includes 18 outcrop exposures of the Westerville and associated units, 1 drill core, 8 Kansas Geological Survey water well reports, subsurface wireline log data from 88 wells in eastern Kansas, and unit thickness data of 129 wells in western Missouri from Sullivan (1969)(Fig. 1). The goals of this study are threefold: (1) Interpret the depositional and relative sea-level history of the Westerville through facies description and paleotopographic reconstruction; (2) Compare results with prior stratigraphic work and hypotheses for

Midcontinent Pennsylvanian cyclothem deposits; and (3) Explore how the Westerville, as an oolitic unit, may enhance or refute the build-and-fill model.

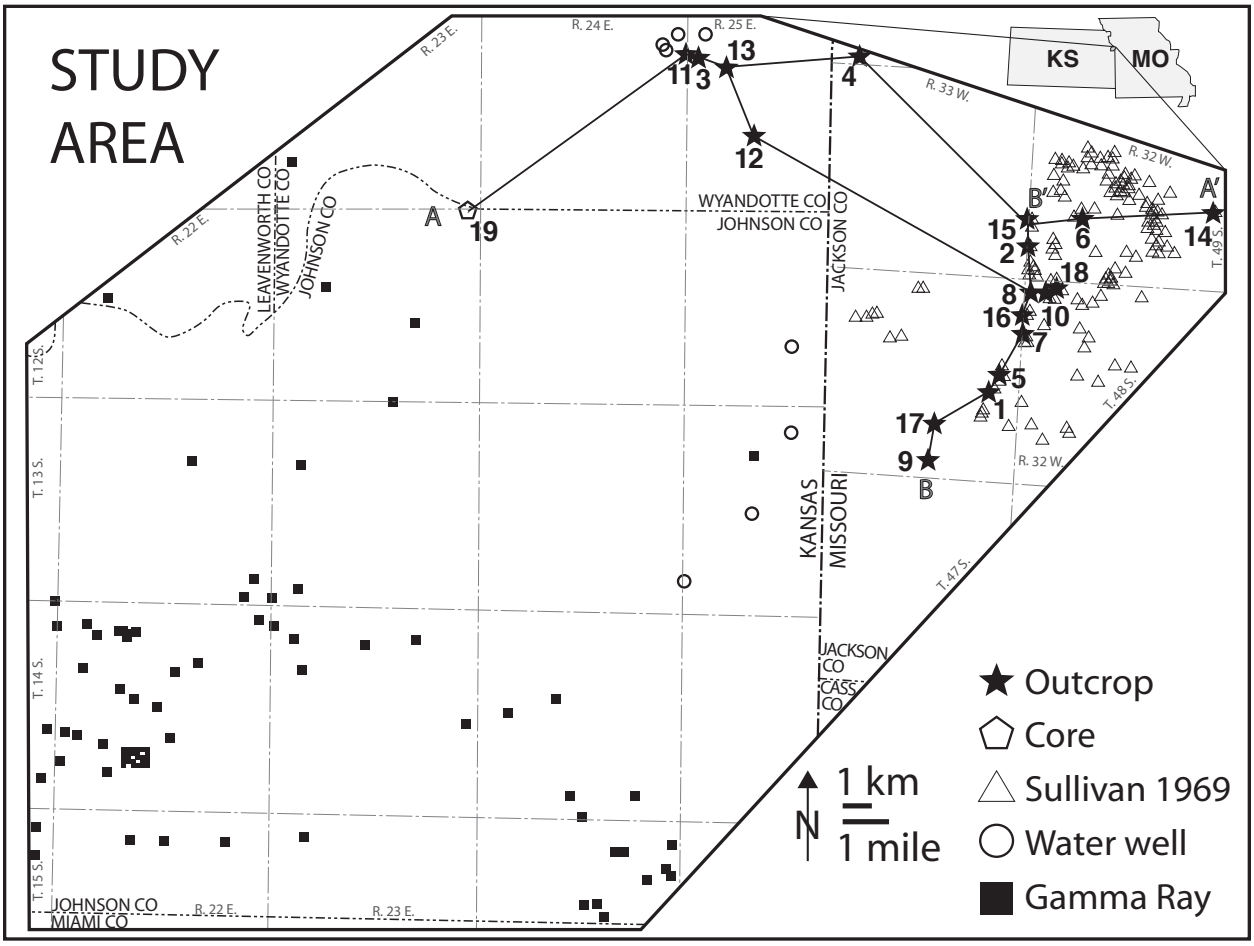


Figure 1. Map of study area. Stars mark locations of outcrops; they are numbered for reference. Open pentagon marks site of Deffenbaugh drill core. Open triangles mark positions of unit thickness data from Sullivan (1969). Open circles mark the sites of Kansas Geological Survey water well reports. Squares mark the location of gamma ray well logs. A–A' and B–B' are lines of cross section (Figs. 19–21). Other lines represent additional cross sections in the fence diagram (Fig. 22).

## Previous Studies And Stratigraphic Context

The type locality of the Westerville was first described by Bain (1898) near Westerville, Iowa. Moore (1936) placed the Westerville, stratigraphically, within the Kansas City Group as part of the Cherryvale Formation, overlying the Wea Shale and underlying the Nellie Bly Formation (Fig. 2). Moore (1936, 1949) grouped Pennsylvanian strata into megacyclothems and placed the Westerville within the Cherryvale Formation and the Drum Cycle. The base of the Drum Cycle is within the Wea Shale and the top is within the Chanute Shale. The Westerville is believed to be stratigraphically equivalent to the Drum Limestone of southern Kansas (Moore, 1936)—this was confirmed by Heckel and Watney (2002)(Fig. 3). Heckel and Baesemann (1975) broke apart the Drum Cycle into the Lower Cherryvale and Quivira Cycles based on conodont diversity and abundance data. They also lowered the boundary between the Lower Cherryvale Cycle (former Drum Cycle) and the Dennis Cycle from the middle of the Wea Shale to the middle of the Fontana Shale to include the Block Limestone and lower Wea Shale (Fig. 4). The upper boundary of the Lower Cherryvale Cycle is the top of the Westerville.

Heckel (1977) proposed a basic cyclothem model which includes, in ascending order: (1) An outside shale; (2) Middle limestone; (3) Core shale; and (4) Upper limestone (Fig 5). The same study introduced a schematic of lateral variation expected from north (proximal) to south (distal) for the Pennsylvanian of the Midcontinent (Fig 6). In the basic cyclothem model the Westerville would be the upper limestone of the Lower Cherryvale Cycle in the mid-ramp setting. This work progressed to create a sea-level curve for the Pennsylvanian depositional cycles of North America (Heckel, 1986). The curve shows the Lower Cherryvale Cycle with the following: subaerial exposure during the deposition of the Fontana Shale; deepening through the

Block Limestone and into the Wea Shale; shallowing upward through the rest of the Wea Shale and the Westerville; and ending with subaerial exposure (Nellie Bly Formation; Fig. 7). From the sea-level curve, estimates were made for the duration of the major cyclothem periods (235–400 ka). Fluctuations in sea level were attributed to changing ice volumes of the Gondwanan ice sheet (Heckel 1986). Sea level periodicity has since been better defined using U-Pb ages to 143+/-64 ka by Rasbury et al. (1998) and 140 ka by Eros et al. (2012).

Several previous studies focused on the sedimentology and diagenesis of the Westerville. Sullivan (1969) described the Westerville in Raytown, Missouri and, in ascending order, divided it into: (1) An ever-present “mat-algal wackestone” overlain by a thin shale deposit; (2) An “algal-lump grainstone” of variable thickness; (3) Two “ooid grainstone” ridges; and (4) A pack-wackestone and shale “cap rock”. No evidence for subaerial exposure was presented. He attributed the thickness variations to accretionary processes. Through the study of outcrops and well logs he observed two northeast-trending ridges capped with oolite deposits, which he interpreted as “tidal current ridges” or ”tidal bars”, and compared them to modern deposits in the Bahamas. Downs (1986) focused on the post-depositional history of the Westerville and attributed the tiger stripe pattern found in some of the oolitic deposits to early cementation of coarser grained laminations. Early cementation protected those stripes against later diagenesis and overcompaction.

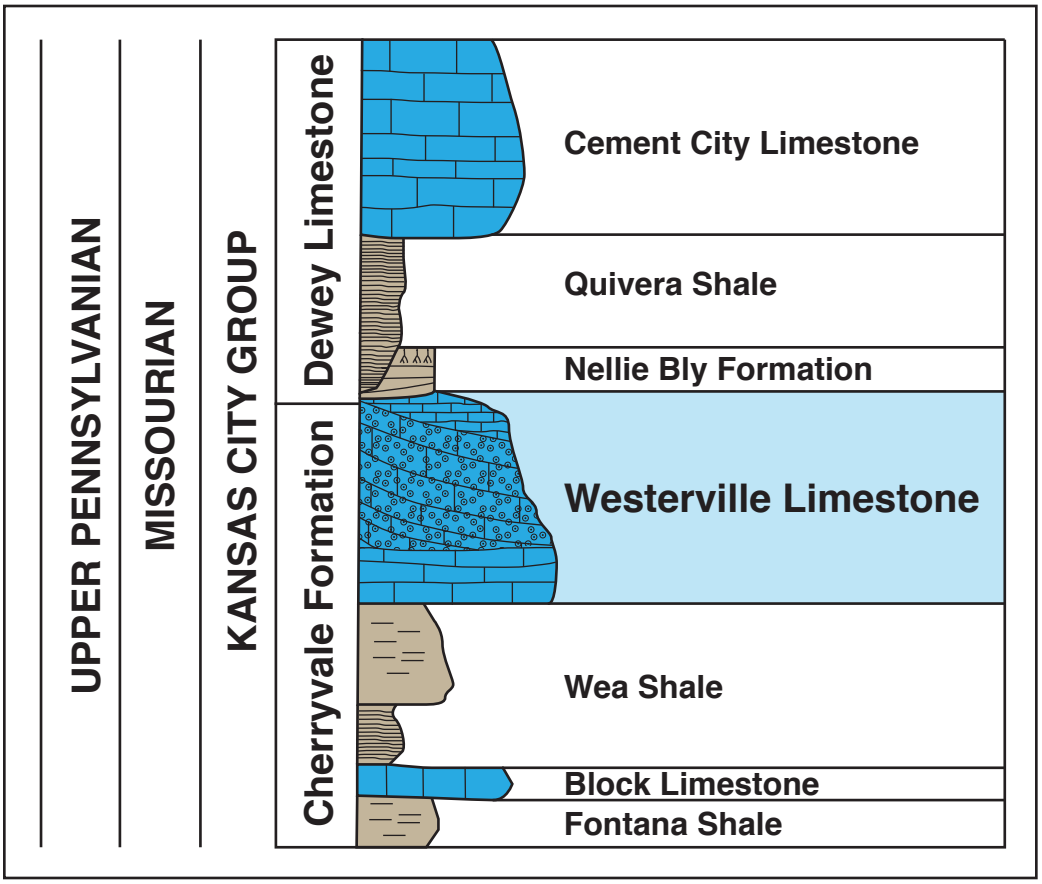


Figure 2. General stratigraphy of the Westerville Limestone and associated deposits (adapted from Heckel, 1999).

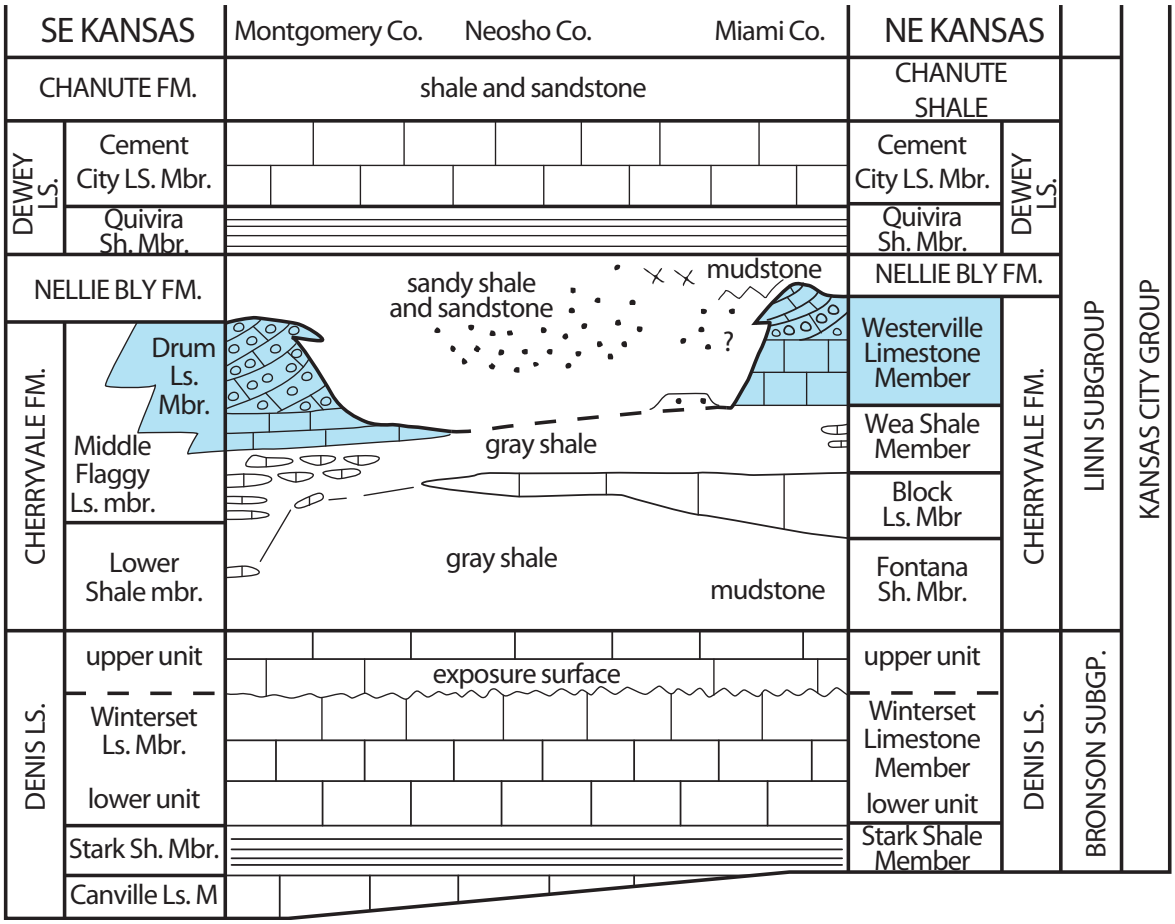


Figure 3. Stratigraphic correlation of Kansas City Group strata. Notice the similar stratigraphic position of the Westerville Limestone Member and the Drum Limestone Member within the Cherryvale Formation (modified from Heckel and Watney, 2002).

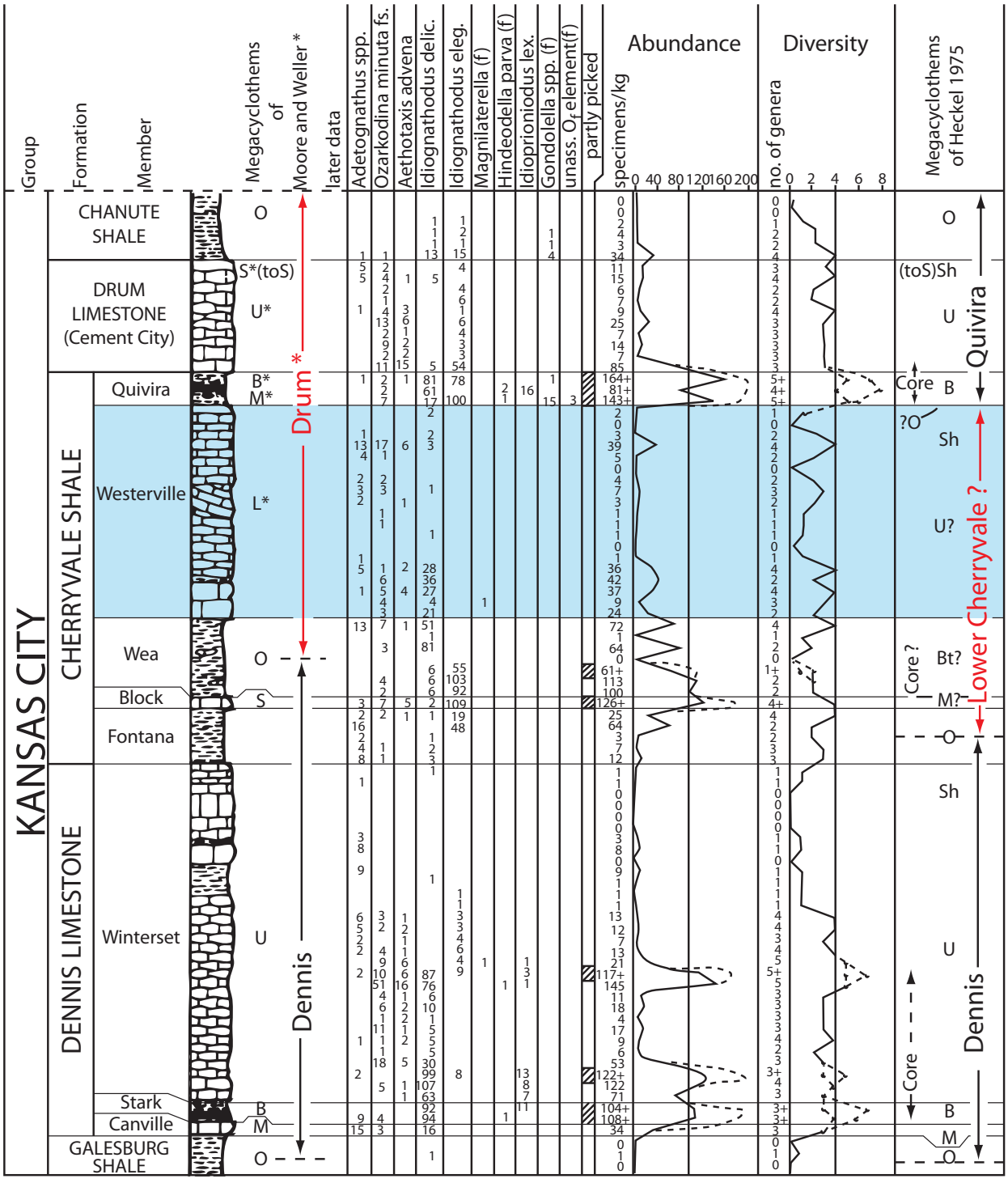


Figure 4. Stratigraphic column of the Kansas City Group. The Westerville Limestone, highlighted in blue, is reassigned from a lower limestone member (L*) of Moore (1949) and Weller (1958) to an upper limestone member (U) of Heckel and Baesemann (1975). Drum cycle is replaced by the lower Cherryvale cycle by Heckel and Baesemann (1975) based on conodont diversity and abundance data. Modified from Heckel and Baesemann (1975).

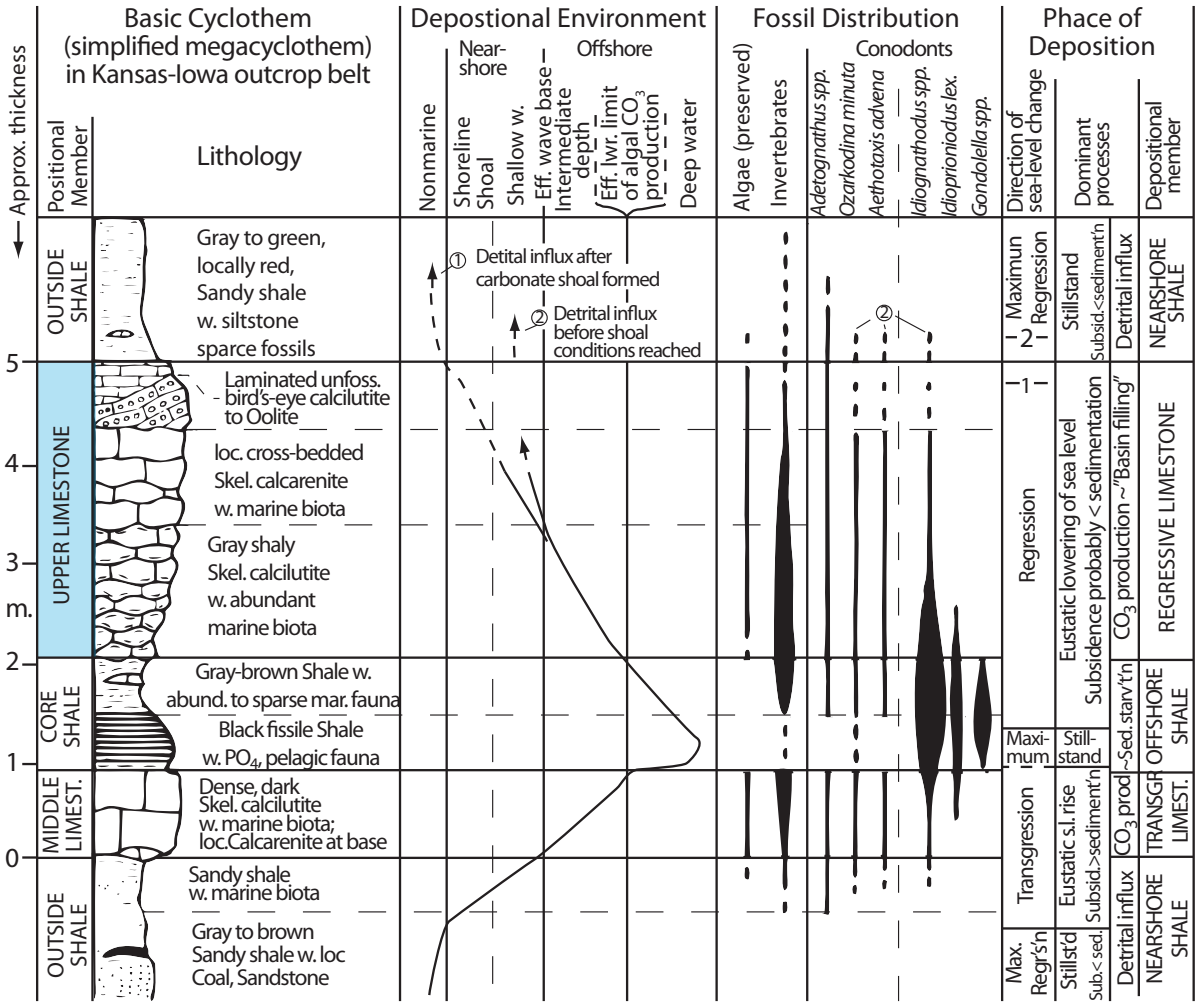


Figure 5. Cyclothem model diagram——Westerville is interpreted as an upper limestone (highlighted in blue) deposited during falling sea level (Heckel, 1977). Modified from Heckel (1977).

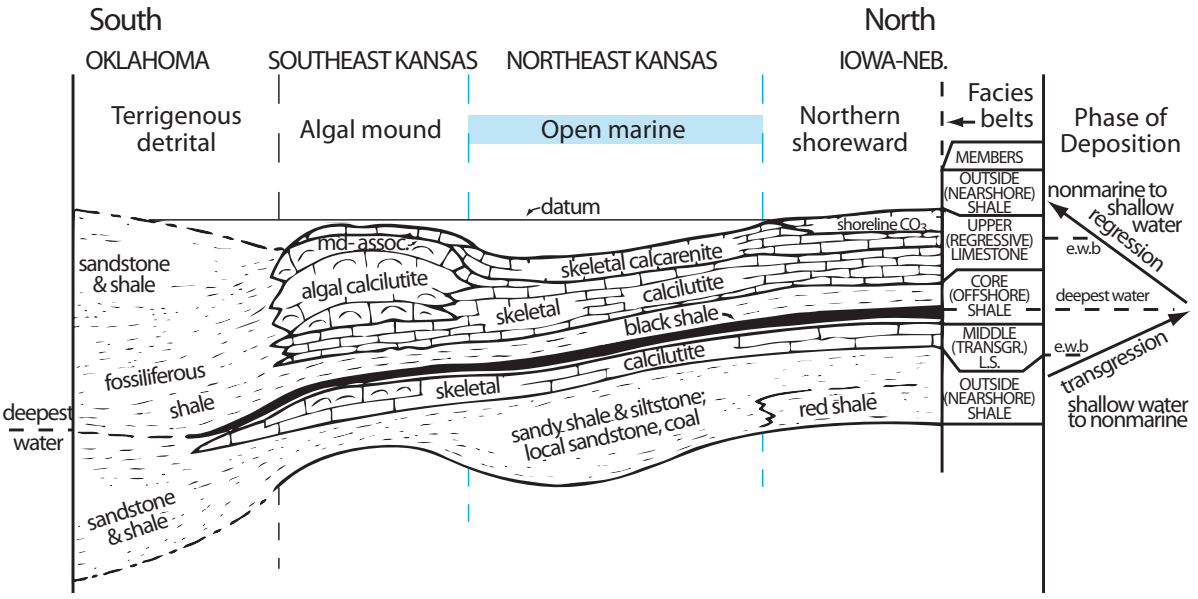


Figure 6. North–South cross section facies belt model (Heckel, 1977). In this model the Westerville is in the open marine section (highlighted in blue). Figure modified from Heckel (1977).

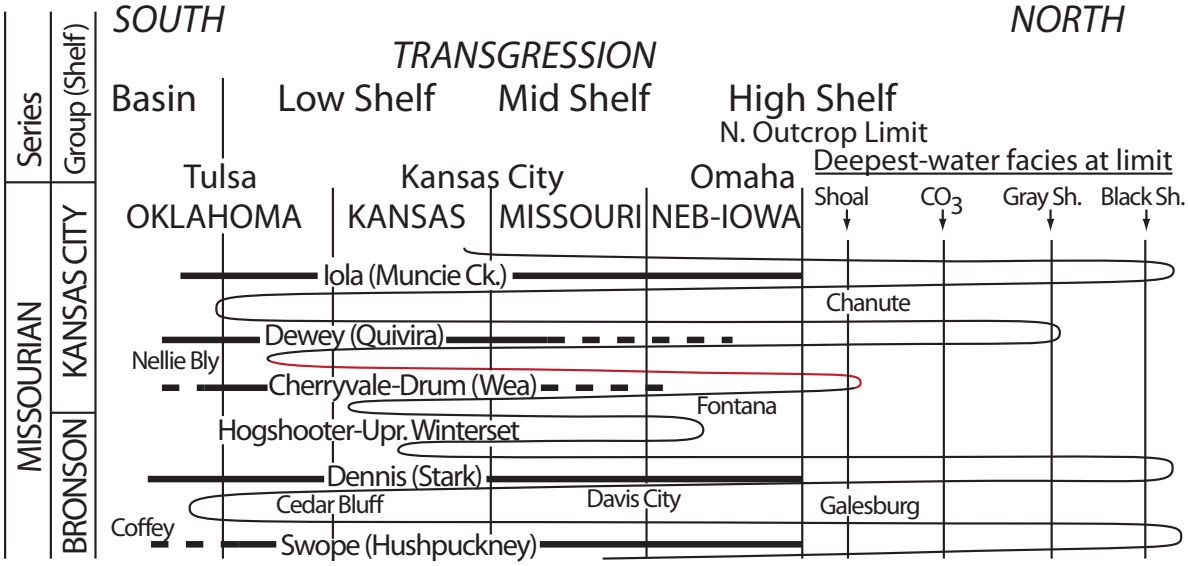


Figure 7. A portion of the sea-level curve from Heckel (1986). Stratigraphic interval of study highlighted in red. Notice the interpreted fall in sea level during this period and mid ramp position of the area of study. Modified from Heckel (1986).

# FACIES

In this section the Westerville is divided into eight lithofacies defined from outcrop observations, slabbed and polished hand-samples, and petrographic study of thin-sections. Facies attributes are summarized in Table 1 and stratigraphic relationships are shown in Figure 8. Facies names reflect the most prevalent attributes. Carbonate rock textures are reported using the Dunham (1962) classification scheme. All percentages reported here were taken as visual estimates from thin section analysis. Component types (e.g., lime mud, grains and cement) are reported as percentages of whole rock volume. Individual grain types (e.g., ooids, bioclastic grains, peloids and intraclasts) are reported as percentages of total grains. Grain size is reported according to the Modified Wentworth scale (Boggs, 2001). Preserved porosity in all carbonate facies is limited to modern weathering of siliciclastic material and minor bioclastic shelter porosity; it totals less than 1% of total rock volume. Inter- and intraparticle space is filled with micrite, blocky spar cement or neomorphic spar.

| Facies Name (textural classification) | Grain types (percent of total grains) and attributes | Bedding | Prominent Structures |
|---|---|---|---|
| **Bioclastic Packstone** (Bioclastic packstone and wackestone) | Abundant coarse-grained fenestrate bryozoan (20–60%), brachiopod (10–15%) and crinoid (15–25%) fragment-sand, and medium- to coarse-grained peloid sand (10–50%)(Fig. 9H). Whole unabraded granule-size brachiopods and phyloid red algae fragments are common. Medium- and coarse-grained bivalve, encrusting foraminifera (Fig. 10A), echinoderm, green algae and rugose coral fragment-sand is less common. Fossil fragment abrasion decreases with increasing grain size. | 5–25 cm thick massive tabular to wavy beds accentuated by 1–2 cm thick siliciclastic-mudstone partings and stylocumulates. | Lime-mud- and siliciclastic-silt-filled burrows common in upper 15 cm of exposure (Fig. 9G). |
| **Fossiliferous Siliciclastic-Mudstone** (Fossil-bearing siliciclastic mudstone and siltstone) | Unabraded very-coarse grained brachiopod and crinoid sand (0–20% of whole rock volume) and sparse whole brachiopod shells (Fig. 15F). Asymmetric coatings on grains are typically present near the gradational boundary with the oncolitic packstone facies and commonly concentrated in the lower portion of the facies where present. | Typically massive. Siltier beds are more likely to be laminated than clay-rich beds | Typically crops out as a thin (5–20 cm) exposure. Can have gradational contact with oncolitic packstone facies |
| **Bioclastic Grainstone** (Grainstone and matrix-poor (<10%) packstone) | Abundant slightly- to well-abraded coarse-grained crinoid (15–50%), dasycladacea green algae—*Mizzia*, *Mastopora*, and *Epimastopora* (3–35%), bryozoan (10–20 %), brachiopod (5–25%) and gastropod (5–20%) fragment-sand (Figure 14E–F). Coarse-grained ooid, peloid, foraminifera, phylloid algae, bivalve, bryozoan, rugose coral, and microbial intraclast fragment-sand is less common. Coated grains are uncommon. Unabraded cm-scale whole fossil brachiopods are present, but rare (Fig. 15C). | Gently dipping cm-scale tabular beds typically show no internal sorting, but cm-scale planar cross-bedding is present locally (Fig. 10E–F and 14G–H). | Centimeter scale bioclastic-grain or spar-filled burrows are common (Fig. 15A), but burrows can also be filled with micrite (Fig. 15B). |
| **Oncolitic Packstone** (Coated-grain rich and matrix poor packstone) | Coarse- to medium-grained phylloid red algae (20–40%), bryozoan (10–40%), brachiopod (5–25%) and gastropod (5–10%) sand present. Very-coarse sand to cobble size oncoids (10–20%) define facies. Fine- to medium-grained ooid, peloid, crinoid, bivalve, and trilobite sand grains are common. Coated grains show little abrasion (Fig. 15D). | Tabular to lenticular beds are 5–25 cm thick, laterally discontinuous at outcrop scale (Fig. 9E–F, 10G–H, and 11A–D). Internal physical sedimentary structures are rare, although imbrication of grains is present in places (Fig. 15E). | Asymmetric grain coatings can be greater than 1 cm thick (Fig. 15E). Coatings are dense, well laminated and rounded. Lime-mud filled burrows are rare. |

| Facies Name (textural classification) | Grain types (percent of total grains) and attributes | Bedding | Prominent Structures |
|---|---|---|---|
| **Oolitic Grainstone** (Grainstone and matrix-poor (<5%) packstone) **Subfacies** defined by bedding type. | Abundant coarse-grained (0.5–1.0 mm) ooid sand (50–80%). Major bioclast contributors include fine- to medium-grained abraded bryozoan (5–15%), dasycladacean green algae (5–15%), brachiopod (5–15%), gastropod (5–10%), and crinoid (0–20%) fragment-sand. Commonly coated, elongate (2–10 mm) fossil fragments are common. Very fine grained siliceous sand is uncommon (< 1%). Whole unabraded and coated brachiopods are rare (Fig. 14E–F). | 5–200 cm thick cross beds. Bidirectional apparent dip (Fig. 13). Climbing ripples present at site 8 (Fig. 12C–D). Herring-bone features present at sites 10 and 14 (Fig. 12G). | Zebra-stripe pattern corresponds to alternating laminations of well-sorted, over compacted, ooid-rich and moderately-sorted, non compacted, ooid-poor very-coarse grained bioclast sand (Fig. 12A–B, 14A–B, 14C). |
| **Planar cross-bedded subfacies** | | **Planar-crossbedded.** Wedge to tabular beds (Fig. 11E–H, 12A–B). | |
| **Trough cross-crossbedded subfacies** | | **Trough-crossbedded.** Dm-scale beds present at location 15 (Fig. 12E–F). | |
| **Peloidal Packstone** (Interbedded fossil-poor peloid-rich packstone and lime mudstone) | Composed of very fine- to fine-grained peloid sand (60–80% of whole rock volume), lime mud (0–35%), chert (0–10%), sparry calcite (0–5%) and quartz void fill (0–5%). Coarse- to very-coarse-grained fossil fragment-sand is rare, and is typically found proximal to other carbonate facies where present. | Mm-scale laminations. Current ripples can alternate apparent flow direction from bed to bed and have mudstone drapes (Fig. 15H). Wave ripples have an average wavelength of 6 cm and amplitude of 0.5 cm. | Mud cracks in beds of massive lime mud. Bedforms and laminations are discontinuous at hand-sample scale. Chert occurs randomly throughout the facies. Fenestrae are common throughout (Fig. 15G–H). |
| **Microbial Boundstone** (Domal microbial boundstone) | 2–4 mm-wide stacked, domal (1 mm tall) layers trap carbonate mudstone, very-fine grained ooid sand, coarse-grained, coated brachiopod fragment-sand, and fine-grained bryozoan and green algal fragment-sand (Fig. 17) | Occurs as <3 cm thick bed which mantles underlying surface (Fig. 16A). Small (mm-scale) domal structures create a bumpy surface expression (Fig. 16B). | Layers and underlying deposits commonly have *gastrochaenolites* borings (Pemberton et al., 1992). Borings are filled with lime mudstone, fossil fragments, and ooids (Fig. 17). |
| **Coarse-Grained Packstone** Portions of facies show grainstone, packstone, and wackestone textures | Packstone contains whole bivalve fossils which are partially filled with peloids. Grainstone contains unsorted coarse coated-grain sand which show no sorting, imbrication, or layering. Wackestone is mottled and contains unabraded fine grained bioclast fragment-sand (Fig. 18). | Occurs as one 10–20 cm thick bed at sites 13 and 19. Lowermost boundary scours into underlying deposits. | Lowermost portion is wackestone. Transitions upward after scour surface to packstone, then grades upward to grainstone. Grainstone grades upward to laminated peloidal packstone. |

Table 1. Facies attribute table. Facies names defined by prominent attributes. Rock texture described below facies name. Individual grain type percentages reported are percent of total grains by number rather than by volume.

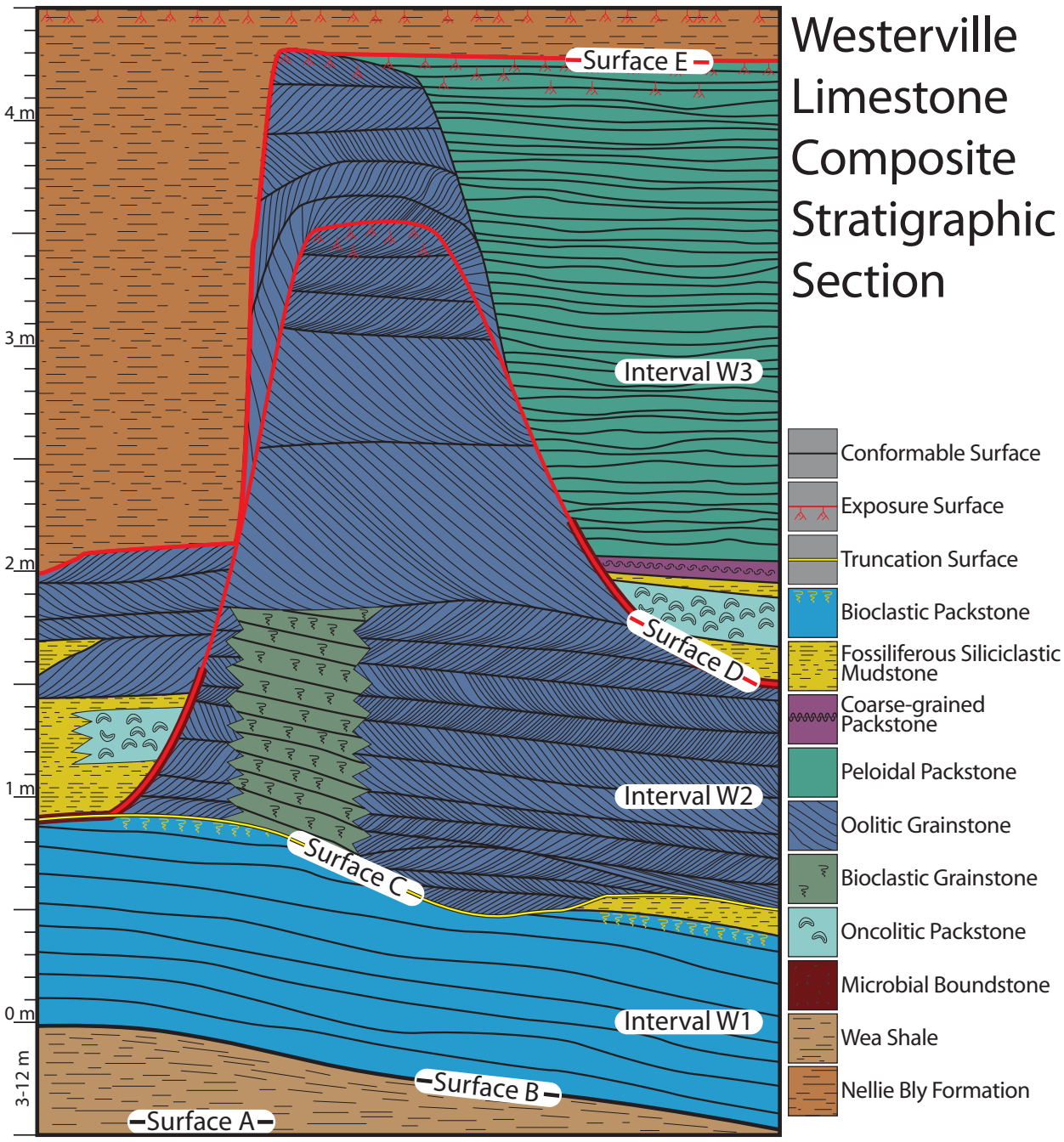


Figure 8. Composite stratigraphic column for the Westerville Limestone encompassing facies and surface relationships as seen across the entire field area.

## Depositional Environment Interpretation

### Bioclastic Packstone Facies

The diverse fossil assemblage of the bioclastic packstone facies is consistent with that found in open marine water systems (Heckel 1972). Whole unabraded brachiopod-shells indicate that the organisms likely lived in or near this environment and were not transported any great distance. The presence of in place algae can indicate a depositional environment within the photic zone (Fornos and Ahr, 1997; Basso, 1998; Wray, 1964; Kirkland, 1993; Baars and Teroes, 1991). Dasycladacean green algae's light dependence indicates a euphotic zone (20–30 m), whereas phylloid red algae and foraminifera can live in the oligophotic zone, extending their possible formation depth to 50–100+ m (Pomar 2001). The light independent or oligophotic organisms present in this facies (phylloid red algae and foraminifera) are preserved whole and unabraded, whereas the euphotic biota (dasycladacean green algae) are abraded. It is therefore possible that the light-dependent organisms were transported from a shallow water environment. This facies does not show graded textures, hummocky stratification or lateral thickness or texture variations within individual beds, which would be expected if deposition occurred by sediment gravity flows or storms. Therefore, the red algae are interpreted to have formed in place and the lower limit of deposition for this facies is placed at 50–100 m. A 50 m lower limit for the bioclastic packstone facies seems reasonable because black phosphatic shale is thought to form in an environment inhospitable to open marine fauna at a minimum depth of 30–50 m in the Midcontinent during the Pennsylvanian (Heckel, 1977). The lack of internal sedimentary structures, except for burrows, and presence of mud indicate a low energy setting. This places

the upper limit of deposition below fair-weather wave base. Fair-weather wave base has been estimated at 5–15 m (Nichols, 1999), the median, 10 m, will be used for this study.

This facies is interpreted to have been deposited in an open-marine subtidal environment away from constant current or wave energy, but shallow enough to be in the photic zone, 10–50 m water depth. Similar Pennsylvanian facies have been interpreted to form below wave base in open marine waters of normal salinity (Krainer and Lucas, 2004; Grammer et al., 1996) and the interpretation is also consistent with Handford's (1988) 7.6–30 m water depth for a similar facies from the Mississippian.

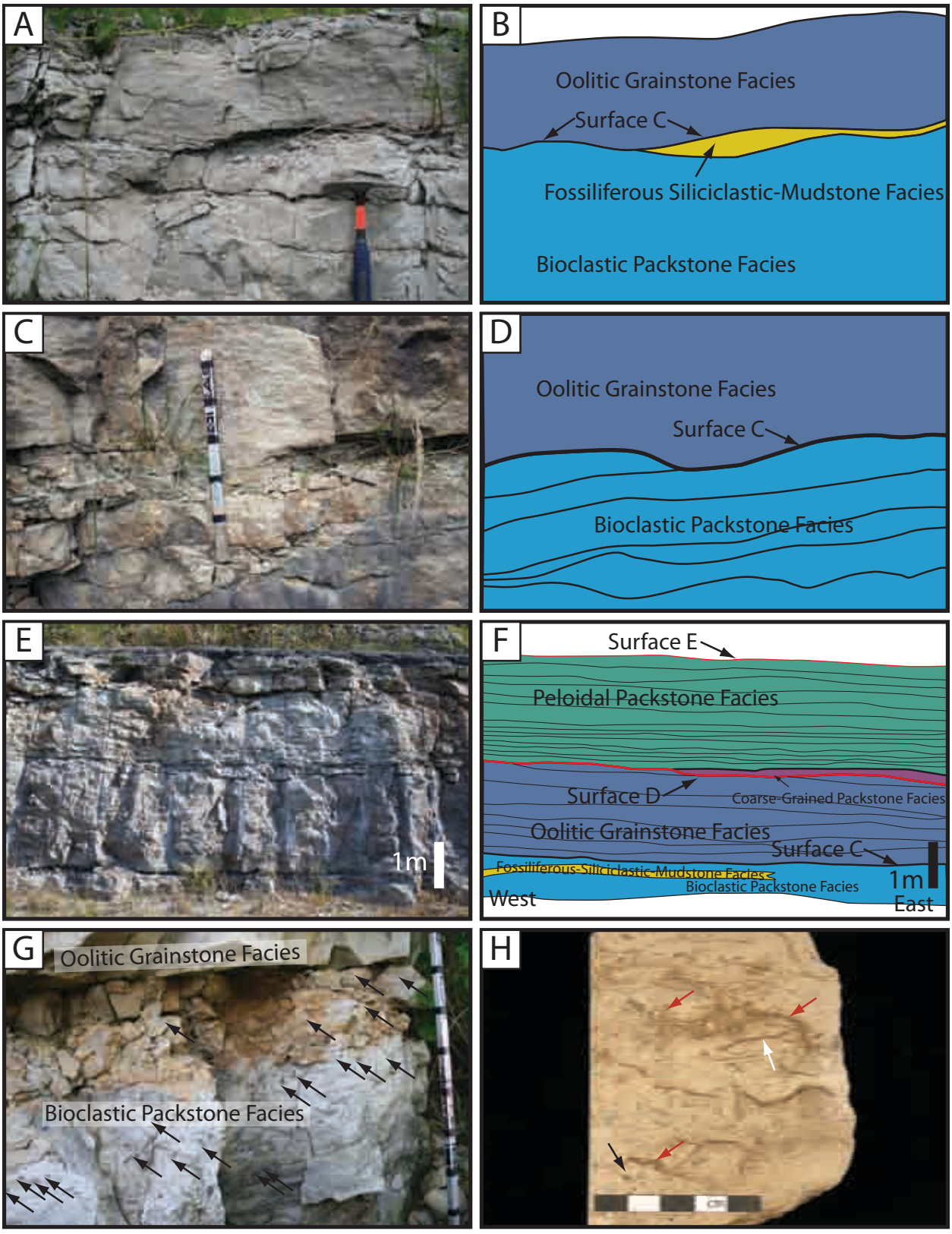
A
B
Oolitic Grainstone Facies
Surface C
Fossiliferous Siliciclastic-Mudstone Facies
Bioclastic Packstone Facies
C
D
Oolitic Grainstone Facies
Surface C
Bioclastic Packstone Facies
E
1m
F
Surface E
Peloidal Packstone Facies
Surface D
Coarse-Grained Packstone Facies
Oolitic Grainstone Facies
Surface C
Fossiliferous Siliciclastic-Mudstone Facies
Bioclastic Packstone Facies
1m
West
East
G
Oolitic Grainstone Facies
Bioclastic Packstone Facies
H

Figure 9. Bioclastic packstone facies photographs and color overlays. Facies color explanation found in Fig. 18. A and B) Photo and color overlay of outcrop at site 7 showing the truncation of the fossiliferous siliciclastic-mudstone facies overlain by oolitic grainstone facies. C and D) Photo and color overlay of outcrop at site 7 showing the truncation of bioclastic packstone facies beds overlain by oolitic grainstone facies. Stick graduated at 10 cm intervals. E and F) Photo and color overlay of outcrop at site 13 showing the gradational lateral boundary between fossiliferous siliciclastic-mudstone and bioclastic packstone. The photo and overlay illustrate the coarse-grained packstone facies onlapping positive relief on oolitic grainstone. Overlying peloidal packstone drapes subtle topography below. G) Photo of outcrop at site 8 showing the boundary between the bioclastic packstone and oolitic grainstone facies. Black arrows point to siliciclastic mud-filled burrows. Stick graduated at 10 cm intervals. H) Polished hand sample of bioclastic packstone facies. White arrow points to phylloid algal fragment. Red arrow points to phylloid algal fragments encrusted with foraminifera. Black arrow points to geopetal feature.

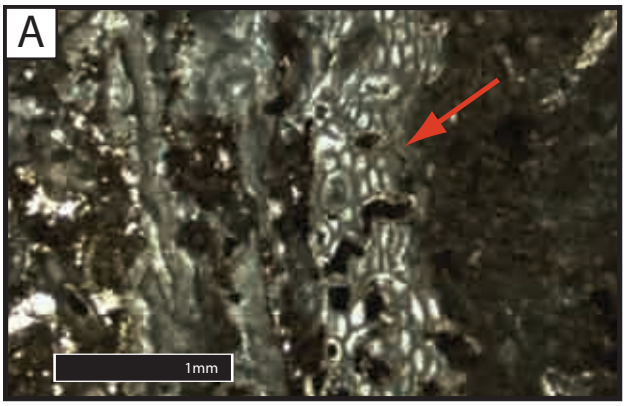
A
1mm


B

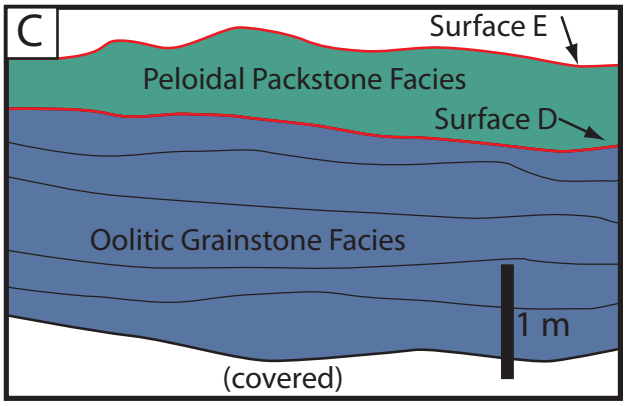
C
Surface E
Peloidal Packstone Facies
Surface D
Oolitic Grainstone Facies
1 m
(covered)


D

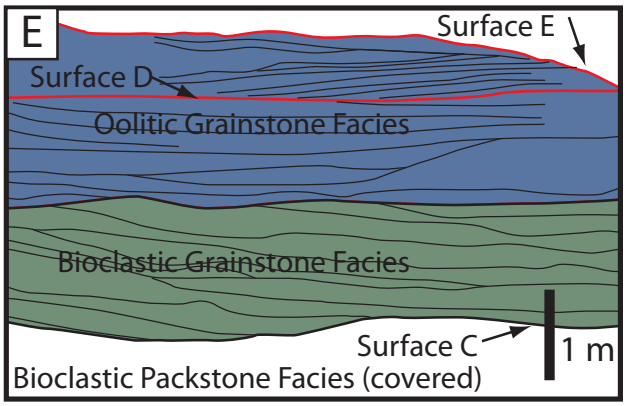
E
Surface E
Surface D
Oolitic Grainstone Facies
Bioclastic Grainstone Facies
Surface C
1 m
Bioclastic Packstone Facies (covered)


F
1 m

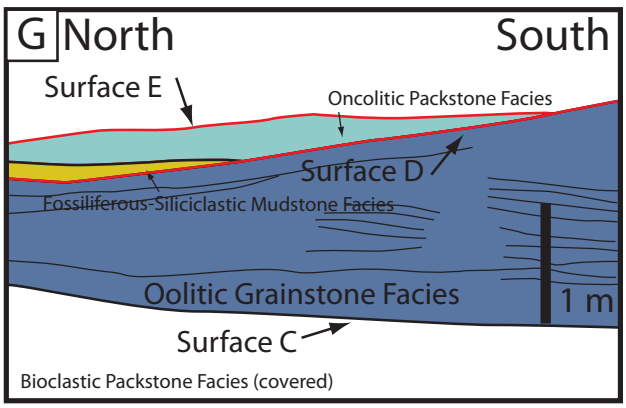
G
North
South
Surface E
Oncolitic Packstone Facies
Surface D
Fossiliferous Siliciclastic Mudstone Facies
Oolitic Grainstone Facies
1 m
Surface C
Bioclastic Packstone Facies (covered)

Figure 10. Facies photographs and overlays. Facies color explanation found in Figure 19. A) Thin section photomicrograph of bioclastic packstone facies. Red arrow points to encrusting foraminifera. B and C) Photo and color overlay of outcrop at site 11 showing peloidal packstone facies overlying oolitic grainstone facies. D and E) Photo and color overlay of outcrop at site 16 showing truncated bioclastic grainstone beds and overlying oolitic grainstone facies. F and G) Photo and color overlay of outcrop at site 2 showing fossiliferous siliciclastic-mudstone and oncolitic packstone onlapping positive relief on oolitic grainstone.

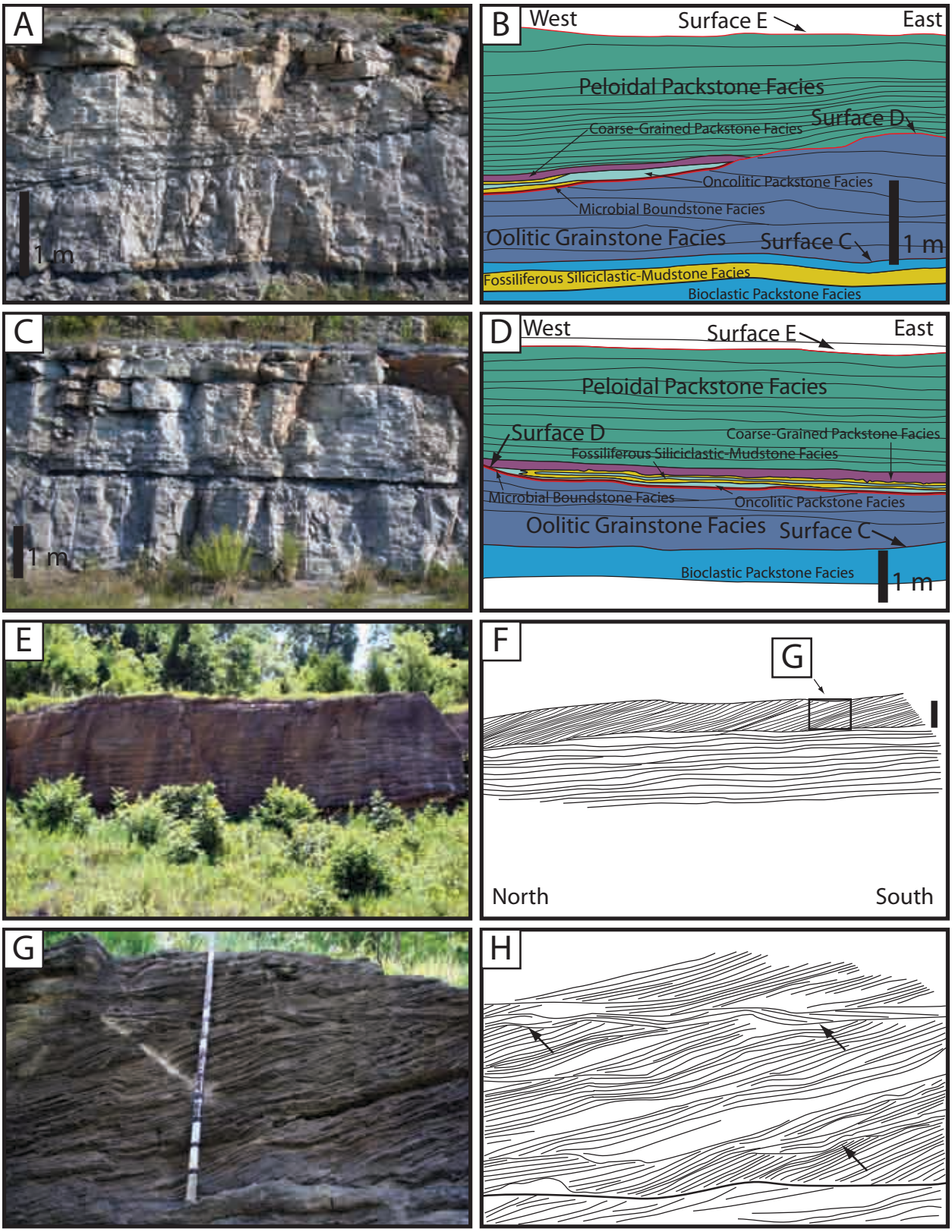
A
1 m
B
West
Surface E
East
Peloidal Packstone Facies
Surface D
Coarse-Grained Packstone Facies
Oncolitic Packstone Facies
Microbial Boundstone Facies
Oolitic Grainstone Facies
Surface C
1 m
Fossiliferous Siliciclastic-Mudstone Facies
Bioclastic Packstone Facies
C
1 m
D
West
Surface E
East
Peloidal Packstone Facies
Surface D
Coarse-Grained Packstone Facies
Fossiliferous Siliciclastic-Mudstone Facies
Microbial Boundstone Facies
Oncolitic Packstone Facies
Oolitic Grainstone Facies
Surface C
Bioclastic Packstone Facies
1 m
E
F
G
North
South
G
H

Figure 11. Facies photographs and overlays. Facies color explanation found in Figure 19. A and B) Photo and color overlay of outcrop at site 13 showing microbial boundstone, oncolitic packstone, and coarse-grained packstone all onlapping against erosional relief on Surface D. The peloidal packstone facies conformably overlies underlying deposits and Surface D. C and D) Photo and color overlay of outcrop at site 13 showing similar facies and onlap relationships seen in A and B on the eastern flank of a local paleotopographic high. Notice the gradational lateral facies transition between the fossiliferous siliciclastic-mudstone and oncolitic packstone. E and F) Photo and line drawing of outcrop at site 8 showing both cm-scale (bottom) and m-scale (top) planar tabular cross beds of oolitic grainstone. One meter vertical scale bar at right. Box shows approximate location of photo in G. G and H) Close-up photo and line drawing of outcrop at site 8 showing m-scale planar tabular cross beds. Black arrows point to reactivation surfaces within the m-scale planar tabular cross beds. Staff graduated at 10 cm interval.

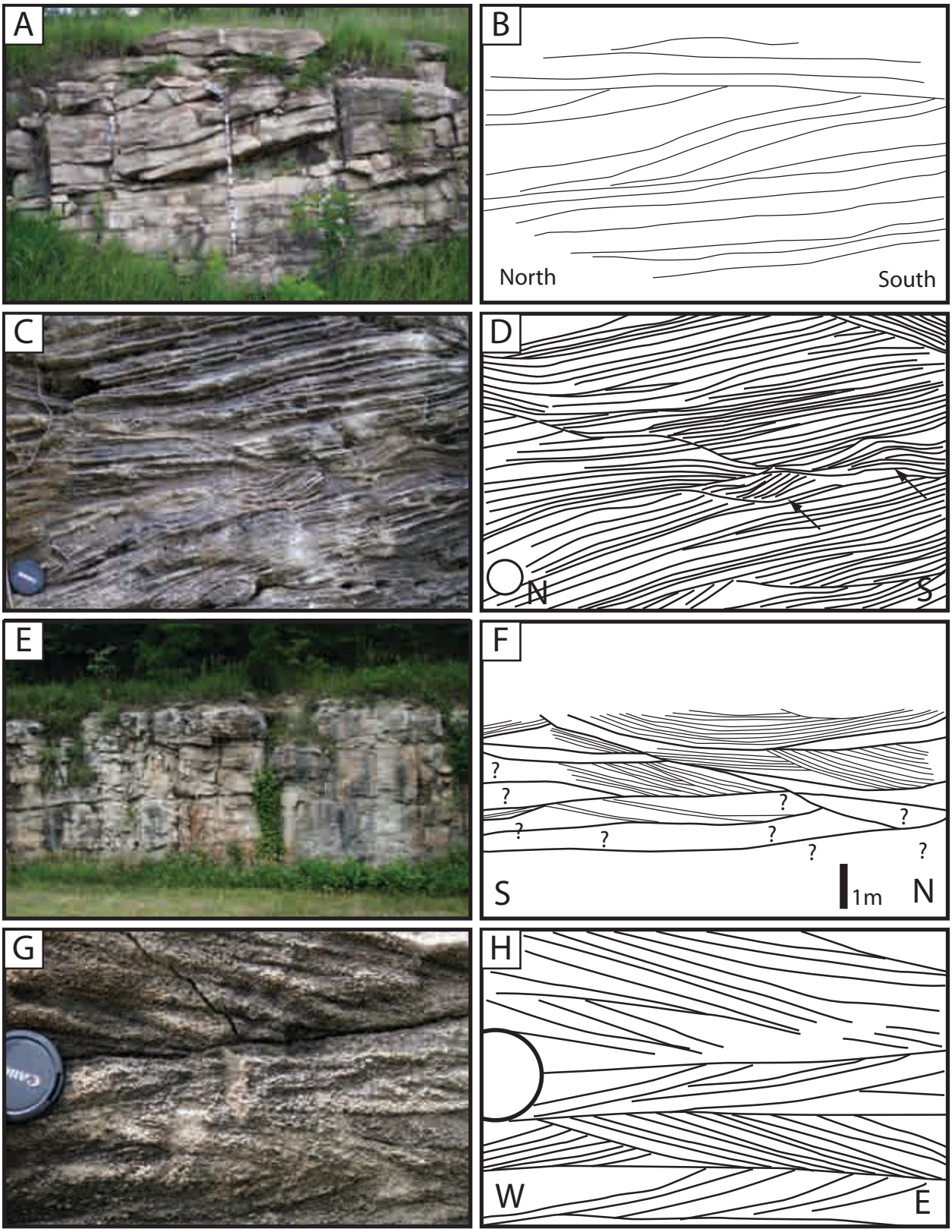
A
B
North
South
C
D
N
S
E
F
?
?
?
?
?
?
?
?
?
?
S
1m
N
G
H
W
E

Figure 12. Oolitic grainstone photos and associated line drawings. A and B) Photo and line drawing of outcrop at site 6 tracing tabular cross bedding in oolitic grainstone. C and D) Close-up photo and line drawing of oolitic grainstone at site 8 showing a north apparent-dip direction to tabular cross beds. Black arrows point to climbing ripples. Lens cap for scale. E and F) Photo and line drawing of oolitic grainstone at site 15 showing bed boundaries (thick lines) and internal laminations (thin lines). This is the only outcrop site studied that displays trough cross bedding in the oolitic grainstone. G and H) Close-up photo and line drawing of cm-scale tabular cross bedding and internal laminations in oolitic grainstone facies at site 14. Notice the apparent opposing orientation of cross beds. Lens cap for scale.

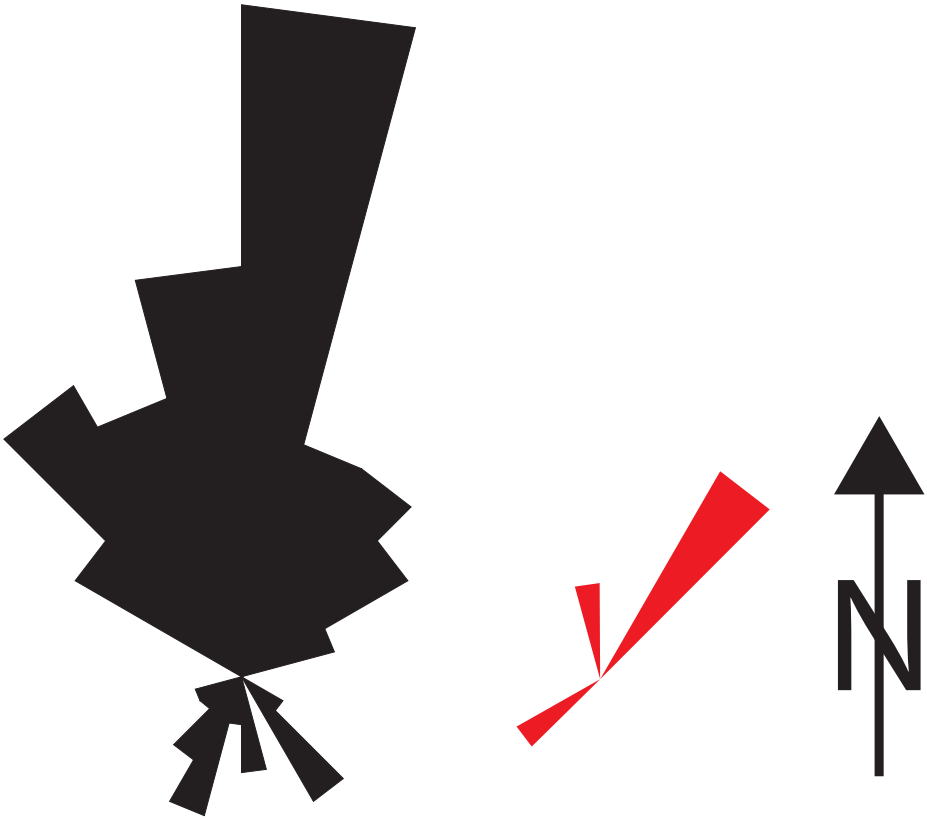


Figure 13. Rose diagram showing tabular cross bed orientations for the oolitic grainstone facies below Surface D (black) and above Surface D (red).

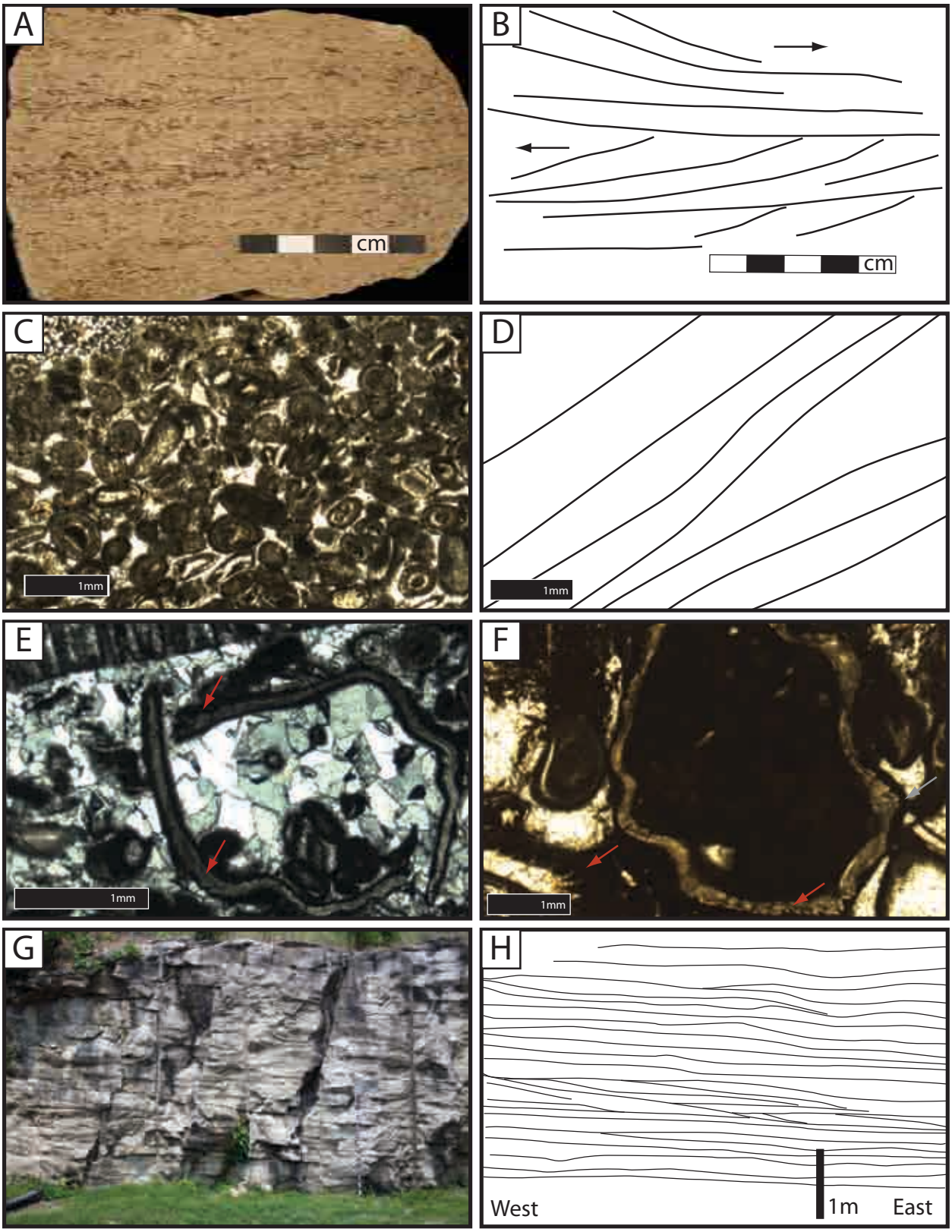
A
cm
B
cm
C
1mm
D
1mm
E
1mm
F
1mm
G
H
West
1m
East

Figure 14. Facies photographs and overlays. A and B) Photo and line drawing of polished hand sample of oolitic grainstone. Notice the color variation between laminations (tiger stripe pattern). Notice the alternating orientations between tabular cross beds. C and D) Thin section photo and line drawing of oolitic grainstone facies. Lines trace approximate boundaries between overcompacted and noncompacted laminations. E and F) Thin section photos of oolitic grainstone with coated whole brachiopod shells. Red arrows point to areas where coating covers preserved ornamentation on brachiopod shells. G and H) Photo and line drawing of outcrop at site 19, tracing bedding contacts in the bioclastic grainstone. Notice the general dip of beds to the east. Measuring staff in photo is divided into 10 cm increments.

Oolitic Grainstone Facies

Modern ooids form in environments where oscillatory fluid flow keep individual grains within the environment, allowing the formation of concentric coatings (Reeder and Rankey, 2008). Handford (1988) summarized modern ooid formation in Bahamas, Abu Dhabi UAE, and Arabian Gulf in water depths from <2–15 m located near bathymetric highs and tidal energy. Small amounts of lime mud and tabular and trough crossbeds are typical in modern ooid-forming environments (Harris, 1984). The alternating laminations of elongate bioclasts and ooid-rich lamina (tiger stripe pattern) within the Westerville are similar in scale and sorting to modern oolitic deposits from the ocean-facing, tidally influenced side of Joulters Ooid Shoal (Harris, 1984). Climbing ripples form during periods of rapid sediment deposition during waning flow (Ashley et al., 1982) and are present in modern tidal systems (Tessier et al., 1995).

The abundance of bioclasts (20–50%) and medium- to coarse-grained sand is similar to deposits in the channels and on the flanks of modern shoals at Double Breasted Cays and ebb and flood tidal deltas around the inlet between Carter's Cay and Jack's Cay, Bahamas (Reeder and Rankey, 2008) and a bar flank from Schooner Cays ooid shoal and channel in Fish Cays shoal complex (Rankey and Reeder, 2011). Stacked planar cross beds showing bidirectional flow (Fig. 10G–H) also indicate a tidal signature.

Today, ooids are also found in modern beach environments, but deposits within the Westerville lack evidence for deposition of beach-accretion beds typical of foreshore environments (i.e. low angle laminations and fenestral fabric) (Inden and Moore, 1983).

Thus, deposition of the oolitic grainstone facies is interpreted to have occurred in a tidally influenced shallow-water (<2–15 m) high-energy environment. Depth constraints similar to

modern Bahamian deposits seem reasonable because the modern Bahamas is a microtidal (1 m tidal amplitude) environment (Gonzalez and Eberli, 1997) and a microtidal environment has been interpreted for the Pennsylvanian Midcontinent (Wells et al, 2007).

Subdivision of oolitic grainstone in the Westerville into the planar cross-bedded and trough cross-bedded subfacies allows for increased precision in paleoenvironmental interpretation. In modern oolitic systems, planar cross-bedding overlies trough cross-bedding in shallowing-upward sequences found in tidal channel, tidal bar, and flood and ebb delta, environments (Harris, 1984). It seems reasonable then to interpret the depositional depth of the trough cross-bedded subfacies to be at the deep end of the interpreted depositional depth (~5–15 m) and the planar cross-bedded subfacies at the shallow end of the range (<2–5 m).

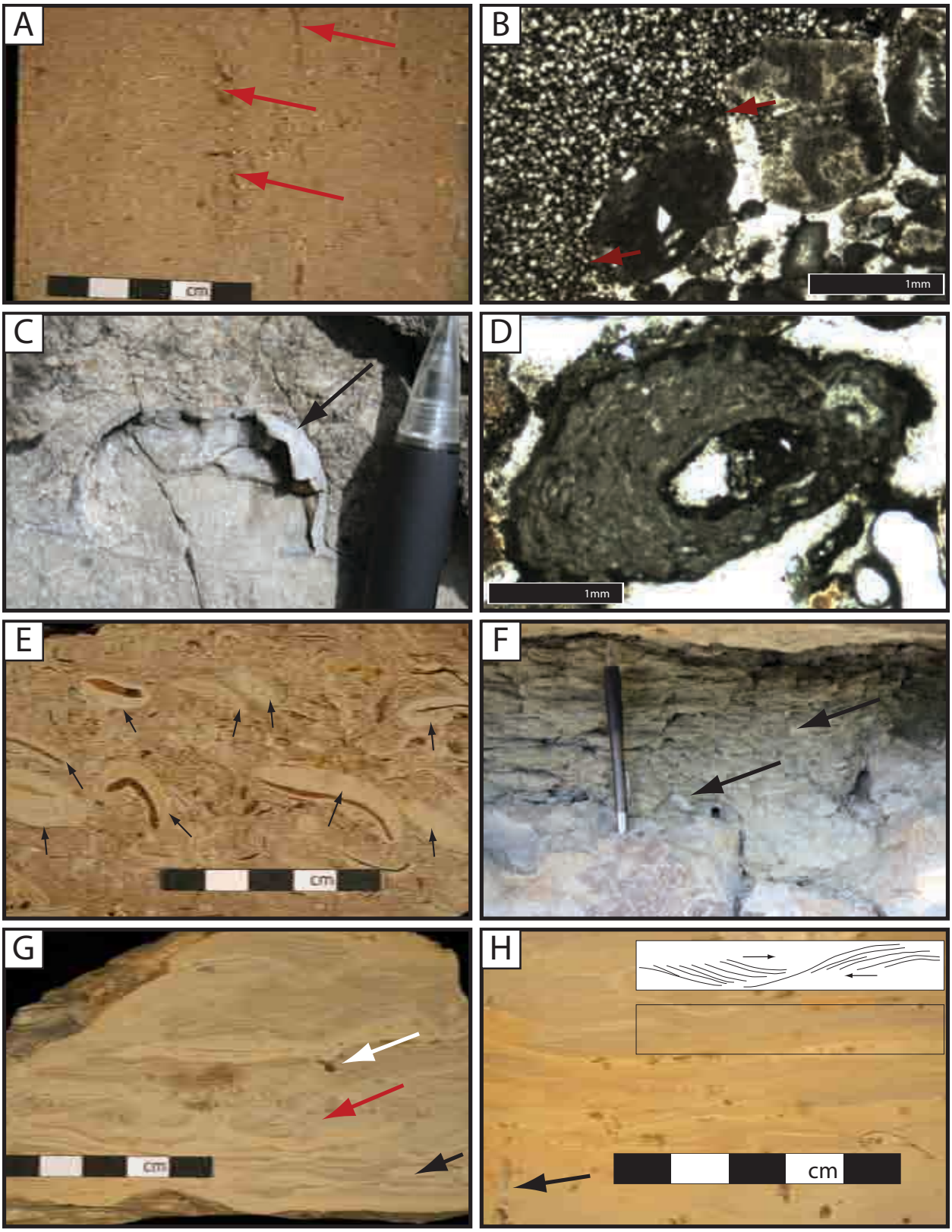
A
cm
B
1mm
C
D
1mm
E
cm
F
G
cm
H
cm

Figure 15. Facies photographs. A) Polished hand sample of bioclastic grainstone. Red arrows point to vertical burrows filled with spar cement. B) Thin section photomicrograph of bioclastic grainstone. Upper left is a filled burrow. Red arrows point to areas where burrow infill conforms to grain boundaries demonstrating that the grains are not truncated. C) Close-up photo of outcrop at site 16. Black arrow points to unabraded whole brachiopod shell within the bioclastic grainstone facies. D) Thin section photo of oncolitic packstone facies showing Girvanella coating around a grain. E) Polished hand sample of oncolitic packstone facies. Black arrows point to asymmetrically coated grains. Notice imbrication of grains and thicker coatings are generally found on the convex side of the coated fragment. F) Close-up photo of outcrop at site 7 of the fossiliferous siliciclastic-mudstone facies. Black arrows point to fossil fragments (crinoids) G) Polished hand sample of peloidal packstone facies. White arrow points to a fenestral pore. Red arrow points to soft sediment deformation. Black arrow points to a mud crack. H) Polished hand sample of peloidal packstone facies. White box shows line drawing from the outlined box below. Lines trace cross-laminations and show evidence for alternating flow directions (arrows). Black arrow (bottom left) points to a quartz cement-filled vertical tube.

Bioclastic Grainstone Facies

The diverse fossil assemblage of the bioclastic grainstone facies indicates open marine water (Heckel, 1972). Tabular cross beds, abraded grains and lack of mud indicate deposition in a high-energy environment. Fossil fragments of *Epimastopora* (a dasycladacean green algae) are present throughout the facies and are interpreted to form in shallow water (5–10 m)(Wilson and Jordan, 1983). Whole unabraded brachiopod fossils, lime mudstone-filled burrows, and lack of internal bedding structures, however, likely indicates that most of this facies was subjected to thorough bioturbation. Oolitic coatings indicate some reworking of sediment or transport of those grains from a nearby active ooid shoal. Transport of ooids from an active shoal is more likely because an ooid-forming environment would not be stable enough to allow for thorough bioturbation. The scattered presence of mud matrix could represent areas of less energy (sheltered or baffled).

This facies was most likely deposited in shallow water exposed to periods of high energy proximal to an active ooid shoal. Similar to modern skeletal grainstone deposits present on the seaward side of the Joulters ooid shoal, Bahamas (Harris, 1984) and forming a depositional band along the southern margin of the modern Persian Gulf at 10 m of water depth (Wilson and Jordan, 1983). The proximity to an active ooid shoal, relatively gentle paleoslope and lack of significant amounts of lime mud means that the depositional depth for the bioclastic grainstone was similar to the interpreted depositional depth of the oolitic grainstone (2–15 m).

Oncolitic Packstone Facies

The diverse fossil assemblage indicates deposition in or near open marine water (Heckel, 1972). The presence of lime and siliciclastic mudstones indicate periods of slack or baffled water energy, whereas the imbrication of asymmetrically coated oncoids, some greater than 3 cm in length, indicate periods of higher energy tractive currents strong enough to move cobble sized grains. Although the ooids could indicate shallow high energy water, the lime mudstone, lime-mudstone filled burrows, and lack of crossbedding, make it more likely that the ooids were transported into the depositional environment during periods of increased water energy. No evidence of subaerial exposure features (i.e. desiccation cracks, fenestral fabric, meniscus or pendant cements) were found in this facies.

Modern oncoids around Grand Cayman Island form 100 m offshore in a reef sheltered shallow lagoon in 1.5 m water depth (Jones and Goodbody, 1985). Dense, rounded, and well laminated oncolitic coatings have been interpreted to form in high energy environments (Wright, 1983). Also, oncoids have been interpreted to develop in shallow restricted waters (Ruf and Aigner, 2004; Qing and Nimegeers, 2008).

I interpret the oncolitic packstone facies to have been deposited in a semirestricted setting, proximal to ooid and siliciclastic sources that was sheltered from open marine waters enough to restrict normal flow, but not restricted enough to limit intermittent tractive currents. The lack of evidence of subaerial exposure supports deposition in a subtidal environment. A depth greater than 1 m would be deeper than the modeled tidal range for the Pennsylvanian Midcontinent (Wells et al, 2007). An upper limit of 1 m would place deposition in the lower intertidal to subtidal. A lower limit for the deposition of the oncolitic packstone is more difficult to define. The lack of current or wave bed forms implies deposition below the assumed wave

base of 10 m. The semirestricted environment of deposition, however, would also protect the area from normal wave energy, shallowing local wave base. Deposition in water depths shallower than ~ 5 m is likely acceptable and agrees with interpretations of Baker (1995) and Washburn (2004) for Pennsylvanian oncolitic deposits. The interpreted depositional depth range of 1–5 m agrees with the modern depositional depth of 1.5 m (Jones and Goodbody, 1985).

Fossiliferous Siliciclastic-Mudstone Facies

The presence of siliciclastic clay and silt in both transgressive and regressive limestones in Pennsylvanian cyclothems has been attributed to deltaic influx (Heckel, 1977; French and Watney, 1993). The influx of siliciclastic material can occur at various depths. The presence of brachiopods and crinoids, which are also present in gradationally underlying and overlying clean carbonate facies in the Westerville, indicates similar environmental conditions during deposition. Therefore, the depositional environment interpretation for this facies is mainly based on its association with surrounding facies. This works well where the facies has a gradational boundary. For example, where present with the oncolitic packstone facies, the fossiliferous siliciclastic-mudstone is interpreted as being deposited in a shallow, semirestricted setting. A different environment is interpreted where the fossiliferous siliciclastic-mudstone occurs between bioclastic packstone facies (10–50 m water depth) and oolitic-or bioclastic-grainstone facies (2–20 m water depth). In these occurrences, the lack of carbonate mud in the oolitic- and bioclastic grainstone facies is attributed to current energy strong enough to remove any fine grained material. The environment of deposition for the fossiliferous siliciclastic-mudstone facies is,

therefore, interpreted to be similar to the bioclastic packstone facies (10–50 m water depth), with the fossiliferous siliciclastic-mudstone reflecting closer proximity to a siliciclastic source.

### Peloidal Packstone Facies

Interbedded mudstone and peloid layers, graded peloids, sparse fossil content, vertical tubular voids, fenestrae, and mud cracks are all consistent with deposition in a supratidal environment (Shinn, 1983). Current ripples (mm-scale) with mud drapes and alternating flow directions indicate waxing and waning flow, likely due to a tidal influence. Mudstone layers can be attributed to storm tide deposits. Wave ripples, generally associated with subtidal deposition, can be common in supratidal deposits (Shinn, 1983). Desiccation structures (mud cracks) indicate periods of subaerial exposure during deposition (Flügel, 2004). Fenestrae are ovoid shaped and can be the product of gas bubble formation or air escape during flooding, processes common to supratidal settings (Shinn, 1983). Although some burrowing organisms were active, the sparse fossil content indicates an environment that was not favorable to abundant biota. Fluctuating temperature, salinity, and periodic subaerial exposure common in modern supratidal environments is hostile toward macrobiologic activity (Shinn, 1983).

The peloidal packstone facies is here interpreted to have been deposited in a supratidal environment. This interpretation is based on the individual features described in the preceding paragraph and similarity to both modern (Sugarloaf Key, Florida) and ancient (West Texas, Cretaceous) examples (illustrated in Shinn, 1983; p. 180–181). Supratidal deposits occur at mean sea level with alternating periods of subaerial exposure and marine influence, so the interpreted depth of deposition range for the peloidal packstone facies is 0–1 m.

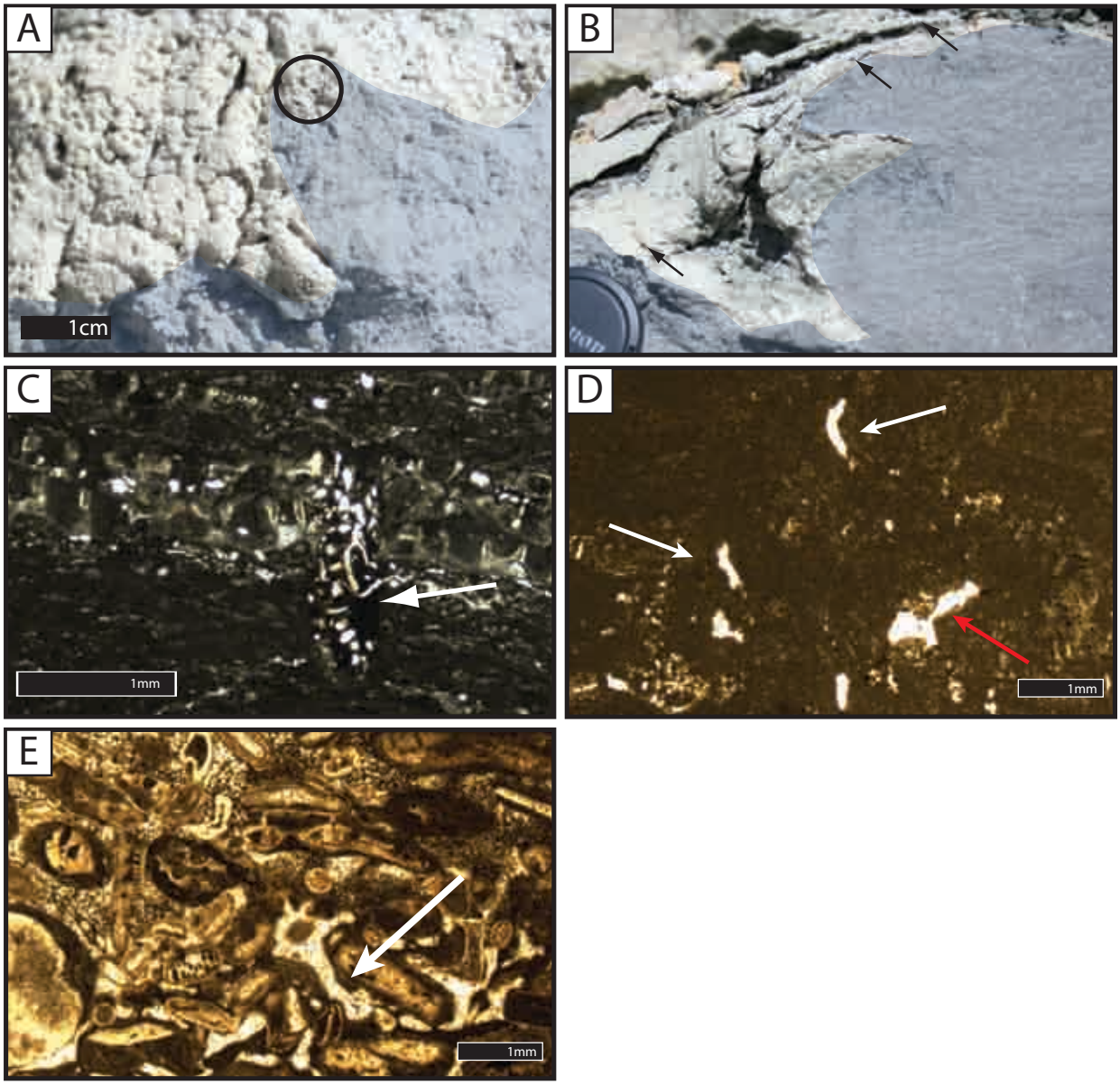


Figure 16. Facies field photographs and micrographs. A) Close-up photo of outcrop at site 13 looking down onto the bedding plane on the left side and at an oblique cross sectional view in the shaded area (right). Notice domal texture of the microbial boundstone (to the left, in sunlit area) encrusting the underlying oolitic grainstone facies (on the right, in shaded area). Black circle around small borings into oolitic grainstone. B) Close-up photo of outcrop at site 13 looking at a cross sectional view of the outcrop shown in A. Black arrows point to layers of microbial boundstone encrusting and draping erosional surface. Area in the shade is the underlying oolitic grainstone. Lens cap for scale is 6 cm. C) Thin section photomicrograph of microbial boundstone facies. White arrow points to mudstone- and fossil fragment-filled boring which crosscuts both the microbial laminations and the encrusting bryozoan. Scale bar equals 1 mm. D) Thin section of peloidal packstone facies near upper contact of the facies. White arrows point

to spar-filled voids, which are interpreted to be rhizoliths based on shape and size distribution. Red arrow points to spar-filled void which is interpreted as a fenestrae desiccation feature. Scale bar equals 1 mm. E) Thin section photomicrograph of oolitic grainstone facies. Notice pendant cement fabrics in lower right portion of sample (white arrow). Scale bar equals 1 mm.

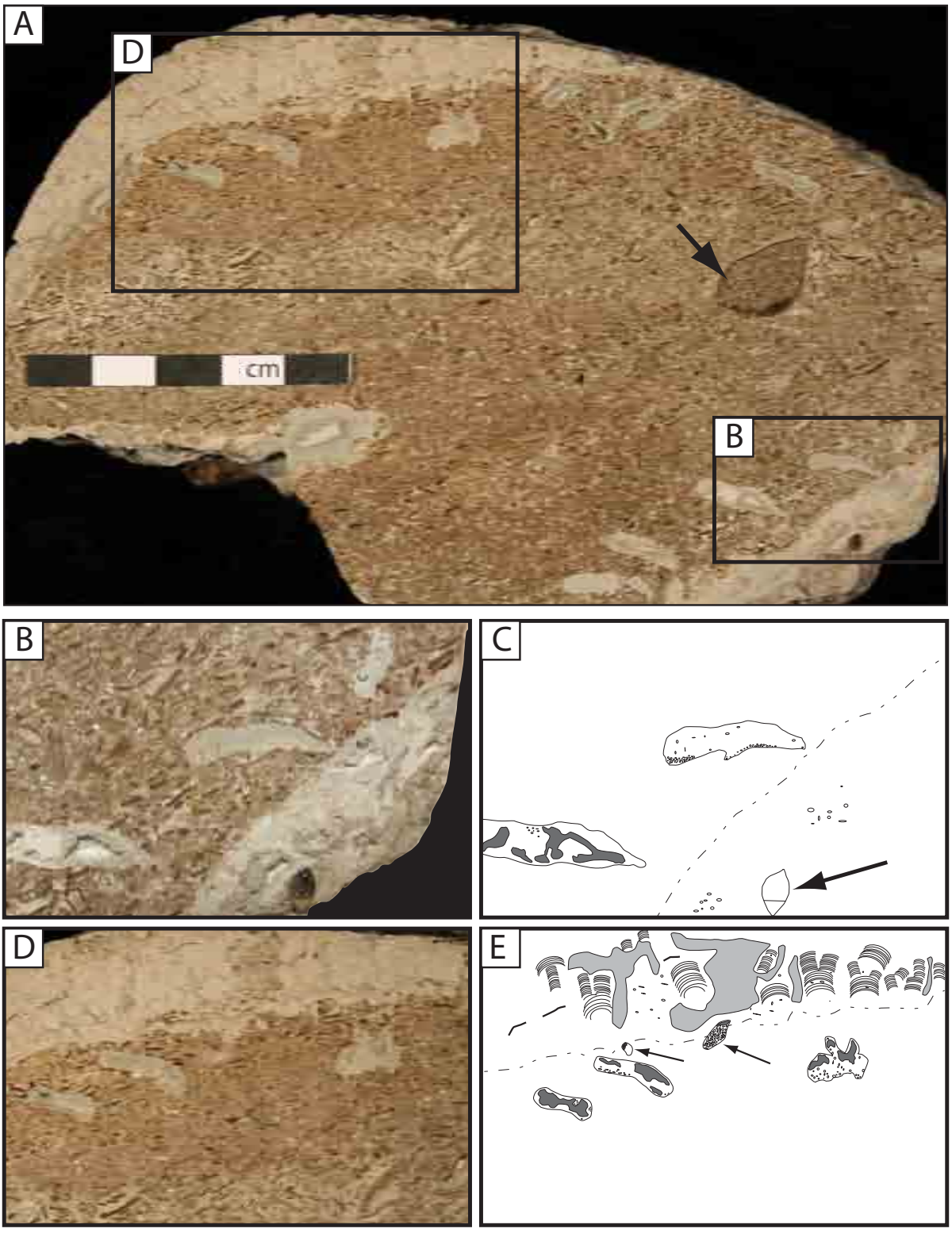


Figure 17. Microbial boundstone facies and associated *gastrochaenolites* borings photographs and overlays. A) Polished hand sample of oolitic grainstone clast encrusted with microbial

boundstone. Boxes show portions enlarged in B and D. Black arrow shows overturned geopetal feature within oolitic grainstone, black cement below grains filling fossil shell. B and C) Close-up photo and line overlay of polished hand sample in A. Lines trace external boundaries of borings within the oolitic grainstone. Dark shaded portions indicate areas in which material was eroded during polishing. Small circles outline grains within the boring fill. Dashed line traces boundary between the oolitic grainstone and the microbial boundstone. Black arrow points to geopetal structure within microbial boundstone. D and E) Close-up photo and line overlay of polished hand sample in A. Lines trace external boundaries of borings. Dark shaded portions indicate areas in which material was plucked during polishing. Small circles outline grains within the boring fill. Dashed line traces boundary between the oolitic grainstone and the microbial boundstone. Light shaded areas represent grain infill between domal microbial features (laminations traced). Black arrows point to borings that cross cut both the microbial boundstone and the oolitic grainstone.

Microbial Boundstone Facies

In the absence of high salinities or other conditions detrimental to grazing organisms, microbial mats are restricted to inter- and supratidal settings (Flügel, 2004). The diverse fossil assemblage found interbedded within the microbial layers, however, are indicative of an environment of normal marine salinity (Heckel, 1972). Ooids present in this facies were most likely transported into the environment as sustained ooid production and deposition would likely terminate microbial deposition. Stromatolites from the Lower Permian of Kansas (Howe Limestone Member, Red Eagle Limestone) show similar domal laminations and are interpreted as shallow-subtidal to intertidal open marine deposits (Shapiro and West, 1999). Stromatolites from the Americus Limestone Member (Lower Permian, Kansas) are subdivided into four nearshore environments by Denver and Kaesler (1992). Of the four environments mentioned as possible, the microbial boundstone facies, described herein, is most similar to the middle to lower intertidal deposits. The lack of desiccation features within the microbial boundstone facies, however, rules out a supratidal or upper intertidal environment where such features are expected to be common. Although the oncolitic packstone contains a more diverse biota, foraminifera in oncolitic coatings are similar to those found in the microbial boundstone, suggesting a similar depositional environment. Lime mudstone, fossil fragment, and ooid-filled *gastrochaenolites* borings crosscut both the microbial layers and underlying deposits thereby indicating that boring organisms were active during deposition. Figure 17 shows a clast with a microbial boundstone coating and *gastrochaenolites* borings near the outer surface of the clast. Variable orientations of way-up indicators within the boundstone and boring fill indicate that the

clast was episodically turned during microbial boundstone formation. The size of the clast (Fig. 15) indicates episodes of high energy current flow.

The similarity to Lower Permian shallow water deposits, lack of subaerial exposure features, and episodic high energy flow suggest a depositional depth range of 1–10 m. The shallow limit assumes a 1 m tidal range, modeled by Wells et al. (2007) and the deep limit assumes the highest energy water to occur within wave base (10 m). Fossil fragments and ooids preserved between the laminations indicate a location that is influenced by open marine water and near an ooid shoal. A probable source of the ooids was the stratigraphically equivalent planar crossbedded oolitic grainstone, deposited in an interpreted water depth of <2–5 m, therefore the depositional depth of the microbial boundstone facies was most likely deeper than 2 m. The stratigraphic location (discussed below) on the flanks of paleohighs, and episodic high energy current flow could indicate formation in a low where currents were focused at times.

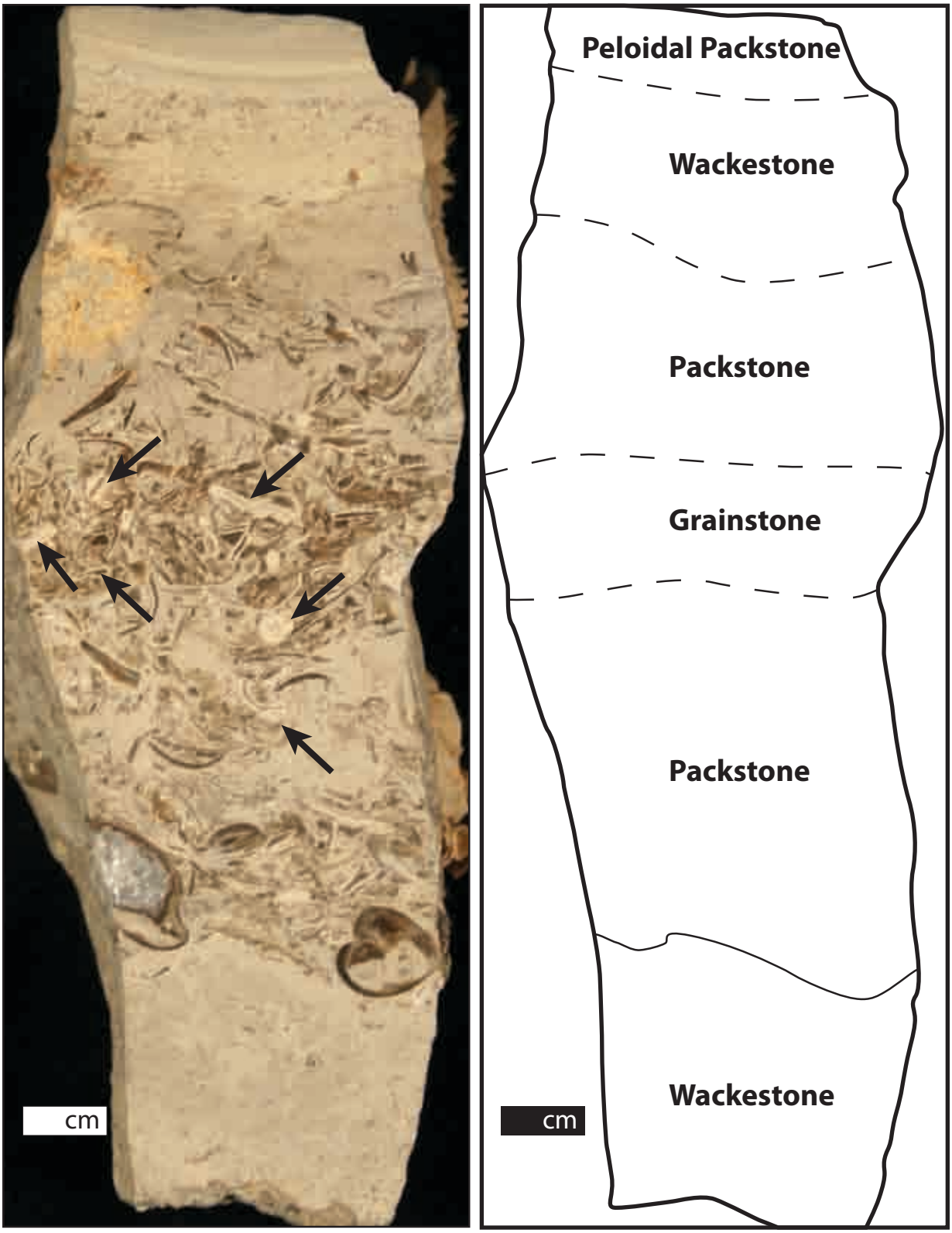


Figure 18. Polished hand sample of coarse-grained packstone facies. Sample shows vertical variation in texture from wackestone (bottom 3 cm), to packstone (next overlying 4 cm), to

grainstone (middle 1.5 cm), to packstone (overlying 2 cm), to wackestone (overlying 2 cm), to peloidal packstone (uppermost 1 cm). Black arrows point to coated grains.

Coarse-Grained Packstone Facies

This facies, contained in one bed, exhibits evidence of fluctuating depositional energies. The lowermost boundary is an erosional surface, evidence of high current energy. Initial deposits have a wackestone texture indicating deposition in a low energy environment. An erosive layer between the lowermost wackestone and overlying packstone and grainstone was caused by an increase in current energy. Large (cm-scale) grains within the packstone and grainstone indicate tractive currents. The gradational upward change from grainstone to packstone to peloidal packstone is indicative of waning flow conditions. The variety of depositional textures within a single bed indicate rapid changes in depositional conditions, in this case, from high energy (erosion), low-energy (lower wackestone) to high-energy (middle packstone and grainstone) back to low energy (laminated peloidal packstone).

According to Flügel (2004), proximal storm beds can be composed of an erosive surface overlain by a basal coarse-grained lag layer, followed by a central well-sorted and matrix-poor calcisiltite and an upper fine-grained rippled calcilutite. The middle coarse grained portion of this facies (packstone and grainstone) partially fits the basal coarse-grained lag layer and central well-sorted and matrix-poor criteria. Although the upper portion does not contain any ripples, sedimentary structures in this portion may have been destroyed by burrowing organisms before deposition of the overlying peloidal packstone. The bottom wackestone portion of the bed is attributed to be a remnant of prior storm events and the uppermost portion is a transition to intertidal deposition.

Deposition of this bed occurs between intertidal and supratidal deposits and is assumed to be deposited at similar depths. It is possible that deposition occurred under a greater water depth as storm surges temporarily raise mean sea level (Flügel, 2004).

## STRATIGRAPHIC CORRELATIONS AND SEQUENCE-STRATIGRAPHIC INTERPRETATIONS

The stratigraphic correlations presented below are displayed graphically in cross sections (Fig. 19–21) and a fence diagram (Fig. 22) that show data collected from stratigraphic description of eighteen outcrops and one drill core. They are used to interpret a genetic stratigraphy for the Westerville and associated units (Wea Shale, Nellie Bly Formation, and the Quivira Shale). This stratigraphy is based on a datum (Surface A), which was used for reasons discussed in the next section. The Wea Shale is separated from the overlying Westerville by Surface B. The Westerville is subdivided into three genetic intervals (W1, W2 and W3). These intervals are truncated by surfaces C, D and E respectively. Surface E separates the Westerville from the overlying Nellie Bly Formation and Quivira Shale.

The following description and interpretation of facies and stratigraphic relationships is intended to identify facies shifts and stratigraphic surfaces that indicate relative rises and falls of sea level. Interpretations of facies and surfaces were used to develop water-depth curves for representative stratigraphic sites 13 and 16 to illustrate the water-depth history during deposition (Fig. 23 and 24). Sites 13 and 16 were chosen because both sections are thought to preserve a nearly complete record for the Westerville. Also, site 13 is laterally extensive (over 2 km in

length) and geographically close to the other exposures in Kansas. Whereas site 16, although small in exposure length, is proximal to many outcrops in Missouri (Fig. 1). Evaluating the water depth histories of the two areas independently allows for the quantitative measurement of relief on paleosurfaces while minimizing any errors in the datum related to the regional westerly dip of 4.7 m/km (Watney, 1999) and differential compaction. Sites 13 and 16 were also chosen because site 13 overlies a relatively thin portion of the Wea Shale and site 16 a thicker portion. So, even though the datum may not reflect exact paleotopography, it is assumed that site 13 occupied a relatively downdip location compared to site 16 (Fig. 21). The genetic relationships interpreted in the following section are compiled to progressively build two water-depth curves for the study area. The interpretation of water-depth history allows other factors that influence sedimentation to be explored. These factors include the evolution of depositional topography and siliciclastic influx. Data for their evaluation are isopach maps for stratigraphic units (Fig. 25, 26 and 27), which were constructed from thickness values measured in the field, gamma-ray logs, water well Kansas Geological Survey reports, and data reported in Sullivan (1969).

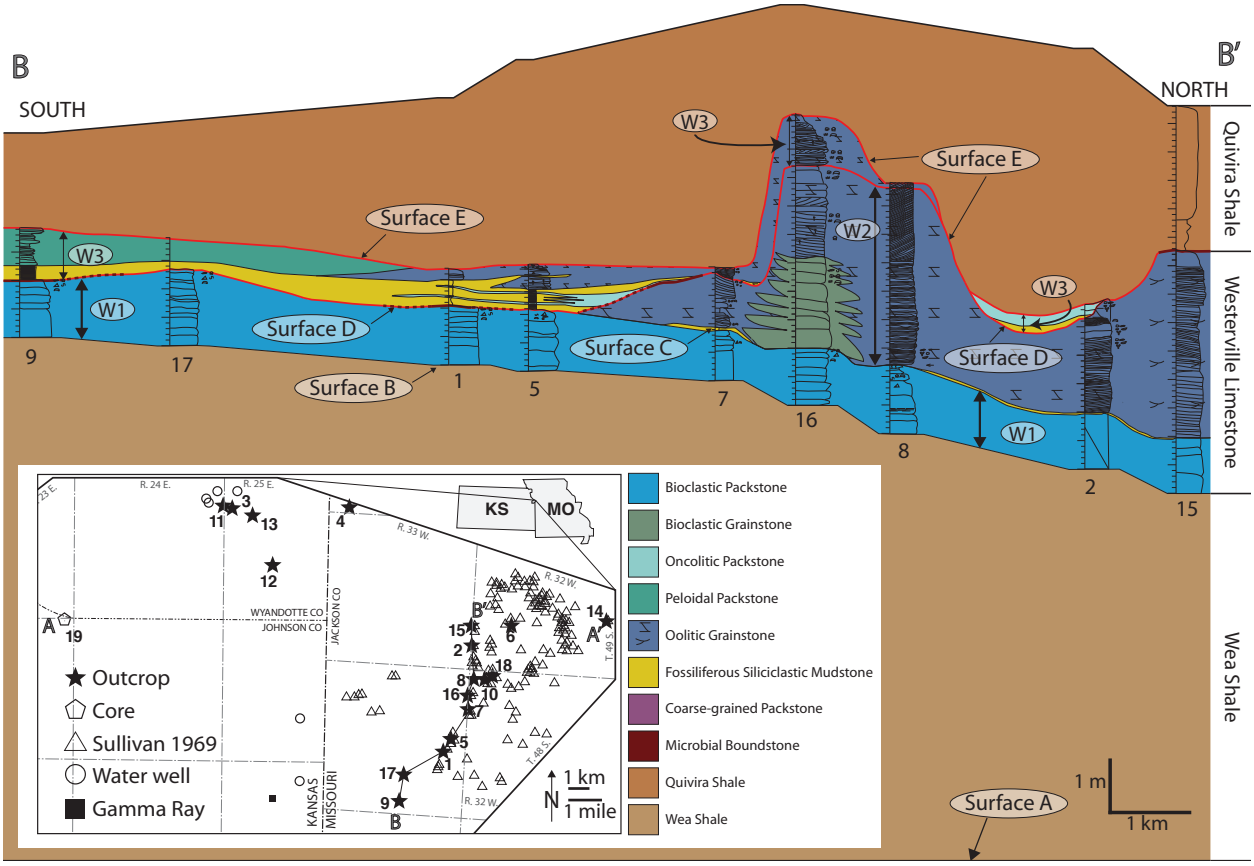


Figure 19. South to north stratigraphic cross section from B at site 9 to B' at site 15. Colored areas represent facies (see inset map). Cross section is hung on Surface A, which is the base of the Wea Shale.

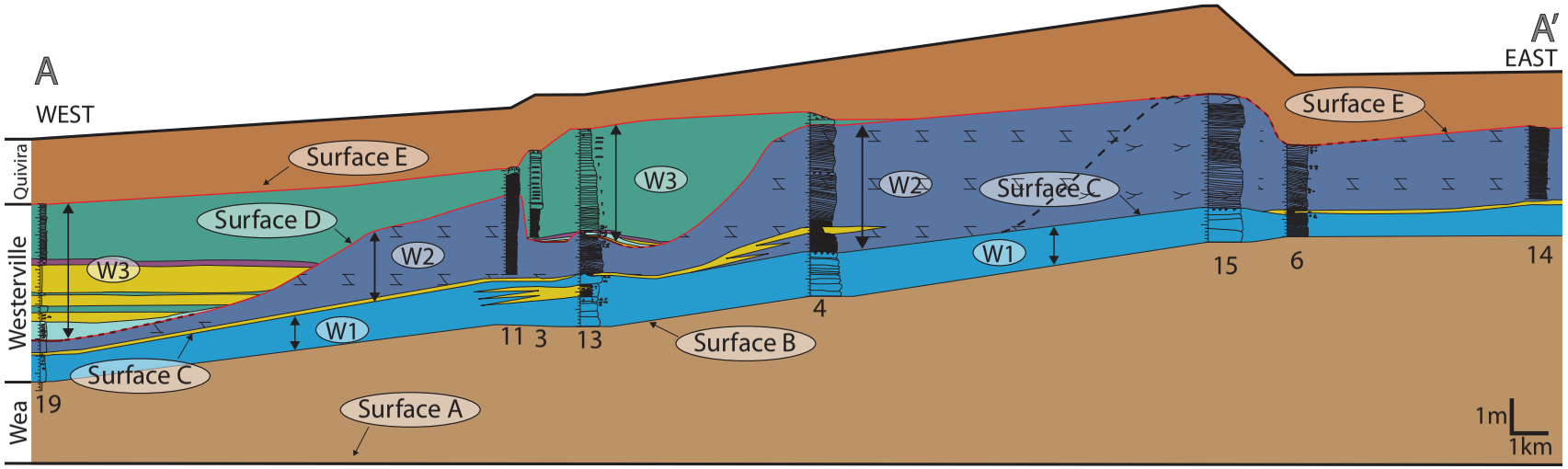
A
WEST
A′
EAST
Quivira
Westerville
Wea
Surface E
Surface D
Surface C
Surface A
Surface B
W1
W2
W3
19
11
3
13
4
15
6
14
1m
1km

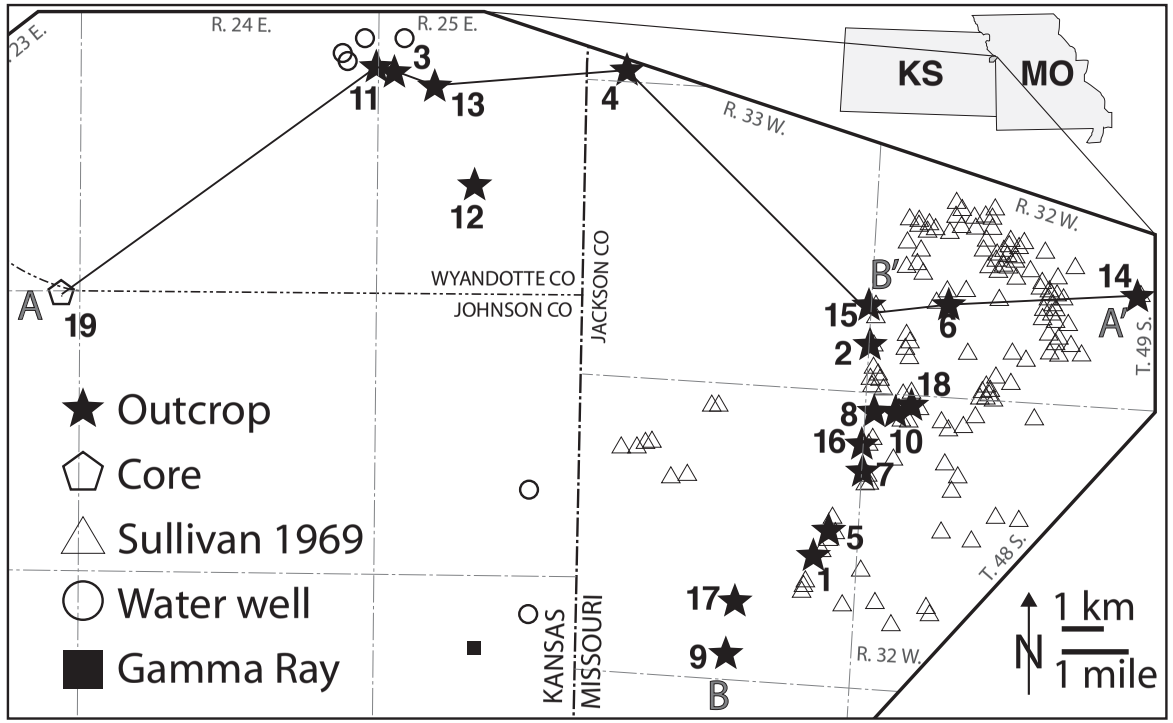
R. 24 E.
R. 25 E.
R. 33 W.
R. 32 W.
KS
MO
WYANDOTTE CO
JOHNSON CO
JACKSON CO
KANSAS
MISSOURI
T. 49 S.
T. 48 S.
A
A′
B
B′
Outcrop
Core
Sullivan 1969
Water well
Gamma Ray
1 km
1 mile
N

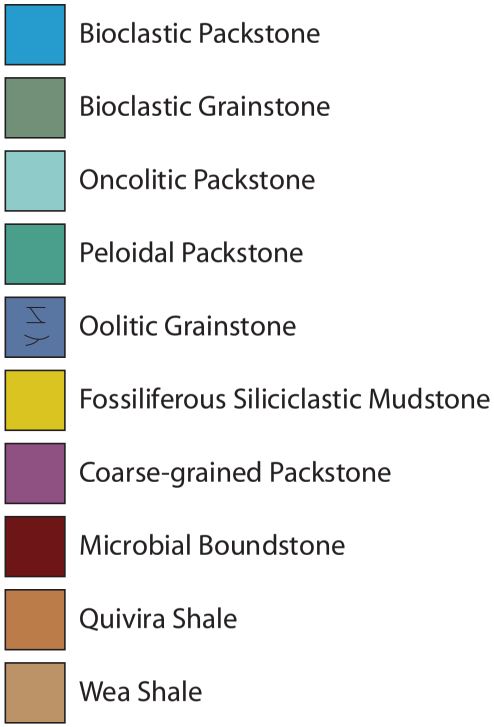
Bioclastic Packstone
Bioclastic Grainstone
Oncolitic Packstone
Peloidal Packstone
Oolitic Grainstone
Fossiliferous Siliciclastic Mudstone
Coarse-grained Packstone
Microbial Boundstone
Quivira Shale
Wea Shale

Figure 20. West to east stratigraphic cross section from A at Deffenbaugh core (19) to A' at site 14 (see inset map). Cross section is hung on Surface A, the base of the Wea Shale.

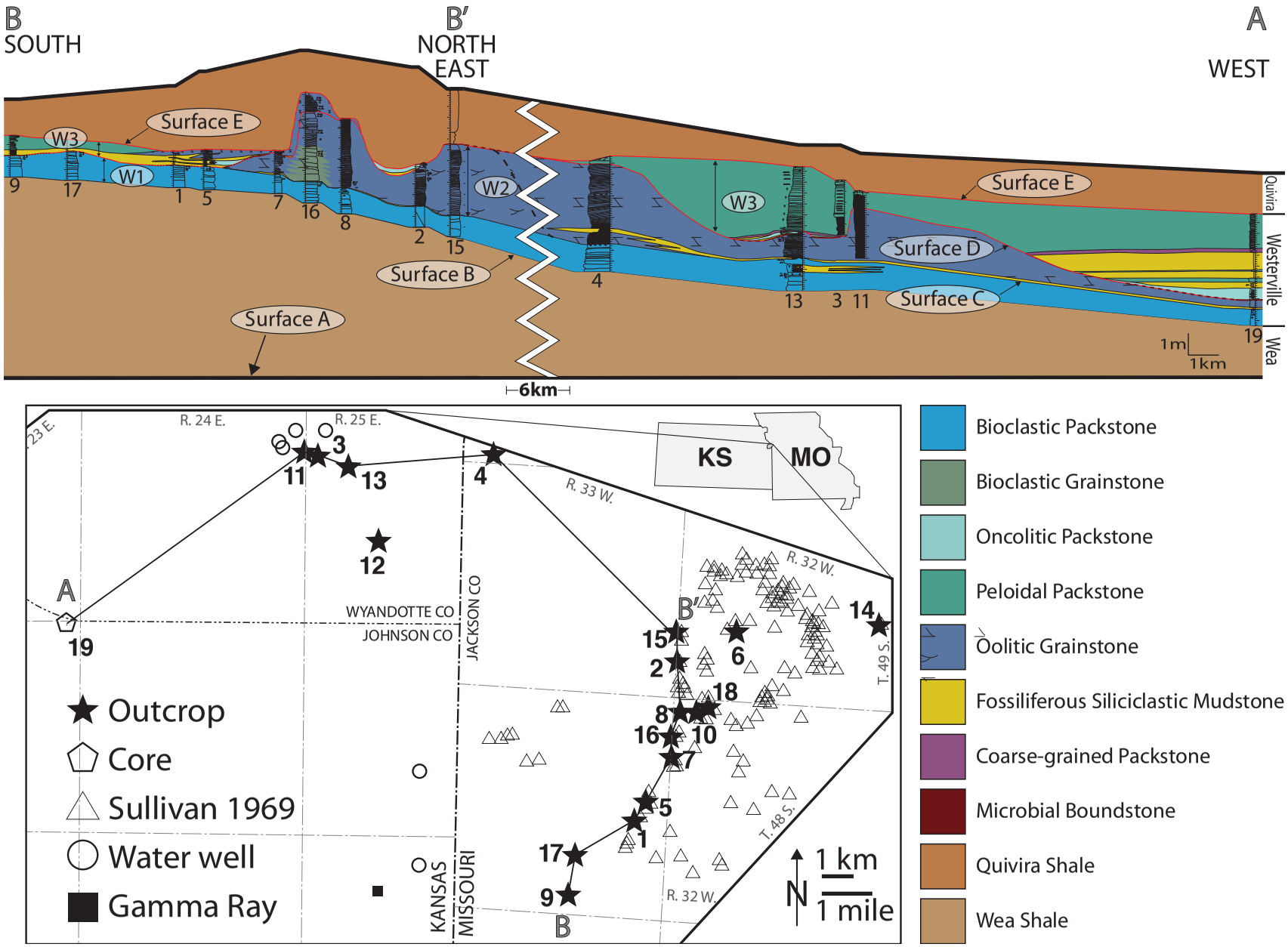
B
SOUTH
B′
NORTH
EAST
A
WEST
Surface E
W3
W1
W2
Surface B
Surface A
Surface D
Surface C
Quivira
Westerville
Wea
1m
1km
6km
R. 24 E.
R. 25 E.
R. 33 W.
R. 32 W.
KS
MO
WYANDOTTE CO
JOHNSON CO
JACKSON CO
T. 49 S.
T. 48 S.
KANSAS
MISSOURI
Outcrop
Core
Sullivan 1969
Water well
Gamma Ray
1 km
1 mile
N
Bioclastic Packstone
Bioclastic Grainstone
Oncolitic Packstone
Peloidal Packstone
Oolitic Grainstone
Fossiliferous Siliciclastic Mudstone
Coarse-grained Packstone
Microbial Boundstone
Quivira Shale
Wea Shale

Figure 21. Combined stratigraphic cross sections shown in Figures 19 and 20. White zig-zag represents 6 km gap. Orientation of cross section line was chosen to illustrate facies associations and stratal geometries within the Westerville that occur over the laterally variable thickness (thinning from left to right) of the underlying Wea Shale.

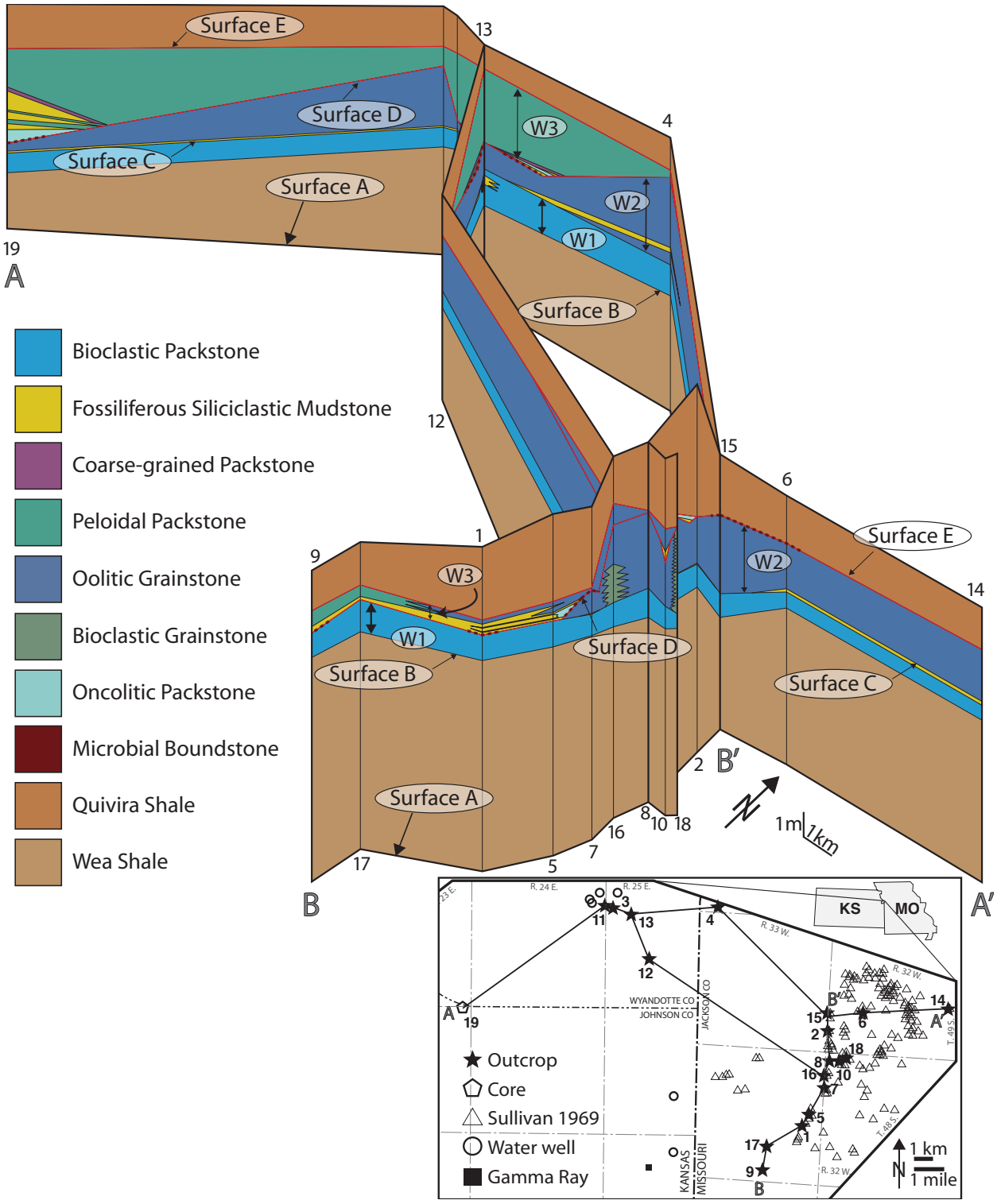


Figure 22. Fence diagram that includes all outcrop and core sites.

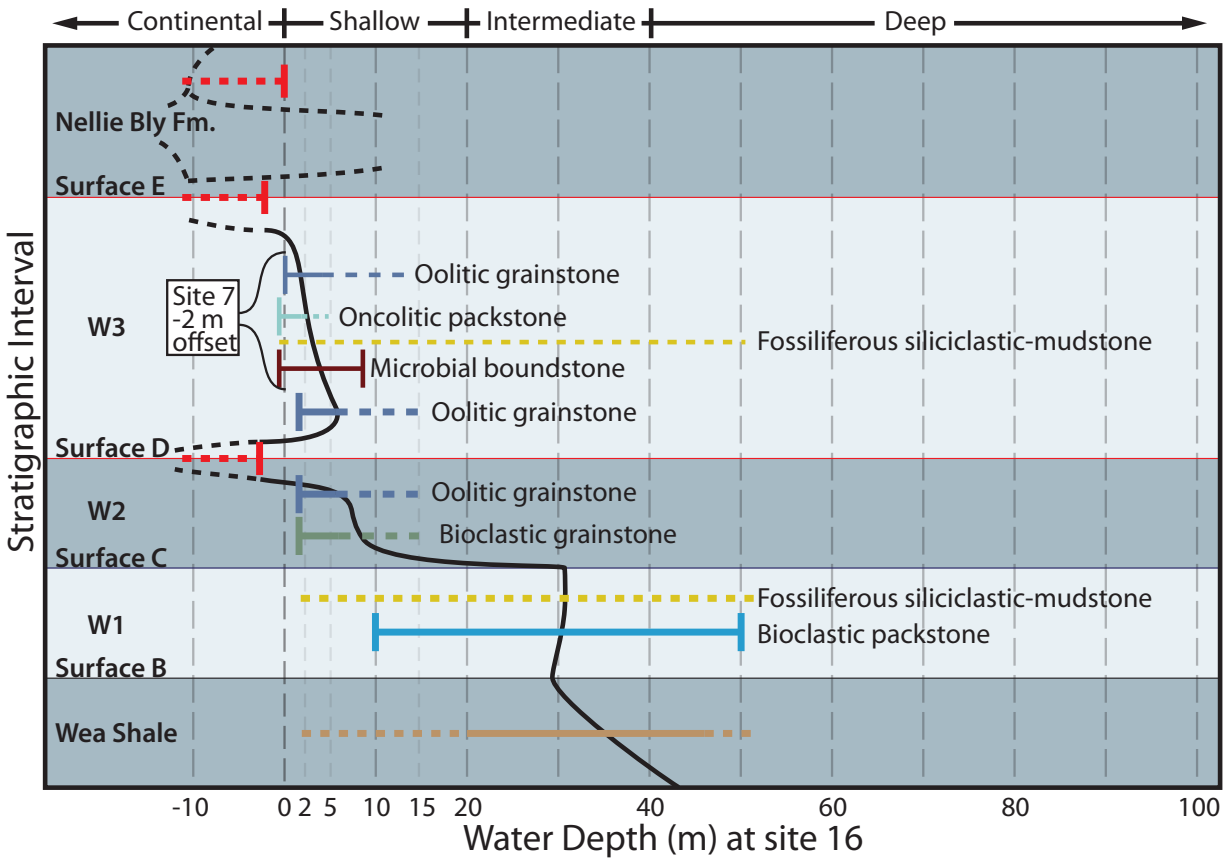


Figure 23. Interpreted water-depth curve for the Westerville and associated units at site 16. Horizontal axis is water depth in meters and the vertical axis is time in a relative sense with the oldest unit at the base. Curve is constrained by facies interpretation. Error bar color is designated by facies type. Dashed portions of curve and error bars indicate no quantitative constraining criteria.

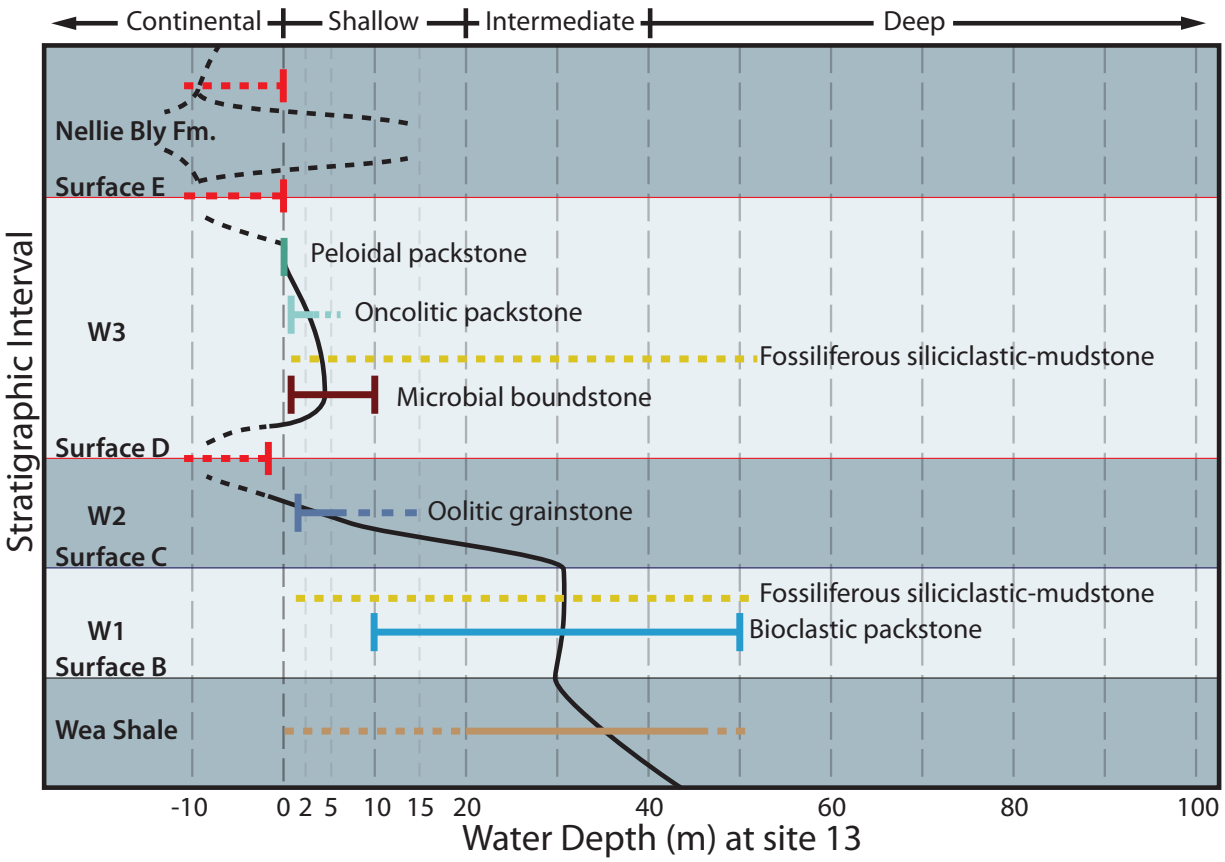


Figure 24. Interpreted water-depth curve for the Westerville and associated units at site 13. Horizontal axis is water depth in meters and the vertical axis is time in a relative sense with the oldest unit at the base. Curve is constrained by facies interpretation. Error bar color is designated by facies type. Dashed portions of curve and error bars indicate no quantitative constraining criteria.

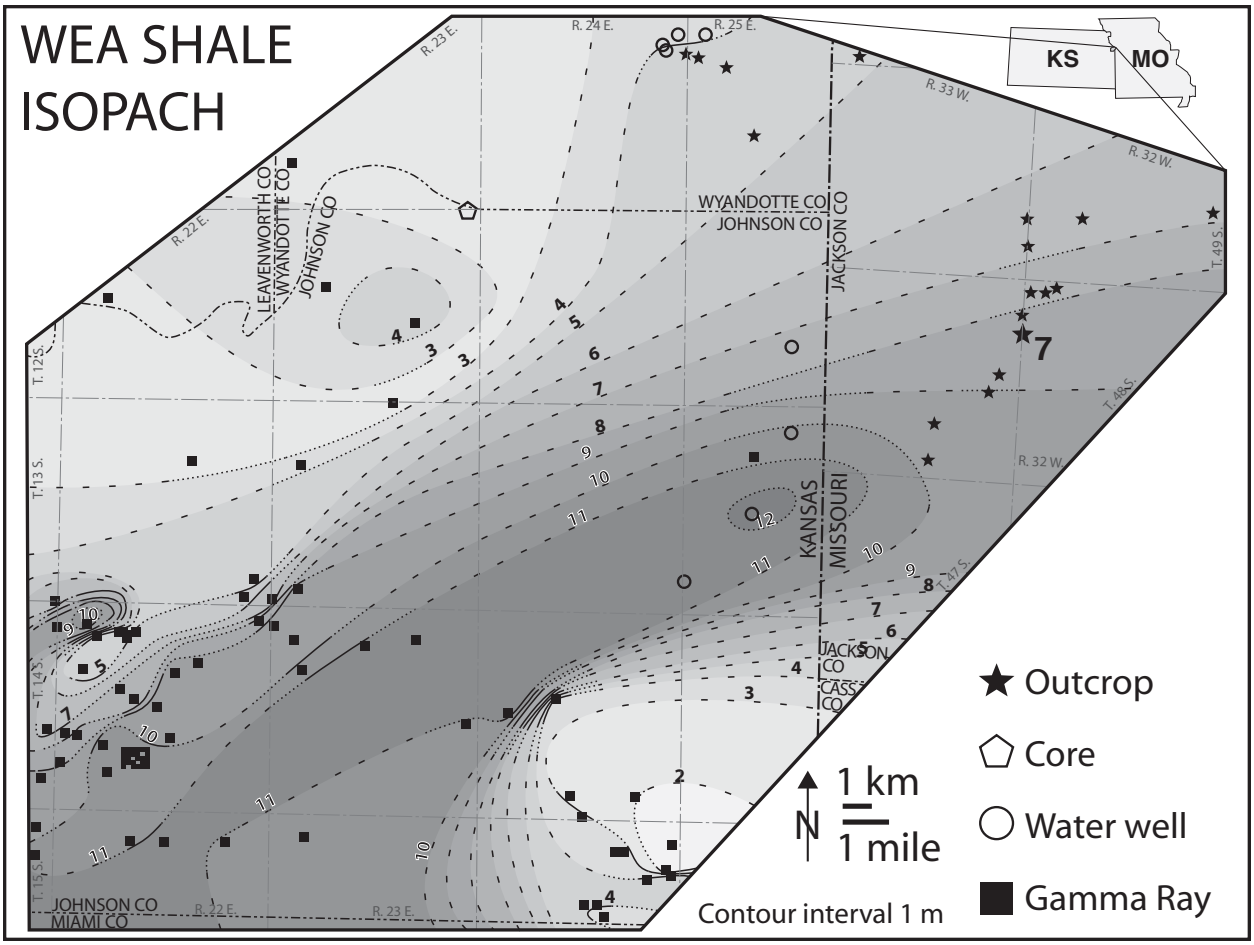


Figure 25. Isopach of Wea Shale. Dark areas are thicker than light areas. If the base of the Wea Shale was flat, then the Wea shale forms a generally flat-topped wedge of sediment with sloped margins. Notice a general thinning to the north and west where the Westerville crops out (stars) and gentle slope near site 7. Contour interval is 1 meter. Solid lines used in areas of highest data concentration. Dashed lines used in areas where data are less concentrated.

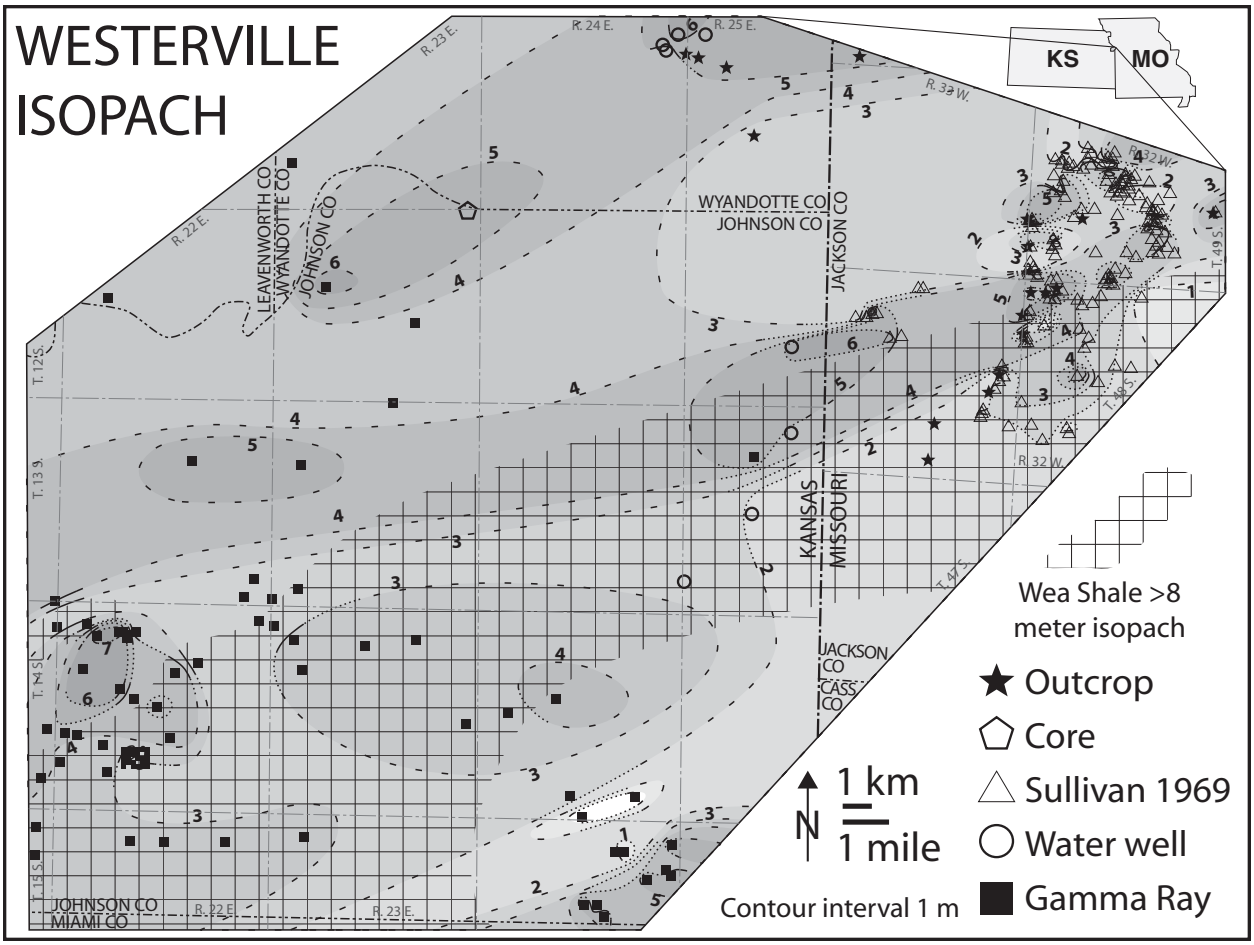


Figure 26. Isopach map for the Westerville Limestone. Cross hatching denotes area where underlying Wea Shale is at least 8 m thick (Fig. 25). Thicker portions (>5 m) of the Westerville correlate with the northern flank of an underlying thick area in the Wea Shale (Fig. 21). Also Westerville thickness variation increases with the concentration of data, indicating that areas between data points are likely to have more variable relief than represented here. Contour interval is 1 meter. Solid lines used in areas of highest data concentration. Dashed lines used in areas where data is less concentrated.

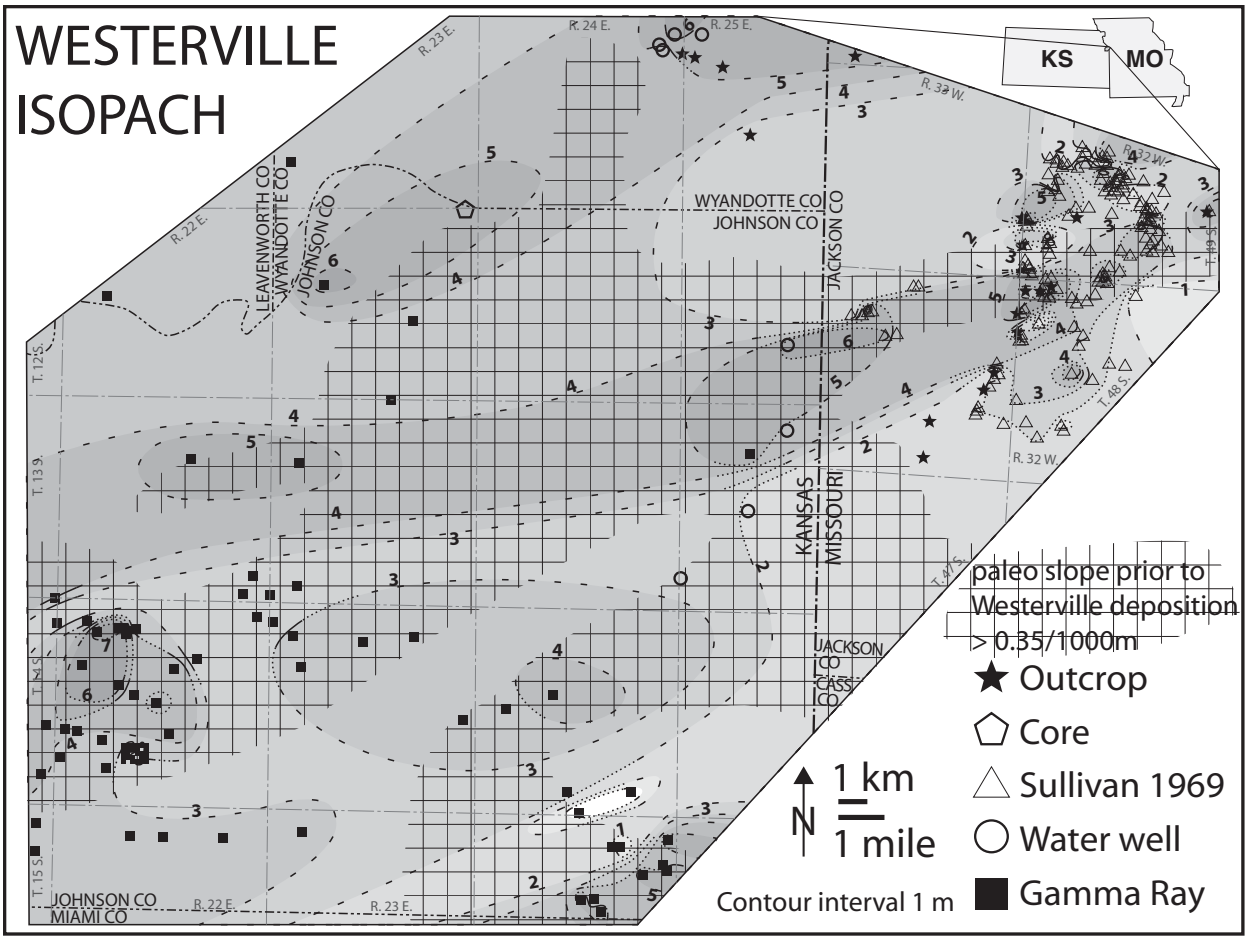


Figure 27. Isopach map for the Westerville Limestone. Cross hatching denotes area where underlying Wea Shale has a slope of 0.35 cm/1000m or greater (Fig 25). Thickest portions of the Westerville Limestone correlate with cross hatched area of steep slope. Contour interval is 1 meter. Solid lines used in areas of highest data concentration. Dashed lines used in areas where data is less concentrated.

## Stratigraphic Datum (Surface A)

The uppermost surface of the Block Limestone (base of the Wea Shale) is used as a stratigraphic datum for this study. The Block Limestone is the fossiliferous marine flooding unit of the Cherryvale Sequence (Watney et al.,1989). It has both a consistent lithologic character and thickness throughout the field area and is interpreted to have been deposited on a relatively flat surface (Heckel, 1999).

Although, differential compaction, chemical dissolution, and structural elements could have affected the strata in the study area, including a regional westerly dip of 4.7 m/km (Watney, 1999; Tucker, 2001), the uppermost surface of the Block Limestone appears to be the best choice for a stratigraphic datum for this study. The horizontal nature of bedding at outcrop scale (at least 400 m in most exposures), and consistent thickness and texture throughout the study area suggest that the current preservation of the top of the Block Limestone is a close approximation of relatively flat depositional topography. Preserved way-up indicators and geopetal features (Fig. 9H), within the Westerville indicate minimal deformation beyond the regional westerly dip.

## Wea Shale

The Wea Shale overlies the Block Limestone. Although not a focus of the study, the Wea Shale thickness was measured from outcrop and wireline-log data (Fig. 25). The Wea Shale was originally designated as an outside shale capping the Dennis Megacyclothem (Moore, 1949). It was later “questionably designated” as a phantom core shale based on a moderately high conodont abundance, although it lacked the three main conodonts normally ascribed to core

shales (Heckel and Baesemann, 1975). Composed of sparsely fossiliferous siliciclastic-mudstone and -siltstone, it was later referred to as a regressive shale (Heckel, 1999).

Unit thickness is variable (1.2–12.2 m). If the chosen datum was indeed a flat surface, the thickest portion of the Wea Shale formed an elongate, flat-topped, topographic feature, which is thickest to the southwest and thinnest to the north and northeast (Fig. 25). The thickness variability is most likely a product of sediment input from the south and not post depositional erosion (see Surface B). Lowland areas to the south have been described as sourcing siliciclastic sediment, during and after the stratigraphically equivalent Drum Limestone in southern Kansas (Stone, 1984), so a southern source for the Wea Shale makes sense.

The Wea Shale is interpreted to be a marine deltaic deposit originating south of the field area because of the south-to-north transition from thick-to-thin deposits and the conformable overlying surface with the Westerville. The nature of deltaic deposits makes any fluctuation of relative sea level during deposition difficult to determine. Sediment thickness variations could be from an autogenic process (e.g. product of distant lobe switching or progradation), or result from an allogenic process, such as shoreline encroachment as sea level falls. The Wea Shale is underlain by a transgressive limestone and overlain by a carbonate facies consisting of light dependent marine organisms requiring deposition in the photic zone and an interpreted depth of 10–50 m (discussed in a later section). Upward decrease in conodont abundance and diversity suggests a general shallowing trend from deposition of the Block Limestone through the Wea Shale (Heckel and Baesemann, 1975)(Fig. 4). Therefore, it seems reasonable to interpret that the Wea Shale was deposited after a sea-level highstand and during a relative fall in sea level (Fig. 28). Water-depth estimates for resulting shallowing are based on interpreted water depth for the

immediately overlying stratigraphic interval (W1). The placement of the shallowing trend is the same for the Wea Shale in both of the constructed water-depth curves (Figs. 23 and 24).

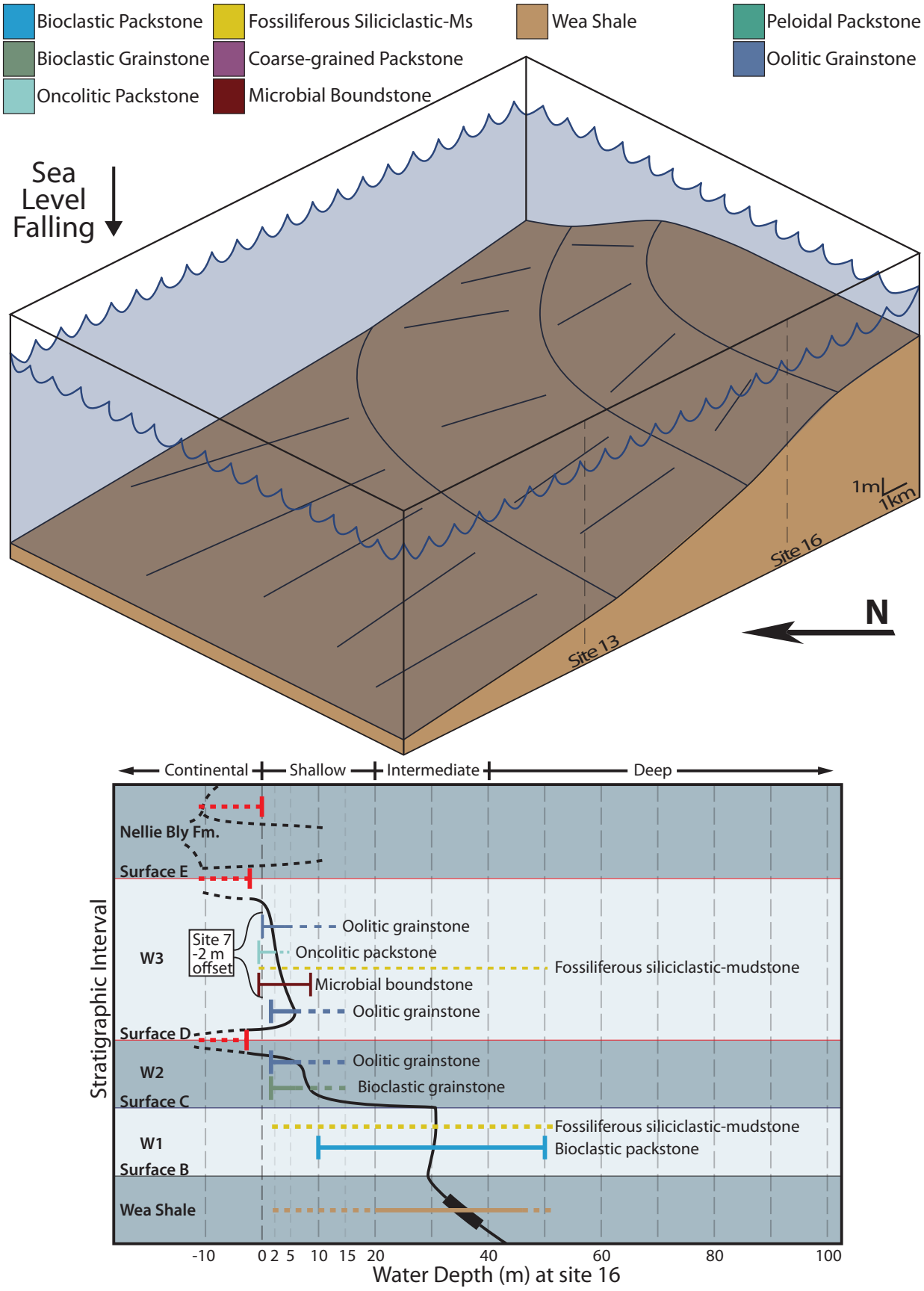
Bioclastic Packstone
Bioclastic Grainstone
Oncolitic Packstone
Fossiliferous Siliciclastic-Ms
Coarse-grained Packstone
Microbial Boundstone
Wea Shale
Peloidal Packstone
Oolitic Grainstone
Sea Level Falling
1m
1km
Site 16
Site 13
N
Continental
Shallow
Intermediate
Deep
Nellie Bly Fm.
Surface E
W3
Site 7 -2 m offset
Oolitic grainstone
Oncolitic packstone
Fossiliferous siliciclastic-mudstone
Microbial boundstone
Oolitic grainstone
Surface D
W2
Oolitic grainstone
Bioclastic grainstone
Surface C
W1
Fossiliferous siliciclastic-mudstone
Bioclastic packstone
Surface B
Wea Shale
Stratigraphic Interval
-10
0 2 5
10
15
20
40
60
80
100
Water Depth (m) at site 16

Figure 28. Block diagram illustrating the interpreted depositional environment during deposition of the Wea Shale. The water column is cloudy due to siliciclastic deposition. Locations of sites 13 and 16 placed in relation to thickness of underlying Wea Shale.

## Surface B

Surface B separates the Wea Shale from the overlying Westerville (Fig. 19–21). Wea Shale outcrops are typically covered with vegetation making it difficult to see the uppermost contact with the overlying Westerville. Although difficult to completely rule out a marine erosional contact (or even subaerial exposure) separating the Wea Shale from the Westerville, there are no truncated beds where the contact is visible. The lowermost Westerville deposits (Interval W1 described in the next section) are interpreted to have been deposited in a low energy environment in a water depth range of 10–50 m. It seems reasonable, therefore, to represent Surface B as a conformable contact, assume a similar water depth for the uppermost Wea Shale and lowermost Westerville deposits, and not show any sea-level fluctuations at the transition between the Wea Shale and Westerville at both sites 13 and 16 (Fig. 23 and 24).

## Westerville Limestone Member

### Interval W1

Interval W1 (Fig. 19–21) is the lower part of the Westerville. The thickness of Interval W1 is relatively consistent throughout the field area, typically ~1 m, but with a range of 0.6–1.3 m (Fig. 19–21). On outcrop the upper surface of the interval is typically flat except at site 13, where there is dm-scale relief across a 2 m wide dome-shaped feature. All bioclastic packstone beds within the dome-shaped feature are of consistent thickness. Interval W1 is composed of bioclastic packstone and fossiliferous siliciclastic-mudstone. Facies relationships within the interval are shown schematically in Figure 8. The interval typically consists of ~1 m of bioclastic packstone overlain by a thin (<5 cm) deposit of fossiliferous siliciclastic-mudstone.

The bioclastic packstone is bioturbated throughout and the uppermost 15–20 cm have open burrows filled with siliciclastic material. In places there is visible truncation of both fossiliferous siliciclastic-mudstone and bioclastic packstone (Fig. 9A–D). A significant amount (5–10 cm thick bed) of fossiliferous siliciclastic-mudstone is interbedded and has a gradational lateral contact with bioclastic packstone at site 13 (Fig. 20 and 21).

The bioclastic packstone facies present at the bottom of Interval W1 is interpreted to have been deposited in an open-marine subtidal environment (below fair-weather wave base) within the photic zone (10–50 m water depth). The fossiliferous siliciclastic-mudstone deposits, which intertongue with the bioclastic packstone at site 13 and form the uppermost portion of Interval W1 at sites 2, 7, and 8, are interpreted as isolated influxes of siliciclastic material into the area. The small dome-shaped feature at site 13 is likely relief inherited from minor relief present on the underlying Wea Shale as all the beds within the dome-shaped feature are of consistent thickness.

As with the underlying Wea Shale, evidence for relative sea-level change during the Interval W1 is lacking. It is possible that the termination of siliciclastic input into the area, ending Wea Shale deposition, created conditions more conducive to carbonate deposition without a change in sea level. Decreased water turbidity allowed light-dependent organisms to flourish. Even light independent organisms would benefit as their potential burial by siliciclastic input would cease. A minor transgression could account for a decrease in water turbidity as the source of siliciclastic input would become more distal (Fig. 29). Conodont diversity and abundance data suggests a minor transgression at the base of the Westerville (the bioclastic packstone portion of Interval W1) after a general regression during deposition of the Wea Shale (Heckel

and Baesemann, 1975; Heckel, 1999)(Fig. 4). The Interval W1 portion of the water-depth curves for both site 13 and 16 show this minor transgression (Fig. 23 and 24).

The siliciclastic input during the end of Interval W1 is interpreted as distal deltaic deposits and the influx of fine-grained siliciclastic material would have increased water turbidity and decreased the amount of light dependent carbonate production. As carbonate production ceased, open burrows were filled with the incoming siliciclastic material (Fig. 30).

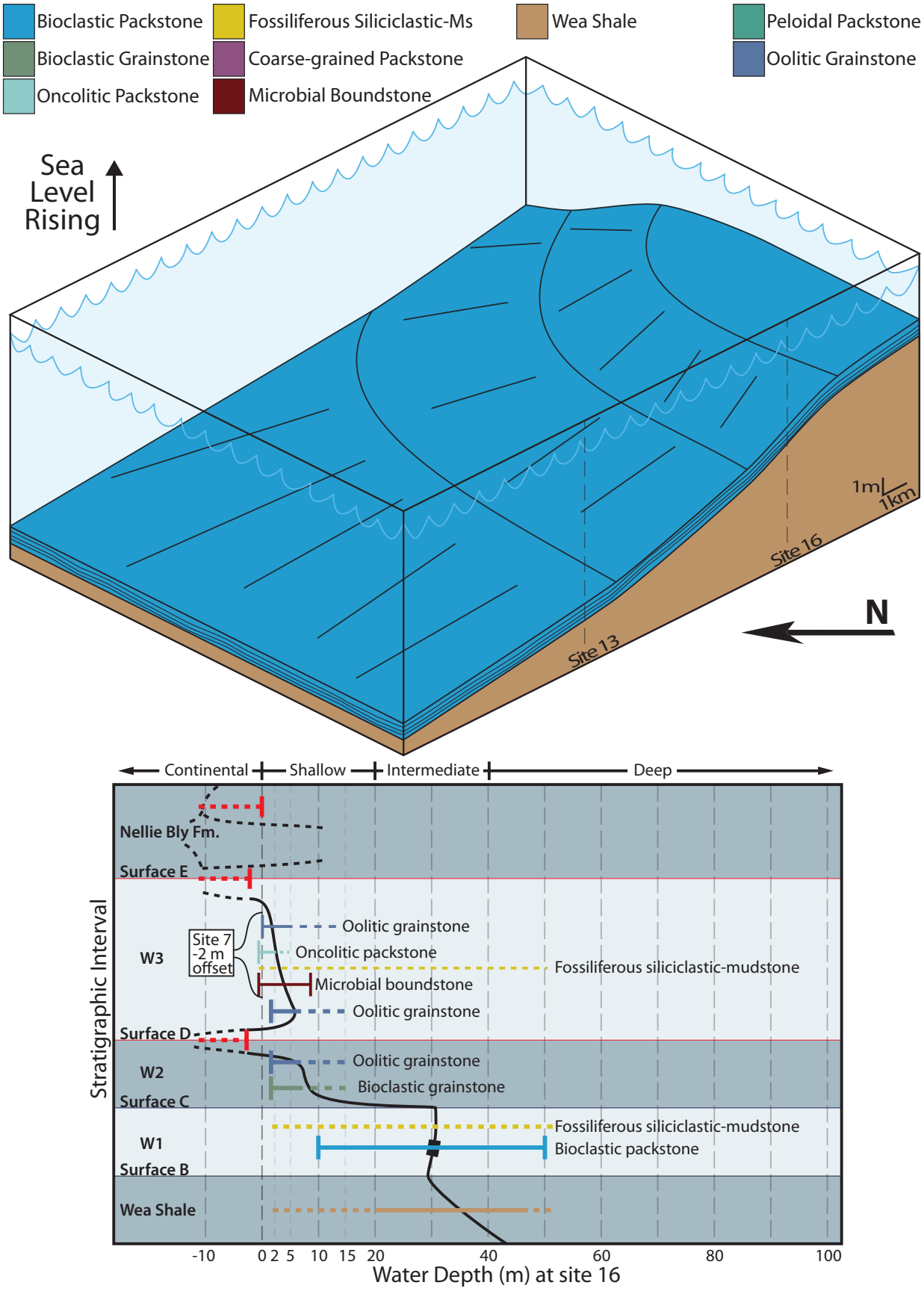
Bioclastic Packstone
Bioclastic Grainstone
Oncolitic Packstone
Fossiliferous Siliciclastic-Ms
Coarse-grained Packstone
Microbial Boundstone
Wea Shale
Peloidal Packstone
Oolitic Grainstone
Sea Level Rising
1m
1km
Site 16
Site 13
N
Continental
Shallow
Intermediate
Deep
Nellie Bly Fm.
Surface E
W3
Site 7 -2 m offset
Oolitic grainstone
Oncolitic packstone
Microbial boundstone
Oolitic grainstone
Fossiliferous siliciclastic-mudstone
Surface D
W2
Oolitic grainstone
Bioclastic grainstone
Surface C
W1
Fossiliferous siliciclastic-mudstone
Bioclastic packstone
Surface B
Wea Shale
Stratigraphic Interval
-10
0 2 5
10
15
20
40
60
80
100
Water Depth (m) at site 16

Figure 29. Block diagram illustrating the interpreted depositional environment during the early stages of Interval W1. Bioclastic packstone is deposited throughout the area, blanketing underlying topography during deepening water depth. Locations of sites 13 and 16 placed in relation to thickness of underlying Wea Shale.

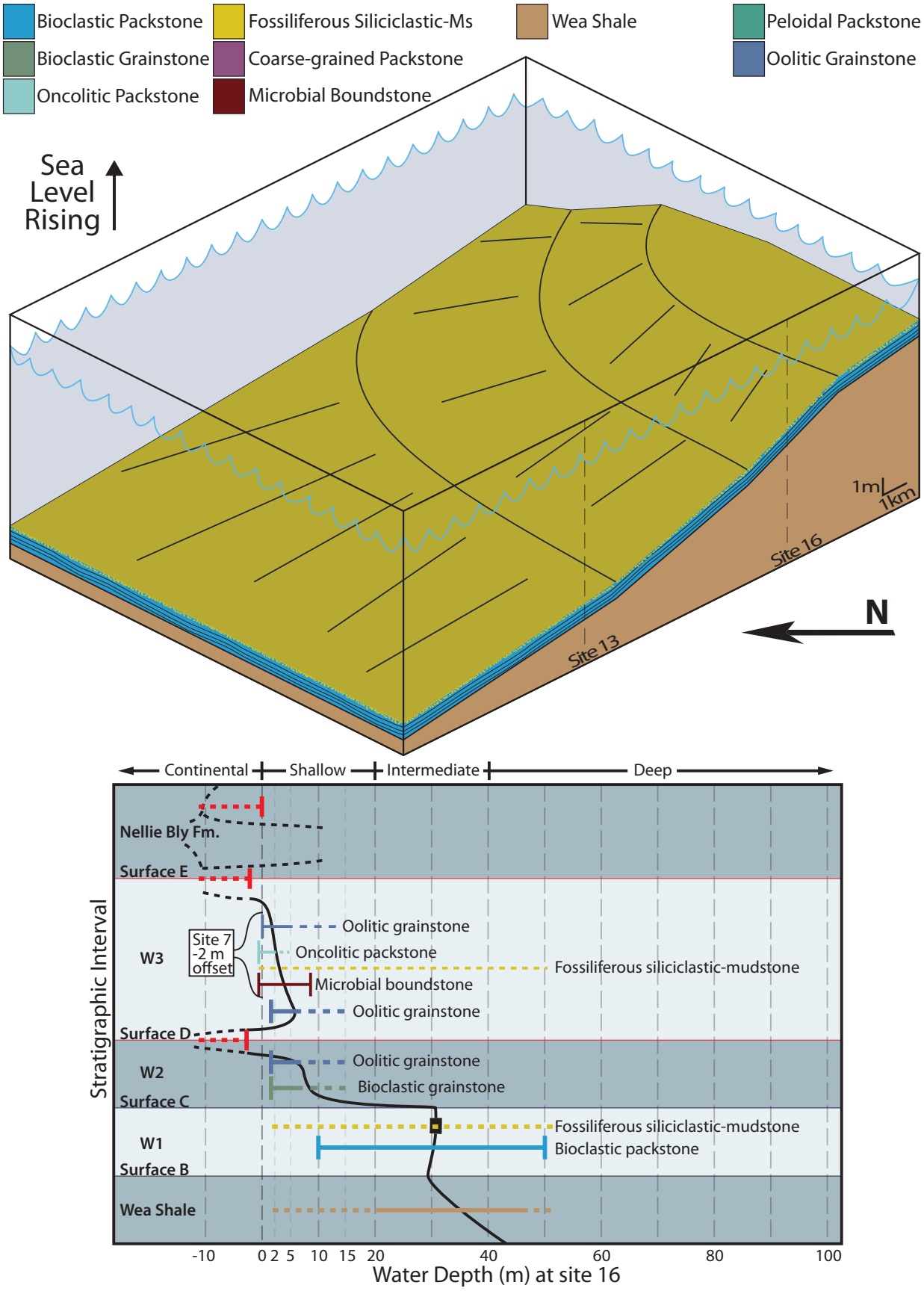
Bioclastic Packstone
Bioclastic Grainstone
Oncolitic Packstone
Fossiliferous Siliciclastic-Ms
Coarse-grained Packstone
Microbial Boundstone
Wea Shale
Peloidal Packstone
Oolitic Grainstone
Sea Level Rising
1m
1km
Site 16
Site 13
N
Continental
Shallow
Intermediate
Deep
Nellie Bly Fm.
Surface E
W3
Site 7 -2 m offset
Oolitic grainstone
Oncolitic packstone
Fossiliferous siliciclastic-mudstone
Microbial boundstone
Oolitic grainstone
Surface D
W2
Oolitic grainstone
Bioclastic grainstone
Surface C
W1
Fossiliferous siliciclastic-mudstone
Bioclastic packstone
Surface B
Wea Shale
Stratigraphic Interval
-10
0 2 5
10
15
20
40
60
80
100
Water Depth (m) at site 16

Figure 30. Block diagram illustrating the interpreted depositional environment during the final stages of Interval W1. Fossiliferous siliciclastic-mudstone deposition blankets the entire area. Locations of sites 13 and 16 placed in relation to thickness of underlying Wea Shale.

Surface C

Surface C truncates Interval W1 deposits (Fig. 19–21). Up to 80 cm of truncation is evident locally in outcrop (site 7, Fig. 31). Where the truncation is greater than 15 cm there are no open burrows in the underlying Interval W1 bioclastic packstone.

Surface C is interpreted to be a marine truncation surface, as there is no evidence of alteration from subaerial exposure. The most obvious evidence for erosion is at site 7 (Fig. 31), where a channel-shaped feature, 100 m wide and up to 80 cm deep, cuts through Interval W1 deposits. Site 7 is located (Fig. 21) on the northeastern edge of the relatively flat-topped area above a thickened Wea Shale (Fig. 25), and the channel-shaped feature is oriented 25 degrees from north and the dip-slope on the edge of the Wea Shale at site 7 is oriented 350 degrees from north. Thus, the paleochannel can be considered to be near parallel (35 degree difference) to paleoslope. It is possible that tidal forces around site 7 were accelerated at the edge of the flat-topped, low-relief area and eroded the underlying substrate (Interval W1). Gomez-Perez et al. (1997) proposed a similar scenario for the stratigraphically equivalent Drum Limestone in southern Kansas, except that there, the channel features form in the underlying Cherryvale Shale, which may be equivalent to the Wea Shale.

In contrast to Interval W1 deposits, Interval W2 deposits overlying Surface C were deposited in a high-energy shallow marine environment. Erosion along Surface C, therefore, is most easily explained with marine erosion associated with shallowing from Interval W1 to Interval W2 (Fig. 23 and 24).

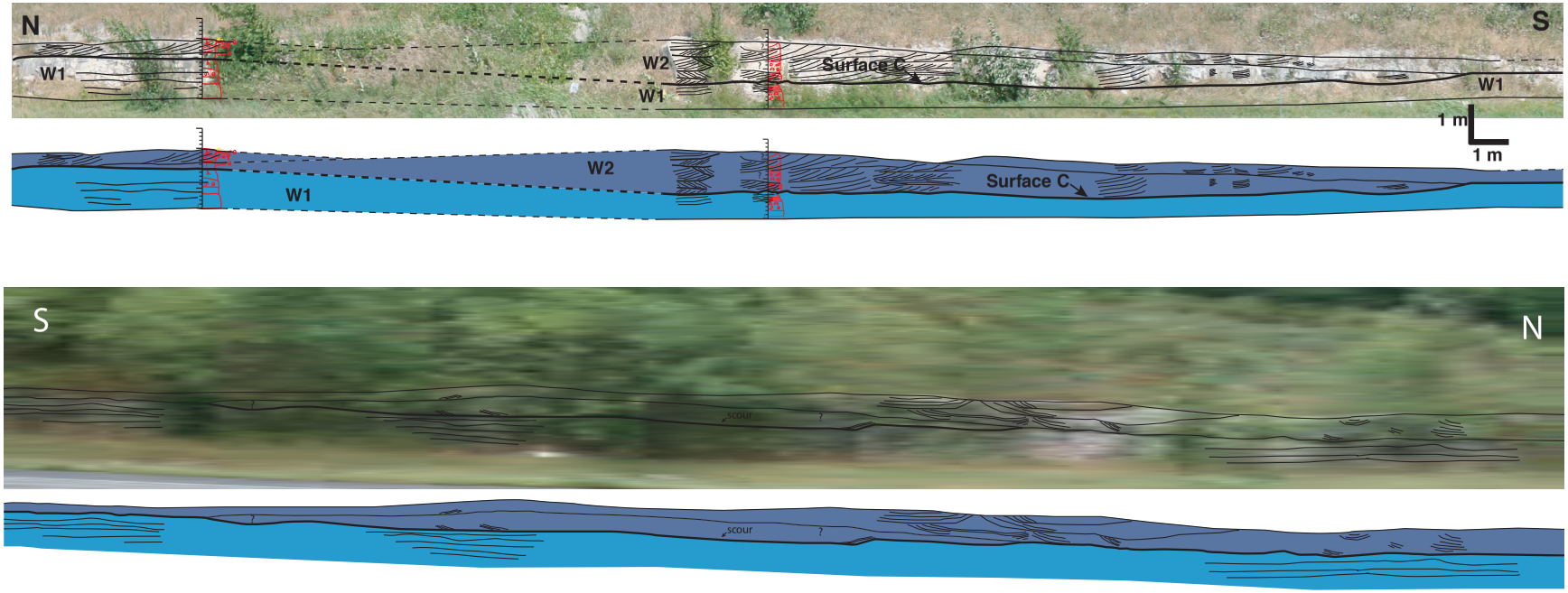
N
S
W1
W2
W1
Surface C
W1
1 m
1 m
W2
W1
Surface C
S
N
scour
?
?
scour
?

Figure 31. Photomosaic of site 7. Upper photo shows the west side of I435, lower photo shows the east side. Channel feature oriented at 025 degrees across interstate. Notice, especially in upper photo, the geometries present within the oolitic grainstone (darker blue above Surface C) showing deposition first within the paleochannel creating positive relief that subsequent strata lap out against. Facies colors match those represented in cross sections (Fig. 19–21).

Interval W2

Interval W2 is the middle part of the Westerville and is preserved throughout the field area except for the southernmost outcrops (1, 5, 9, and 17, Fig. 19). These southern outcrops coincide with the thickest portions of the underlying Wea Shale. The thickness of Interval W2 is highly variable at both outcrop, 0.5–2.0 m (Fig. 10G–H), and field area, 0.0–3.7 m (Fig. 21), scales. It is composed mostly of planar crossbedded oolitic grainstone with a thick (3.5 m) occurrence of crossbedded oolitic grainstone at site 15, thick (1.6 and 3.3 m) occurrences of bioclastic grainstone at sites 16 and 18 (Fig. 22). A thin (5 cm) bed of fossiliferous siliciclastic-mudstone is present between beds of planar crossbedded oolitic grainstone at site 4 (Fig. 20 and 21). Facies relationships within the interval are shown schematically in Figure 8. Lowermost Interval W2 oolitic grainstone deposits fill in minor relief along underlying Surface C. At site 7, geometries present within the oolitic grainstone show deposition first within and then above the margins of a paleochannel creating positive relief that subsequent strata lap out against (Fig. 31).

Interval W2 is mostly composed of shallow-water high-energy facies and provides evidence for a shallowing trend over the entire field area (Fig. 32). The fossiliferous siliciclastic-mudstone at site 4 is attributed to deltaic influence from the north—similar to the occurrence at site 13 in Interval W1. The stratigraphic record at and around sites 16 and 13 differ slightly. At site 16 bioclastic grainstone overlies Surface C (Fig. 19). Initial strata were deposited in 2–15 m water depth and were followed by planar crossbedded oolitic grainstone, deposited in <2–5 m water depth. This relationship is represented in the water-depth curve for site 16 by the curve passing first through the depositional depth range for the bioclastic grainstone facies and then the depositional depth range for the oolitic grainstone facies, a shallowing trend (Fig. 23). At site 13,

Interval W2 is composed solely of planar crossbedded oolitic grainstone, so the curve for site 13 also follows a shallowing trend, but only by passing through the depositional depth range for the oolitic grainstone facies (Fig 24).

Along with the shallowing trend throughout the field area, there is also evidence for downdip migration of oolitic grainstone deposits. At updip locations (sites 2, 7, 8, 10, and 16) planar crossbedded oolitic grainstone is present, at site 15, an intermediate location, trough crossbedded oolitic grainstone is present, and at down dip locations (sites 3, 4, 11, 12, and 13) planar crossbedded oolitic grainstone is also present (Fig. 21). The transition from planar to trough crossbedded oolitic grainstone from up-to-intermediate dip locations would be possible during a stagnant relative sea-level position because the trough crossbedded oolitic grainstone facies had a deeper depositional environment than the planar crossbedded oolitic grainstone facies. The presence of planar crossbedded oolitic grainstone in locations downdip of the trough crossbedded oolitic grainstone, however, is evidence of a prograding system (Fig. 33).

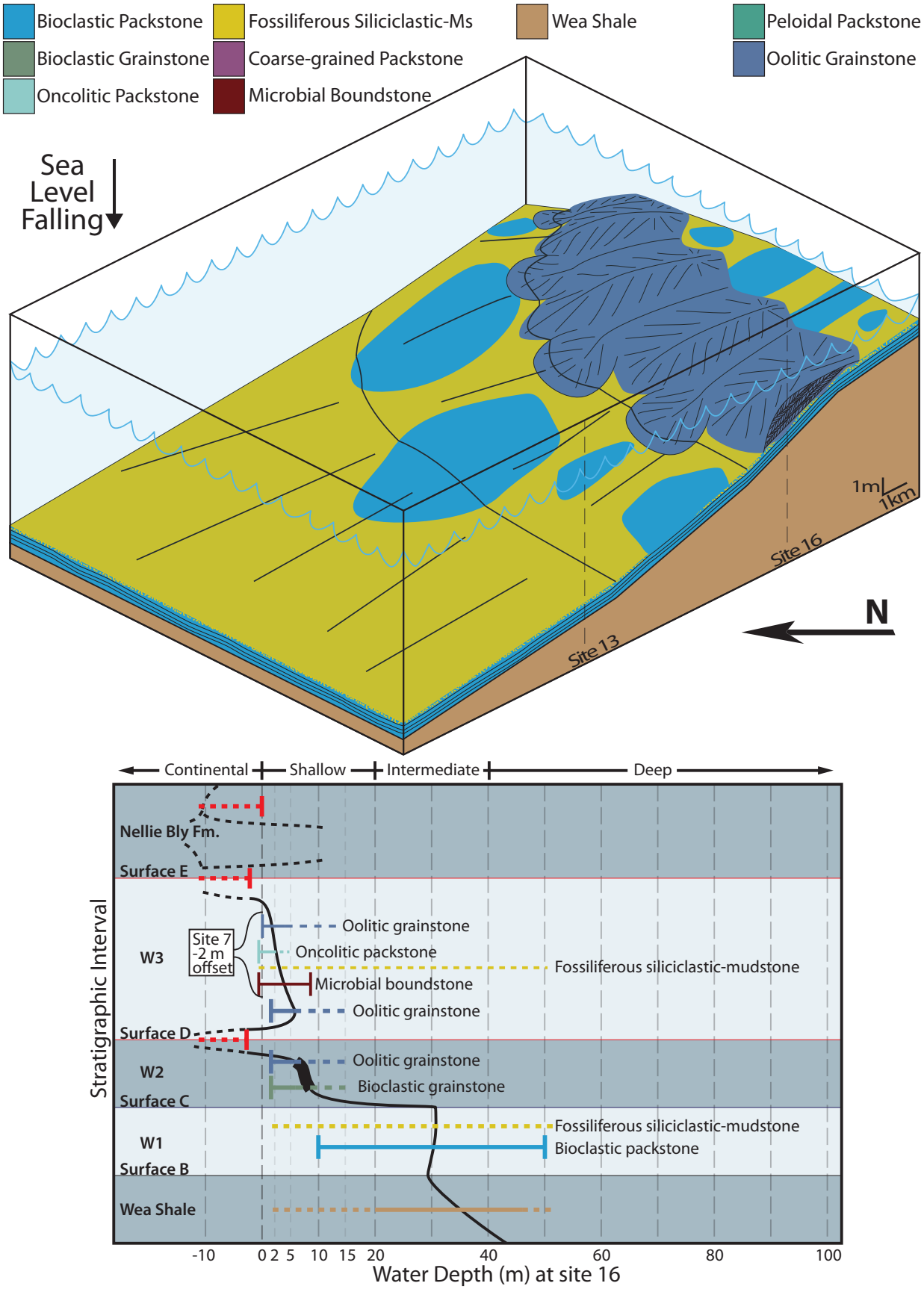
Bioclastic Packstone
Bioclastic Grainstone
Oncolitic Packstone
Fossiliferous Siliciclastic-Ms
Coarse-grained Packstone
Microbial Boundstone
Wea Shale
Peloidal Packstone
Oolitic Grainstone
Sea Level Falling
1m
1km
Site 16
Site 13
N
Continental
Shallow
Intermediate
Deep
Nellie Bly Fm.
Surface E
W3
Site 7 -2 m offset
Oolitic grainstone
Oncolitic packstone
Fossiliferous siliciclastic-mudstone
Microbial boundstone
Oolitic grainstone
Surface D
W2
Oolitic grainstone
Bioclastic grainstone
Surface C
W1
Fossiliferous siliciclastic-mudstone
Bioclastic packstone
Surface B
Wea Shale
Stratigraphic Interval
-10
0 2 5
10
15
20
40
60
80
100
Water Depth (m) at site 16

Figure 32. Block diagram illustrating the interpreted depositional environment during the formation of Surface C and early stages of Interval W2. Marine truncation of Interval W1 occurs as shallow, high energy, water erodes the underlying substrate. Oolitic grainstone deposits form in the portions of the field area where the water is shallowest. Locations of sites 13 and 16 placed in relation to thickness of underlying Wea Shale.

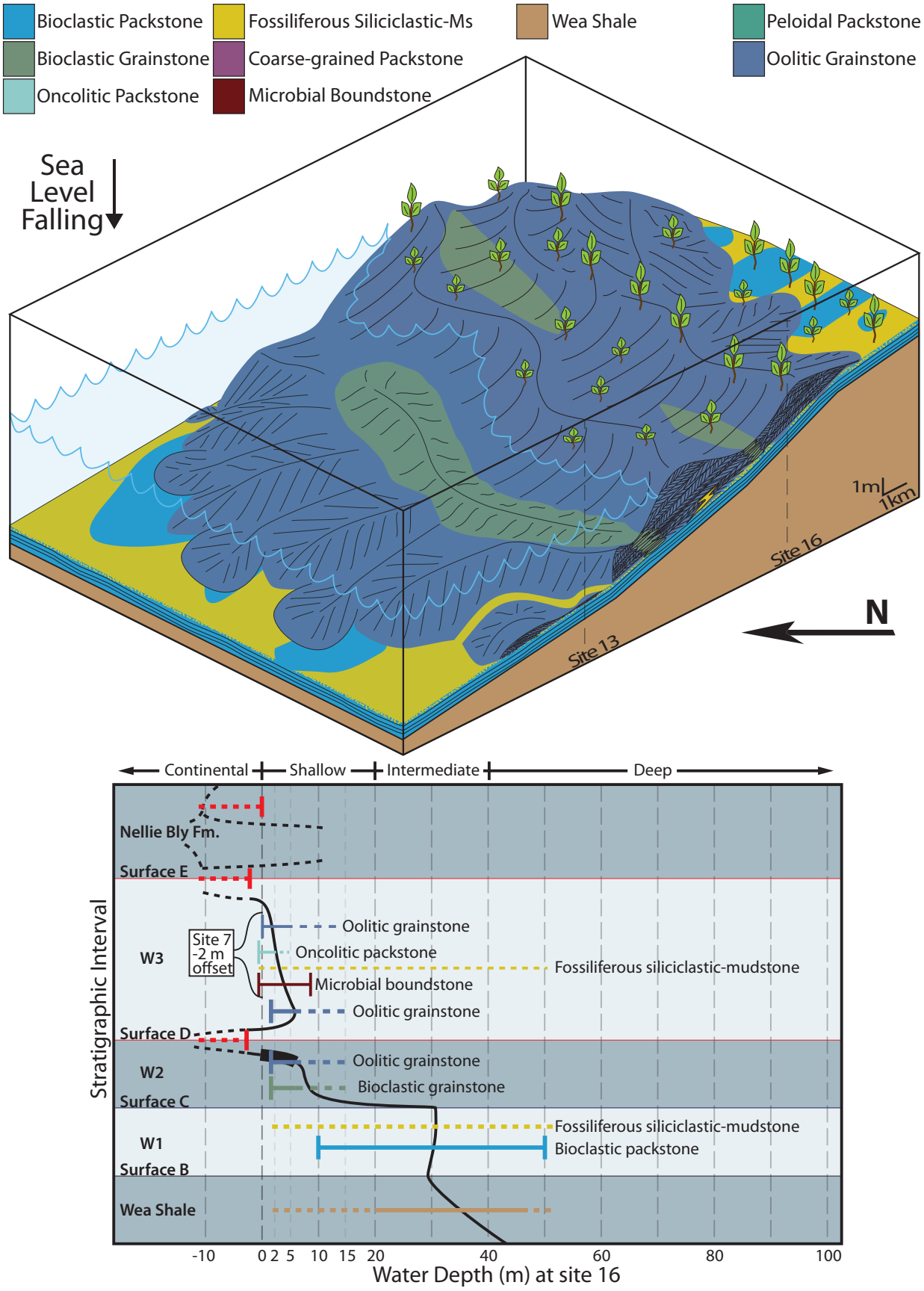
Bioclastic Packstone
Bioclastic Grainstone
Oncolitic Packstone
Fossiliferous Siliciclastic-Ms
Coarse-grained Packstone
Microbial Boundstone
Wea Shale
Peloidal Packstone
Oolitic Grainstone
Sea Level Falling
1m
1km
Site 16
Site 13
N
Continental
Shallow
Intermediate
Deep
Nellie Bly Fm.
Surface E
W3
Site 7 -2 m offset
Oolitic grainstone
Oncolitic packstone
Microbial boundstone
Oolitic grainstone
Fossiliferous siliciclastic-mudstone
Surface D
W2
Oolitic grainstone
Bioclastic grainstone
Surface C
W1
Fossiliferous siliciclastic-mudstone
Bioclastic packstone
Surface B
Wea Shale
Stratigraphic Interval
-10
0 2 5
10
15
20
40
60
80
100
Water Depth (m) at site 16

Figure 33. Block diagram illustrating the interpreted depositional environment during the final stage of Interval W2. Portions of the field area are subaerially exposed and underlying deposits are truncated. Oolitic and bioclastic grainstone deposition is forced down dip by limited accommodation. Locations of sites 13 and 16 placed in relation to thickness of underlying Wea Shale.

Surface D

Surface D truncates all of Interval W2 and the southernmost exposures of Interval W1, sites 1, 5, 9, and 17 (Fig. 19–21). Deposits immediately beneath Surface D at site 16 show pendant fabrics in thin section, whereas deposits of the same facies above Surface D at site 16 show no pendant fabrics. Meter-scale erosional truncation at the base of Surface D is observed at site 13. Features that may be rhizoliths are present directly beneath Surface D at site 13. At sites 1, 7, 9, 13, 15, and 19 microbial boundstone directly overlies Surface D. *Gastrochaenolites* borings associated with the microbial boundstone facies crosscut both grains and cements in deposits underlying Surface D at site 13 (Fig. 17).

Surface D is interpreted as a surface of subaerial exposure (Fig. 34). Pendant fabrics are evidence of subaerial exposure or vadose zone processes (Tucker and Wright, 1990). Although these fabrics could have developed during later subaerial exposure (Surface E discussed in another section), the concentration of these fabrics below Surface D leads to the interpretation of an earlier timing. The crosscutting relationship between the *Gastrochaenolites* borings, microbial boundstone facies in Interval W3, and the cemented grains below Surface D indicate, that at the very least, cementation below Surface D occurred before deposition of Interval W3.

The maximum amount of relief exposed subaerially along Surface D is unknown and represented in the water-depth curves for both sites 13 and 16 by an open-ended dashed line (Fig. 23 and 24). The amount of relief subaerially exposed on outcrop at site 13 is at least 1 m (Fig. 11A–D). This minimum relief is represented in the water-depth curve for site 13 as at least 1 m of exposure (Fig. 24). Considering reconstructed paleotopography, the trace of Surface D from site 16 to site 7, a distance less than 1 km, indicates two meters of subaerially exposed relief

(Fig. 19). This minimum relief is represented in the water-depth curve for site 16 as at least two meters of exposure (Fig. 23).

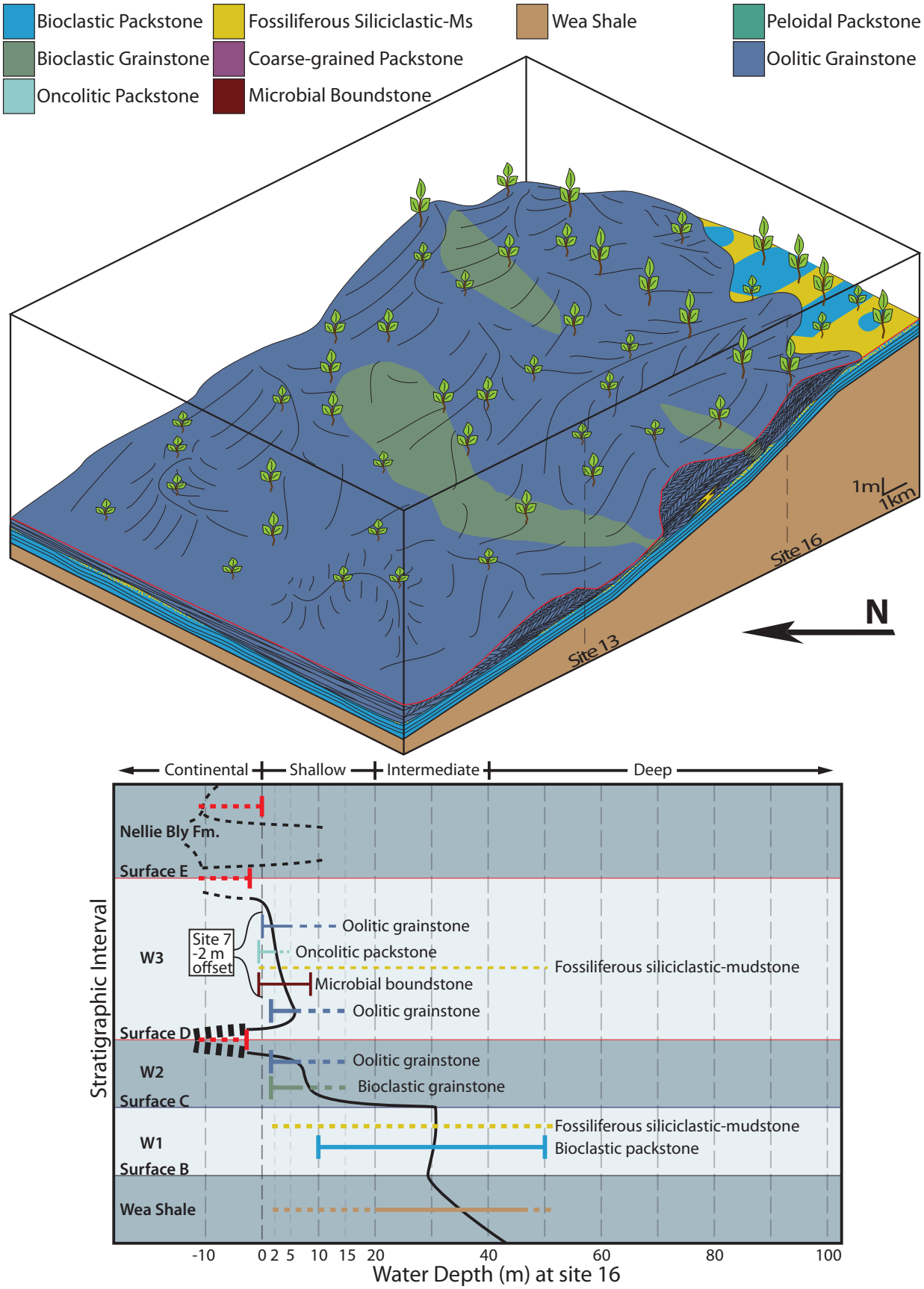
Bioclastic Packstone
Bioclastic Grainstone
Oncolitic Packstone
Fossiliferous Siliciclastic-Ms
Coarse-grained Packstone
Microbial Boundstone
Wea Shale
Peloidal Packstone
Oolitic Grainstone
1m
1km
Site 16
Site 13
N
Continental
Shallow
Intermediate
Deep
Nellie Bly Fm.
Surface E
W3
Site 7
-2 m
offset
Oolitic grainstone
Oncolitic packstone
Microbial boundstone
Oolitic grainstone
Fossiliferous siliciclastic-mudstone
Surface D
W2
Oolitic grainstone
Bioclastic grainstone
Surface C
W1
Fossiliferous siliciclastic-mudstone
Bioclastic packstone
Surface B
Wea Shale
Stratigraphic Interval
-10
0 2 5
10
15
20
40
60
80
100
Water Depth (m) at site 16

Figure 34. Block diagram illustrating the interpreted environment during the formation of Surface D. The entire field area is subaerially exposed. Locations of sites 13 and 16 placed in relation to thickness of underlying Wea Shale.

Interval W3

Interval W3 represents the uppermost portion of the Westerville. It immediately overlies Surface D throughout the field area, except at sites 10, 12, 15 and 18 (Fig. 21 and 22) where Interval W3 overlies Surface C. Interval thickness is highly variable (0.0–4.0 m) with the thickest portions coinciding with the thinner portions of the combined underlying Interval W1, Interval W2, and Wea Shale portions (Fig. 21). Interval W3 is composed of microbial boundstone, oncolitic packstone, fossiliferous siliciclastic-mudstone, peloidal packstone, coarse-grained packstone and oolitic grainstone facies. The lowermost portion of W3 is composed of microbial boundstone, which mantles underlying topography at sites 1, 9, 13 (Fig. 11A–D), 15, and 19 (Fig 21). All of the oncolitic packstone and a majority of the fossiliferous siliciclastic-mudstone and coarse-grained packstone facies present in Interval W3 onlap against paleotopographically higher areas. This onlapping relationship is found at sites 2 (Fig. 10F and G), 7, and 13 (Fig. 11A–D) and inferred at sites 1, 5, 10, and 19 (Fig. 21 and 22). Peloidal packstone (sites 3, 9, 11, 13, and 19) and planar crossbedded oolitic grainstone (sites 1, 5, 7, 8, 10, and 16) form the uppermost portion of Interval W3 (Fig. 21 and 22). Facies relationships within the interval are shown schematically in Figure 8.

Interval W3 represents marine sedimentation after a period of subaerial exposure (Surface D). Lowermost W3 deposits throughout the field area consist of microbial boundstone, fossiliferous siliciclastic-mudstone, and oncolitic packstone (Fig. 21). All of these deposits are interpreted to be marine in nature. The microbial boundstone and oncolitic packstone have depositional depth ranges of 2–10 m and 2–5 m respectively. The interbedded and gradational nature of the contact between the fossiliferous siliciclastic-mudstone and oncolitic packstone

would indicate a similar depositional depth (2–5 m) for both facies. The position of shallow water marine facies on top of a subaerial exposure surface leads to an interpretation that initial deposition in Interval W3 was transgressive in nature. This may not be the case, however, as the complexity within Interval W3 makes interpretation of the depositional history difficult. For that reason, the interpretation of depositional history and associated water-depth curves is presented first for site 16 and then for site 13.

Initial W3 deposits at sites 16 and 10, paleotopographically high areas are planar crossbedded oolitic grainstone deposits and are thought to have been deposited prior to or at the same time as the microbial boundstone and oncolitic packstone found in paleotopographically lower areas (Fig. 19). This conclusion is based on the presence of ooids in both the microbial boundstone and oncolitic packstone facies. Both the microbial boundstone and oncolitic packstone were deposited in environments where ooids would not have formed and the presence of ooids has been interpreted here to be a product of proximity to an ooid shoal. Whereas the source for the ooids found at site 7 within the microbial boundstone and oncolitic packstone may not have actually been sites 10 and 16 specifically, ooid production proximal to and paleotopographically higher than microbial boundstone and oncolitic packstone deposits within Interval W3 makes sense. Also, the depositional depth of planar crossbedded oolitic grainstone is <2–5 m and the tracing of Surface D from site 16 to site 7 (<1 km horizontal distance) shows 2 m of relief (Fig. 19). If water depth was <2–5 m at site 16, during deposition of oolitic grainstone, and the paleotopographic reconstruction is correct, the water depth at site 7 would have been two meters greater (<4–7 m) and overlap with the range of interpreted depositional depth for the microbial boundstone (2–10 m) and to a lesser extent the oncolitic packstone (2–5

m). Deposition of the oncolitic packstone at site 7, therefore, could have occurred during the Interval W3 highstand, but most likely occurred during falling sea level, after oolitic grainstone deposition in the paleotopographically highest areas (e.g. Site 16), and as ooid production moved to lower areas during a forced regression.

Whereas the oolitic grainstone is not preserved in Interval W3 at or near site 13, there is evidence for a water-depth curve at site 13 similar to the curve for site 16. Interval W3 deposits at site 13 consist first of microbial boundstone, oncolitic packstone, fossiliferous siliciclastic-mudstone, and coarse-grained packstone onlapping underlying topographical relief and an overlying, blanketing deposit of peloidal packstone (Fig. 11A–D). There are ooids incorporated within the domal layers of the microbial boundstone, the fill of the cross cutting *gastrochaenolites* borings and the overlying oncolitic packstone deposits. The ooids within these deposits are interpreted to have originated in an ooid shoal proximal to and at a higher paleoelevation than site 13, for the same reasons as discussed for similar deposits near site 16. The coarse-grained packstone is interpreted to have been deposited during a storm surge event at an undetermined water depth. The regression during Interval W3 must have continued in order to deposit the supratidal peloidal packstone at site 13 in 0–1 m water depth. Water depth at site 13 then remained at 0–1 m during the deposition of 3 m of peloidal packstone (Fig. 24). A relative rise in sea level or sediment compaction must have occurred during the final part of Interval W3 to accommodate 3 m of peloidal packstone at site 13.

Thus, sedimentation during Interval W3 initiated with oolitic grainstone at the paleotopographically highest areas and microbial boundstone within the surrounding paleolows during highstand or falling sea level (Fig. 35). Initial sedimentation was followed by deposition

of oolitic grainstone at paleotopographically lower areas and deposition of oncolitic packstone and fossiliferous siliciclastic-mudstone in sheltered paleolow areas (Fig. 36). Lastly, supratidal peloidal packstone deposition filled regional paleotopography (Fig. 37).

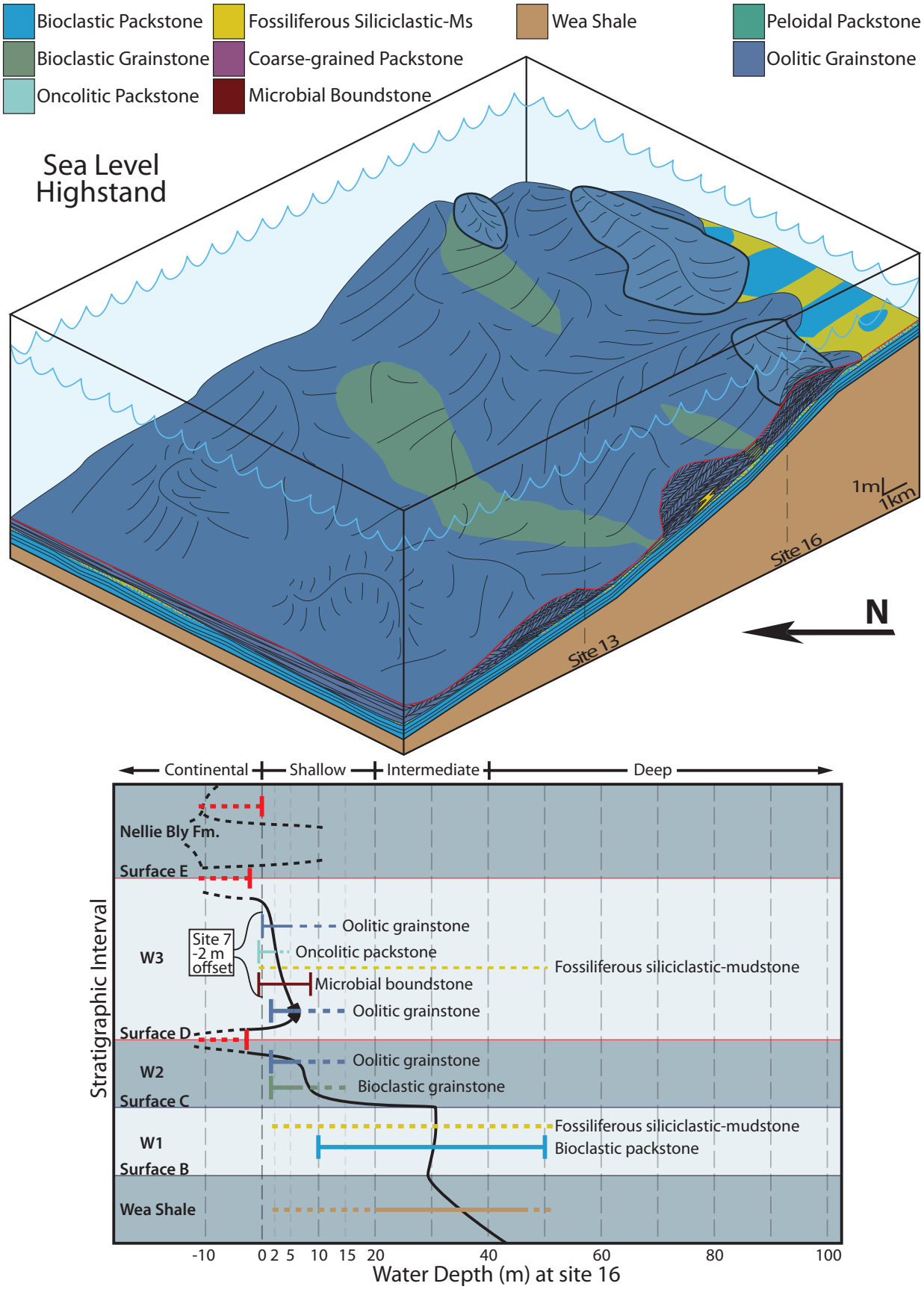
Bioclastic Packstone
Bioclastic Grainstone
Oncolitic Packstone
Fossiliferous Siliciclastic-Ms
Coarse-grained Packstone
Microbial Boundstone
Wea Shale
Peloidal Packstone
Oolitic Grainstone
Sea Level Highstand
1m
1km
Site 16
Site 13
N
Continental
Shallow
Intermediate
Deep
Nellie Bly Fm.
Surface E
W3
Site 7 -2 m offset
Oolitic grainstone
Oncolitic packstone
Fossiliferous siliciclastic-mudstone
Microbial boundstone
Oolitic grainstone
Surface D
W2
Oolitic grainstone
Bioclastic grainstone
Surface C
W1
Fossiliferous siliciclastic-mudstone
Bioclastic packstone
Surface B
Wea Shale
Stratigraphic Interval
-10
0 2 5
10
15
20
40
60
80
100
Water Depth (m) at site 16

Figure 35. Block diagram illustrating the interpreted depositional environment during the sea-level highstand period of Interval W3. Deposition of oolitic grainstone (lighter blue) modifies local relief on the flank of a paleotopographically high area. Locations of sites 13 and 16 placed in relation to thickness of underlying Wea Shale.

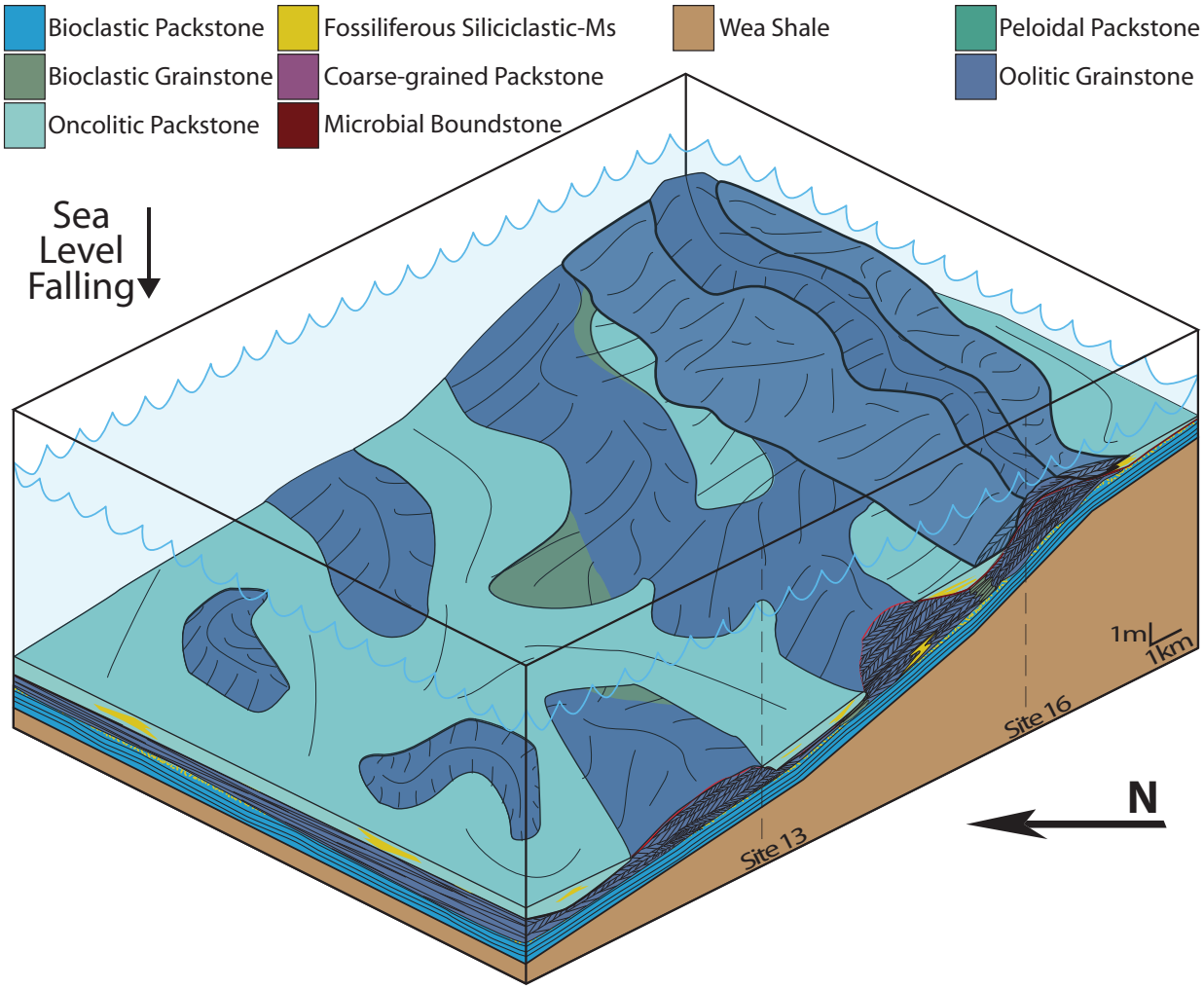
Bioclastic Packstone
Bioclastic Grainstone
Oncolitic Packstone
Fossiliferous Siliciclastic-Ms
Coarse-grained Packstone
Microbial Boundstone
Wea Shale
Peloidal Packstone
Oolitic Grainstone
Sea Level Falling
1m
1km
Site 16
Site 13
N

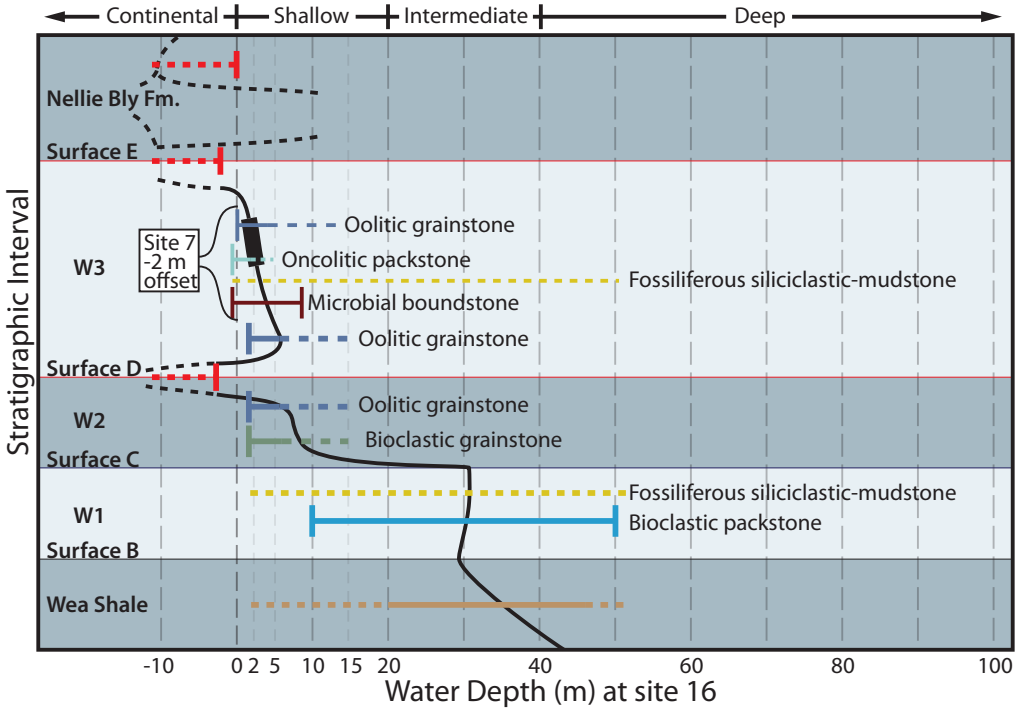
Continental
Shallow
Intermediate
Deep
Nellie Bly Fm.
Surface E
W3
Site 7
-2 m
offset
Oolitic grainstone
Oncolitic packstone
Fossiliferous siliciclastic-mudstone
Microbial boundstone
Oolitic grainstone
Surface D
W2
Oolitic grainstone
Bioclastic grainstone
Surface C
W1
Fossiliferous siliciclastic-mudstone
Bioclastic packstone
Surface B
Wea Shale
Stratigraphic Interval
-10
0 2 5
10
15
20
40
60
80
100
Water Depth (m) at site 16

Figure 36. Block diagram illustrating the interpreted depositional environment during the falling sea-level stage of Interval W3. Oolitic grainstone (lighter blue) deposition moves from the top to the flanks of local paleohighs. Microbial boundstone drapes underlying topography. Oncolitic packstone and fossiliferous siliciclastic-mudstone onlap paleotopography and fill paleolows. Locations of sites 13 and 16 placed in relation to thickness of underlying Wea Shale.

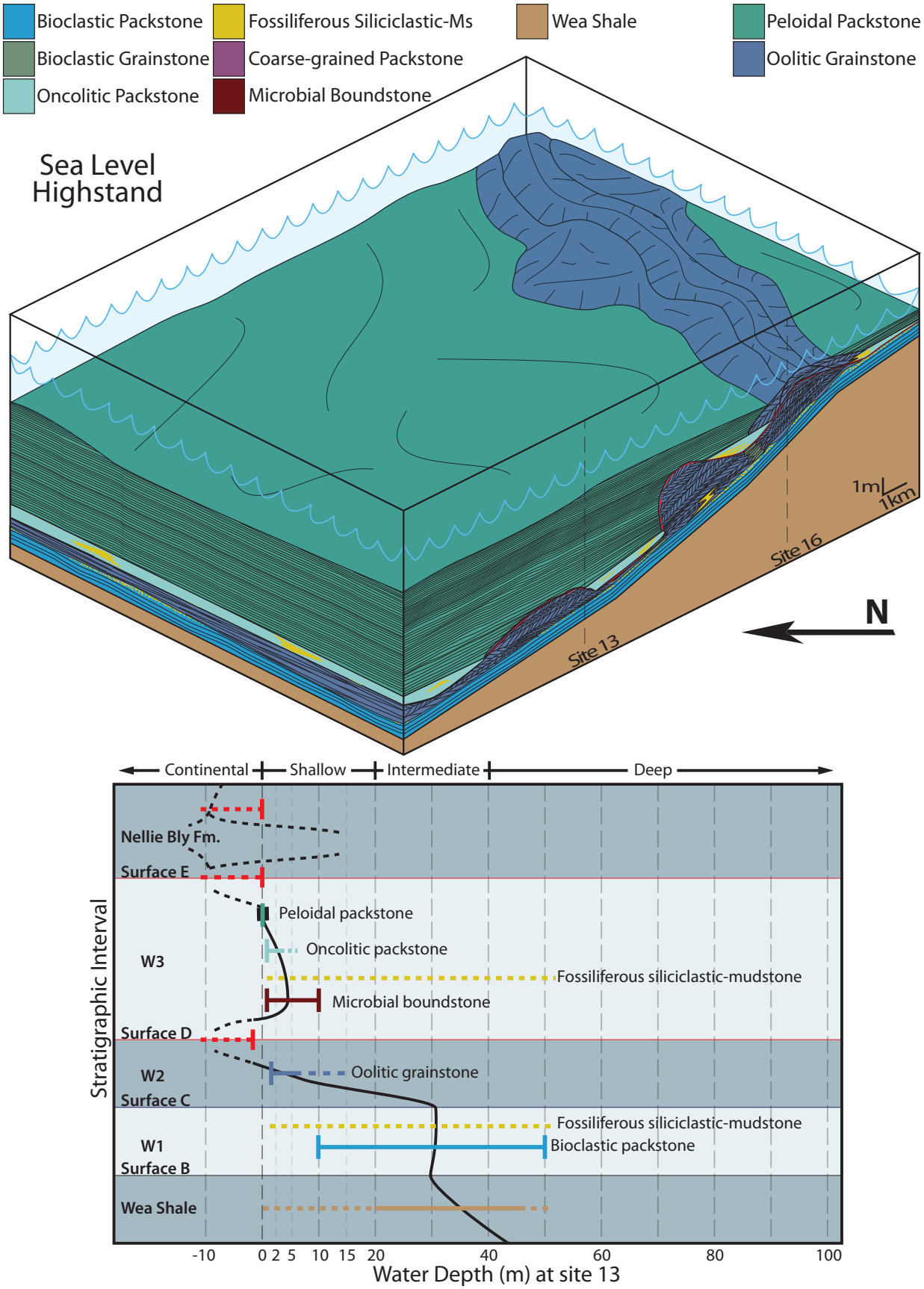
Bioclastic Packstone
Bioclastic Grainstone
Oncolitic Packstone
Fossiliferous Siliciclastic-Ms
Coarse-grained Packstone
Microbial Boundstone
Wea Shale
Peloidal Packstone
Oolitic Grainstone
Sea Level Highstand
1m
1km
Site 16
Site 13
N
Continental
Shallow
Intermediate
Deep
Nellie Bly Fm.
Surface E
Peloidal packstone
Oncolitic packstone
W3
Fossiliferous siliciclastic-mudstone
Microbial boundstone
Surface D
W2
Oolitic grainstone
Surface C
Fossiliferous siliciclastic-mudstone
W1
Bioclastic packstone
Surface B
Wea Shale
Stratigraphic Interval
-10
0 2 5
10
15
20
40
60
80
100
Water Depth (m) at site 13

Figure 37. Block diagram illustrating the interpreted depositional environment during the final stages of Interval W3. Supratidal peloidal packstone deposition fills regional paleotopography. Locations of sites 13 and 16 placed in relation to thickness of underlying Wea Shale.

## Surface E

Surface E separates the Westerville (below) from the Nellie Bly Formation and the Quivira Shale Member (above) (Fig. 19–21). This surface is recognized both at outcrop and thin section scale. On outcrop, relief along the truncation surface is minimal (cm-scale). At sites 4, 10, 11, and 13 rhizoliths are present in the upper 15–20 cm of the peloidal packstone deposits (Fig. 16D). At the top of Interval W3 at site 6 pendant fabrics are present in thin section (Fig. 16E) and at site 15 void space is filled with crystal silt.

The rhizoliths are interpreted as casts of the roots of land plants present when the upper surface of the Westerville was subaerially exposed. The crystal silt is interpreted as weathered spar cement. This cement formed in the marine environment and then was subsequently eroded in a vadose environment and filled void space below (e.g. Dunham 1969). Pendant fabrics are evidence of subaerial exposure or vadose zone processes (Tucker and Wright, 1990).

Subaerial exposure is interpreted to have occurred throughout the field area. Water depth fell at least 2.5 m at site 16 to account for the relief on Surface E from site 16 to site 7 (Fig. 23). At site 13, relief on Surface E is minimal (dm-scale) and the water-depth curve shows subaerial exposure initiating at 0 m (Fig. 24). The water-depth curves for both sites 13 and 16 show subaerial exposure beginning after deposition of Interval W3 and continuing with an open-ended dashed line (Fig. 23 and 24).

## Nellie Bly Formation and Quivira Shale Member

The Nellie Bly Formation and the Quivira Shale Member overlie the Westerville throughout the field area. Although these rocks were not a focus of the study, thickness

measurements were made in the field where exposure allowed. It should be noted, however, that the outcrops were almost always covered with vegetation and thickness estimates were based on the distance from the top of the Westerville to the bottom of the Cement City Limestone, which overlies the Quivira Shale Member.

The Nellie Bly Formation is reported as a thin paleosol with a possible coal bed near Kansas City, MO. It has been interpreted as a 50 m thick sandy shale and sandstone lowstand deposit at the type location in northern Oklahoma. The paleosol portion extends from the Kansas City area northward into Iowa (Heckel, 1999). The Quivira Shale is a phosphatic grey-to-black shale that forms the transgressive and highstand portions of the Dewey cyclothem (Heckel, 1999). In Nebraska it is interpreted as a nearshore shale deltaic sequence from observed progradational wedges and deltaic sequence characteristics (Burchett, 1971).

The thin paleosol deposits of the Nellie Bly Formation are further evidence of exposure after deposition of the Westerville. It is unknown if the paleosol deposits of the Nellie Bly Formation developed during a continuation of the exposure event on Surface E or if it is separated from Surface E by an event of relative rise and fall in sea level. For this reason both scenarios are represented as dashed lines in the water-depth curves for sites 13 and 16 (Fig. 23 and 24). The sequence boundary above the Nellie Bly Formation represents the end of the Cherryvale cyclothem. The Quivira Shale represents a return to marine deposition in the area and the beginning of the Dewey cyclothem (Heckel, 1999).

## Relative Sea-Level Curve

The depositional history interpreted in the previous sections was used to construct water-depth curves for sites 13 and 16. This section proposes the combination of the constructed water-depth curves into one curve that will serve as a relative sea-level history curve. Due to the relative similarity in the fluctuations in the water-depth curves for sites 13 and 16, it seems reasonable to assume that the entire field area experienced a similar sea-level history. The combined curve (referred to as the relative sea-level curve) was constructed using the water-depth histories from sites 13 and 16 and the top of the Block Limestone (Surface A) as a reference point. Thickness of sediment deposited above Surface A is accounted for by shifting interpreted facies depositional water depths relative to that surface. Minimum amounts of sea-level fall are taken from relief on exposure surfaces traced across the entire field area (Fig 38).

Water depth is a result of multiple factors. Water depth can vary with relative changes in sea level. Water depth can also vary due to autogenetic processes: shallowing as sediment fills accommodation, deepening as currents erode sediment, or remaining consistent as wave energy reworks sediment. The data on the Westerville and associated units show that both allogenic and autogenic processes affected water depth.

During deposition of the Wea Shale the filling of accommodation could have been the only effect on water depth, and for that reason, the Wea Shale portion of the relative sea-level curve is dashed. The relative sea-level curve mimics the water-depth curves for sites 13 and 16 during deposition of Interval W1 and shows a slight deepening or stillstand in relative sea level interpreted from an increase in conodont abundance and diversity. This portion of the curve is dashed. After deposition of Interval W1, however, there is a relative fall in sea level. Interval W1, composed mostly of bioclastic packstone with an interpreted depositional depth of 10–50 m,

is overlain by shallow high-energy deposits. The relatively thin nature of the bioclastic packstone (~1 m) makes shallowing due to sediment accumulation unlikely. If the bioclastic packstone and associated fossiliferous siliciclastic-mudstone deposits of Interval W1 were deposited near the shallow end of their interpreted depositional depth range (10 m), one would expect to see a more gradational contact with the overlying high-energy deposits. The sharp overlying contact and facies dislocation across Surface C and the lack of coated grains or ooids in Interval W1 suggests that a relative fall in sea level caused the shallowing from Interval W1 to Surface C and on to Interval W2 (Fig. 38).

The situation in Interval W2 is not as clear. It is worth considering that Interval W2 could have filled accommodation and led to the exposure of Surface D, but Interval W2 facies lack gradational facies shoaling into the subaerial realm. Further, there is local m-scale erosional truncation on Surface D, and Surface D overlies subtidal deposits. Thus, ascribing a portion of the shallowing of water depth during deposition of Interval W2 to a relative fall in sea level seems reasonable—even more so considering the high frequency and rate of relative sea-level changes during the Pennsylvanian (Rasbury et al., 1998; Eros et al., 2012). Tracing relief along Surface D from site 16 to site 19 represents at least a 9.5 m relative fall in sea level after exposure at site 16.

After subaerial exposure, which created Surface D, a relative rise in sea level must have occurred in order to explain the subtidal facies found in Interval W3. This is evident because the uppermost Interval W2 deposits were exposed to vadose zone processes and they are initially overlain by subtidal deposits, including planar crossbedded oolitic grainstone that was deposited in <2–5 m water depth at site 16. The last Interval W3 deposits were deposited in shallower

water than earlier Interval W3 deposits and must have occurred after a relative fall in sea-level because supratidal deposits, which were deposited after the oolitic grainstone at site 16, are present immediately overlying Surface D at site 13 (Fig. 21 and 38). There is evidence for a relative rise in sea level during the latest stage of Interval W3 in the 2.5–3.0 m thick peloidal packstone deposits at site 13 (Fig. 20). The interpreted depositional depth for the peloidal packstone is supratidal (0–1 m), but the peloidal packstone deposits at site 13 are 2.5–3.0 m thick. In order to deposit a sediment wedge thicker than the depositional depth range, there must have been a small relative rise in sea level to create the necessary accommodation. The relative rise could have been a product of subsidence, compaction of underlying sediment, or a eustatic rise, and is included in the solid portion of the sea-level curve for Interval W3 (Fig 38).

The full relative sea-level curve for the Westerville and associated units is composed of three minor relative rises in sea level during an overall relative fall in sea level (Fig. 38). The overall relative fall in sea level is interpreted to have begun after deposition of the Block Limestone and continued during deposition of the Wea Shale and Westerville until the succession was subaerially exposed (Nellie Bly Formation)(Heckel, 1986)(Fig. 7).

The relative rise in sea level during Interval W1 is interpreted from conodont abundance and diversity data (Heckel and Baesemann, 1975), and not assigned a quantitative value (dashed line for Interval W1 in Figure 38).

The relative fall in sea level after Interval W1, during the formation of Surface C, deposition of Interval W2, and formation of Surface D, is evidenced by a facies dislocation across Surface C and truncation of subtidal facies by Surface D. This represents at least a 15.5 m relative fall in sea level. The 15.5 m value is calculated by subtracting the elevation of the

lowermost occurrence of Surface D (3.5 m above datum, #8 in Fig. 38) from the shallowest depositional depth elevation of bioclastic packstone deposited at site 16, an updip location, during Interval W1 (19 m above datum, #3 in Fig. 38). The 19 m value is calculated at #3 in Figure 38 by adding the thickness of the underlying Wea Shale and the thickness of the bioclastic packstone at site 16 (9 m) to the lowermost depositional depth value for the bioclastic packstone (10 m).

Deposition of oolitic grainstone (site 16) on top of the subaerial exposure surface (Surface D) evidences a second relative rise in sea level of at least 11.5 m. The 11.5 m value is calculated by subtracting the elevation of the lowermost occurrence of Surface D (3.5 m, #8 in Fig. 38) from the shallowest depositional depth elevation of the latest oolitic grainstone deposits at site 16 during Interval W3 (15 m, #9 in Fig. 38). The 15 m value is calculated at #9 in Figure 38 by adding the thickness of the sediment beneath Surface D (12 m) and the thickness of the oolitic grainstone of Interval W3 (1 m) at site 16 to the lowermost depositional depth value for the planar bedded oolitic grainstone (<2 m).

A relative fall in sea level of at least 8.2 m during the middle stages of Interval W3 (#10–15 in Fig. 38) is evidenced by deposition of supratidal deposits on top of Surface D at a lower paleoelevation (site 13) than the planar crossbedded oolitic grainstone at site 16 (Fig. 21). The 8.2 m value is calculated by subtracting the elevation the lowermost deposition of the supratidal peloidal packstone at site 13 (6.8 m, #15 in Fig. 38) from the elevation of the uppermost oolitic grainstone deposits at site 16 (15 m, #9 in Fig. 38). The 6.8 m value at #15 in Figure 38 is calculated by adding the thickness of the underlying deposits at site 13 (6.8 m) with the depositional depth value for the peloidal packstone (0–1 m)(Fig. 21).

The third relative rise in sea level of at least 3 m occurred during the final stage of Interval W3 as evidenced by an accumulation of supratidal deposits (peloidal packstone) that are thicker than the depositional depth range for the facies. The 3 m value is taken from the greatest thickness of the peloidal packstone at site 13.

Tracing relief on Surface E from site 13 to site 19 shows a relative fall in sea level of at least 2.3 m. Although relief on Surface E is greatest from site 16 to site 19, site 13 is used here because the higher paleoelevations, such as site 16, would already have been exposed during deposition of the latest Interval W3 supratidal deposits described in the previous paragraph.

The stratigraphic succession and relative sea-level history observed in this study is strikingly similar to that of the supposedly correlative Drum Limestone (Feldman et al., 1993; Gomez-Perez et al., 1997). The Drum Limestone crops out near Independence in southeastern Kansas. The lower Drum Limestone facies succession indicates a shallowing trend (similar to Interval W2), which is capped by a subaerial exposure surface (similar to Surface D). The upper Drum Limestone is interpreted as a transgressive sequence, indicating marine deposition (similar to Interval W3) (Gomez-Perez et al., 1997). The subaerial exposure event and relative rise recorded in Surface D and Interval W3, respectively, were previously undocumented in the Westerville but compare favorable to that observed ~250 km away in the Drum Limestone.

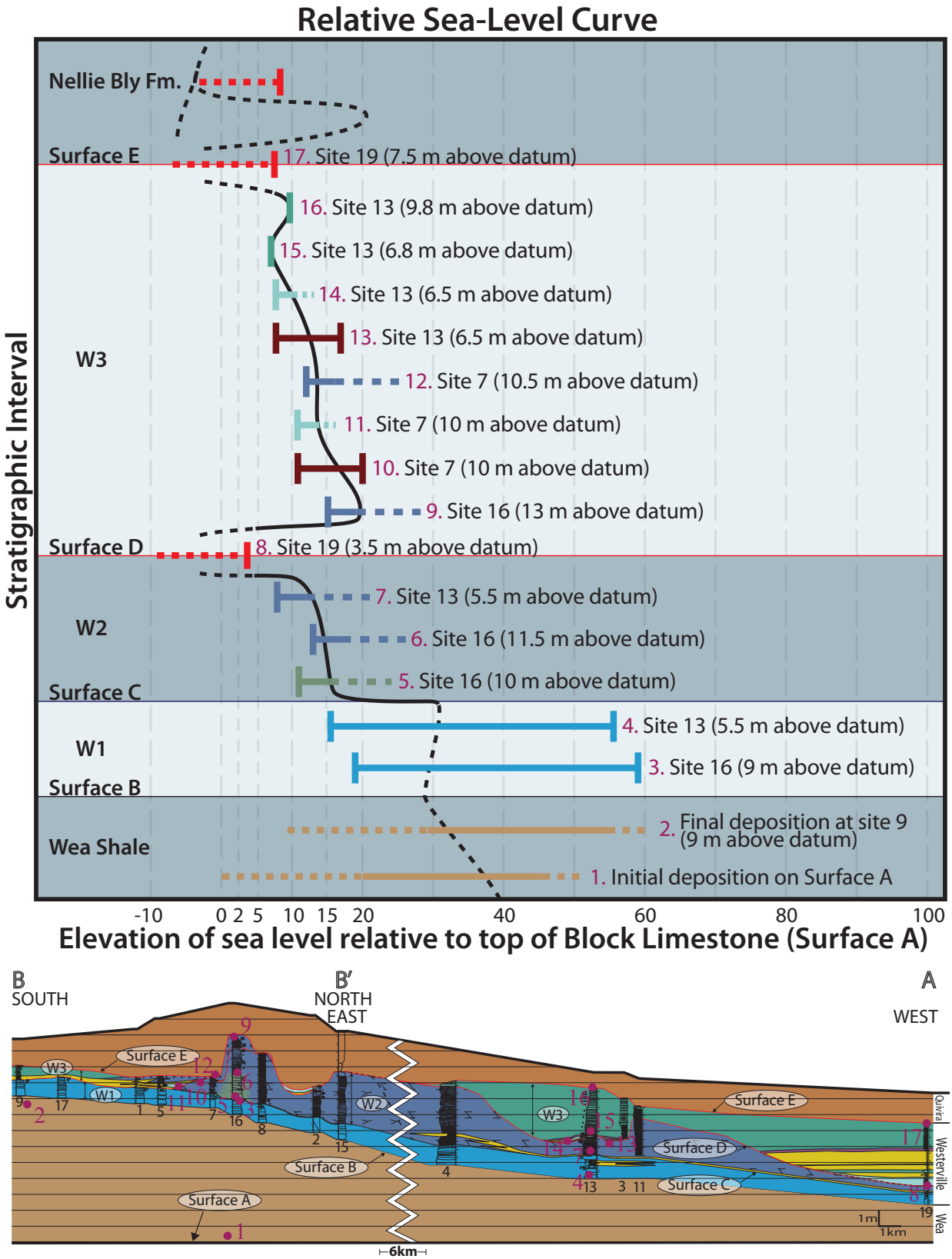





Cross section from Figure 21

Figure 38. Relative sea-level curve. Interpreted depth ranges for facies are shifted to account for the thickness of underlying sediment. The thickness and location of measurement are numbered and marked by purple dots on the combined cross section. Horizontal lines on combined cross section are placed at 1 m intervals.

# DISCUSSION

## Relative Sea-Level Curve

Heckel (1986) interpreted a sea-level curve for the Pennsylvanian Midcontinent which showed a relative fall in sea level during deposition of the Wea Shale, Westerville Limestone Member and Nellie Bly Formation (Fig. 7). The relative sea-level curve created in this study for the Westerville and associated units has three relative rises in sea level, each of which interrupt an overall relative fall in sea level (Fig. 38). The three relative rises in sea level and a subaerial exposure event within the Westerville (Surface D) were not documented by Heckel (1986) and show a more complicated relative sea-level history during deposition of the Westerville and associated units. This can call into question the validity of the estimates to the length of fifth order eustatic fluctuations made by Heckel (1986). Estimates from that study were 235–393 ka. Those estimates were taken from the total number of sea-level fluctuations recognized by the variations in conodont abundance and diversity. If the conodont data do not provide enough resolution and underestimate the number of fifth order sea-level fluctuations then the time estimates given would be too long. Although it is more likely that the sea-level fluctuations seen in this study are of a shorter period and amplitude than fifth order fluctuations, the shortening of the estimated length of sea-level fluctuation periods would bring values closer to the 143+/-64 ka period length reported by Rasbury et al. (1998) from U-Pb ages of paleosols from the Pennsylvanian and Early Permian of the Sacramento Mountains, New Mexico, U.S.A. and the 140 ka U-Pb calibrated period length for older deposits from the Donets Basin (Moscovian), Ukraine (Eros et al., 2012). Martin et al. (2012) also reported an average of 103 ka for

Moscovian equivalent deposits, but reported 358+/-180 and 398+/-133 ka period lengths for the Missourian portion of the Bird Spring Formation, southern Great Basin, U.S.A. based on biostratigraphy and using thickness to estimate time. The shorter period length values (~150 ka) agree more with the length of Pleistocene sea-level fluctuation periods, and both the Pleistocene and the Pennsylvanian have Milankovich cyclicity as proposed forcing mechanisms for glacioeuastatic fluctuations. The longer period values (~400 ka) are also in tune with Milankovich cyclicity (Heckel, 1986).

## Paleotopography, Relative Sea Level, and Carbonate Production

This section evaluates the effect paleotopography and relative sea level had on carbonate production during deposition of the Westerville and associated units. Paleotopographic reconstructions used for the study are suggested to be a close approximation to depositional topography. Where possible, the evaluation of paleotopography is constrained by relationships of facies and surfaces within individual outcrops. The interpreted relative sea-level curve is based on facies depositional depth interpretations and stratigraphic relationships as well as the tracing of truncation surfaces and published conodont abundance data. The interpreted relationship between the evolution of facies distribution within the Westerville and associated units, and relative fluctuations in sea level are shown schematically in Figure 39.

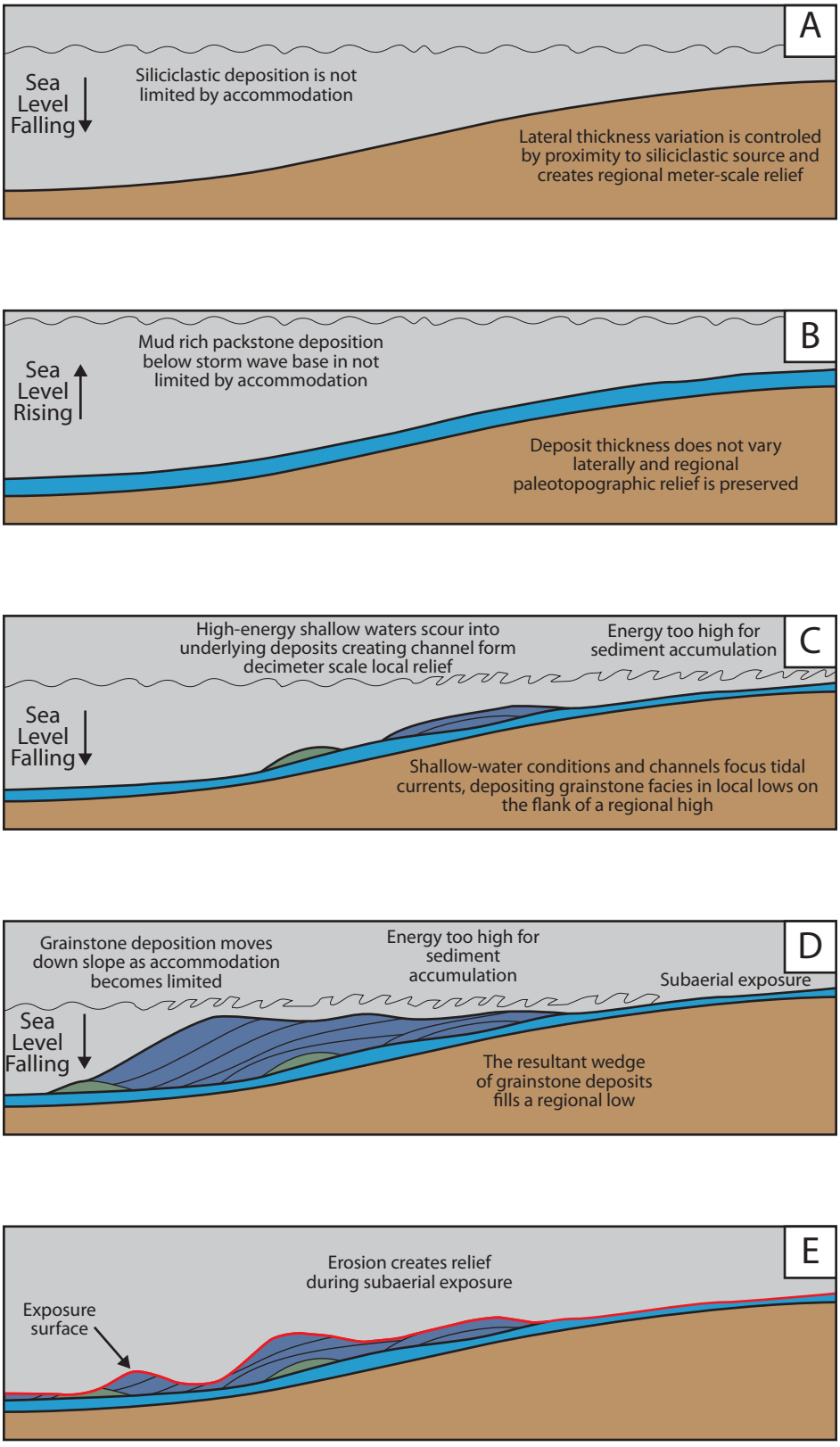
A
Sea Level Falling
Siliciclastic deposition is not limited by accommodation
Lateral thickness variation is controled by proximity to siliciclastic source and creates regional meter-scale relief
B
Sea Level Rising
Mud rich packstone deposition below storm wave base in not limited by accommodation
Deposit thickness does not vary laterally and regional paleotopographic relief is preserved
C
High-energy shallow waters scour into underlying deposits creating channel form decimeter scale local relief
Energy too high for sediment accumulation
Sea Level Falling
Shallow-water conditions and channels focus tidal currents, depositing grainstone facies in local lows on the flank of a regional high
D
Grainstone deposition moves down slope as accommodation becomes limited
Energy too high for sediment accumulation
Subaerial exposure
Sea Level Falling
The resultant wedge of grainstone deposits fills a regional low
E
Erosion creates relief during subaerial exposure
Exposure surface

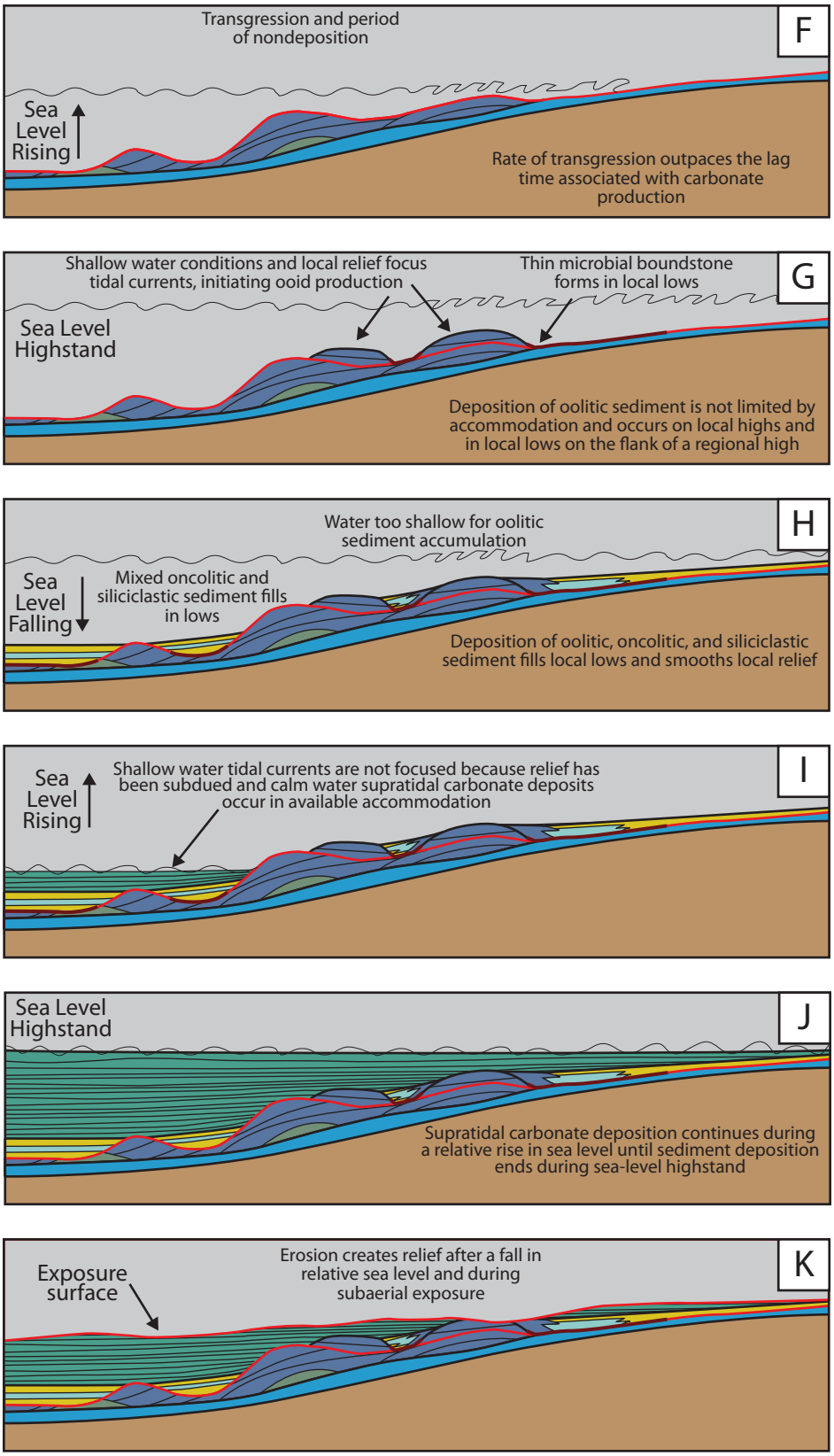
F
Transgression and period of nondeposition
Sea Level Rising
Rate of transgression outpaces the lag time associated with carbonate production
G
Shallow water conditions and local relief focus tidal currents, initiating ooid production
Thin microbial boundstone forms in local lows
Sea Level Highstand
Deposition of oolitic sediment is not limited by accommodation and occurs on local highs and in local lows on the flank of a regional high
H
Water too shallow for oolitic sediment accumulation
Sea Level Falling
Mixed oncolitic and siliciclastic sediment fills in lows
Deposition of oolitic, oncolitic, and siliciclastic sediment fills local lows and smooths local relief
I
Sea Level Rising
Shallow water tidal currents are not focused because relief has been subdued and calm water supratidal carbonate deposits occur in available accommodation
J
Sea Level Highstand
Supratidal carbonate deposition continues during a relative rise in sea level until sediment deposition ends during sea-level highstand
K
Exposure surface
Erosion creates relief after a fall in relative sea level and during subaerial exposure

Figure 39. Schematic diagram showing the facies distribution within the Wea Shale and Westerville during relative fluctuations in sea level. A) Deposition of the Wea Shale during a relative fall in sea level. B) Deposition of the carbonate portion of Interval W1 during a relative rise in sea level. C) Formation of Surface C and the earliest stage of deposition of Interval W2 during a relative fall in sea level. D) Later stage of deposition of Interval W2 during a relative fall in sea level. E) Subaerial erosion modifies topography before the initiation of the next sequence. F) Transgression after period of subaerial exposure. G) Oolitic grainstone buildups form in shallow water during sea level highstand (Interval W3). H) Limited accommodation during falling sea level forces oolitic grainstone deposition onto the flanks of local highs. Mixed carbonate and siliciclastic facies accumulate in local lows. I) Deposition of supratidal peloidal packstone during a relative rise in sea level. J) Peloidal packstone deposition during a slight relative rise in sea level until sea-level highstand. K) Subaerial erosion modifies topography before the initiation of the next sequence.

Wea Shale

Deposition of the Wea Shale occurred on a regionally flat surface during a relative fall in sea level, before accommodation became limited, and modified topography creating a gentle slope with 7 m of relief across the field area (Fig. 39A). Siliciclastic wedges deposited during relative falls in sea level are not uncommon in the Pennsylvanian Midcontinent; the Island Creek and Lane Shale are examples (McKirahan et al., 2003). The Wea, Island Creek, and Lane Shales all modified local relief. A notable difference between the Wea Shale and the McKirahan et al. (2003) examples is that deposition of the Wea Shale was not limited by accommodation and built regional relief, whereas the location of the Island Creek and Lane Shales is attributed to limited accommodation and the deposits filled regional lows. There is the possibility that regional paleotopography focused deposition of the Wea Shale, although there is no evidence for this within the field area.

Interval W1

Deposition during Interval W1 occurred during a relative rise in, or stable, sea level (Fig. 38) on a wedge of underlying Wea Shale that thinned to the north and northwest (Fig. 39B). Carbonate production consisted of bioclastic packstone deposited below normal wave base. As was demonstrated in the building of the relative sea-level curve, sedimentation did not fill accommodation——one meter of bioclastic packstone was deposited in a minimum 10 m of water depth, and Interval W1 deposits are truncated by a shallowing event. It is possible that the relative fall in sea level, which formed Surface C, occurred before the system had time to fill accommodation, or that carbonate production was not optimal during Interval W1. Whereas the rate of sea level-fall is unknown, there was siliciclastic input into the area both before (Wea

Shale), during (siliciclastic-mudstone partings), and after (fossiliferous siliciclastic-mudstone) deposition of the bioclastic packstone during Interval W1. Fine-grained siliciclastic material would add turbidity to the water column, may raise nutrient levels through the introduction of trophic resources, and hinder carbonate production during Interval W1.

Interval W1 draping carbonate facies were deposited during a stable or relative rise in sea level and not limited by accommodation. The carbonate factory was most likely perturbed by elevated turbidity or nutrient content of water laden with siliciclastic material intermittently entering the area. Reduced carbonate production likely resulted in unfilled accommodation. Less-than-maximum carbonate production could account for the lack of any carbonate mound formation and relief building, which is possible during a period of stable or a relative rise in sea level in water of moderate depth (Samankassou and West, 2002; McKirahan et al., 2003). The lack of mound formation could also be explained by the relatively flat, although sloping, paleotopography with no local highs, or relief, on which carbonate mounds could initiate or focused currents could localize deposition.

Surface C

Surface C is interpreted to have formed during a relative fall in sea level. High energy currents scoured into and truncated underlying Interval W1 deposits. The most significant truncation is a 100 m wide, 80 cm deep channel shaped feature located at site 7 (Fig. 31). Scouring during formation of Surface C enhanced local relief on an originally relatively flat, sloping surface after deposition of Interval W1.

Interval W2

Interval W2 is interpreted to have occurred during a relative fall in sea level (i.e. forced regression). The oolitic and bioclastic grainstone facies deposited during Interval W2 formed in high energy normal marine waters and are preserved in local low areas along Surface C on the flank of the regional high (Fig. 39C).

Modern oolitic shoals form in shallow high-energy environments (Harris, 1984; Reeder and Rankey, 2008). For this reason, ancient oolitic deposits are commonly interpreted to form on paleohighs, where the shallowest, highest energy water would have been. This relationship has been found in ancient examples, such as the Lansing and Kansas City Groups in southern Kansas (Raef et al., 2005). The geometries present in Interval W2 of the Westerville, however, provide an example of an oolitic-rich facies being preserved in paleolow areas (Fig. 31). Regionally, the thickest portions of grainstone deposits are found along a sloping surface in a slightly downslope position and not on top of the thickest or thinnest portions of the underlying sediment (Fig. 21).

The thick portions of oolitic grainstone are also present where the Westerville as a whole is at its thickest. If this relationship is considered when looking at the Westerville isopach maps, then the elongate thick areas are assumed to be mostly oolitic and are found on the flanks of the underlying flat-topped deposit of Wea Shale (Fig. 26 and 27). Modern examples of heterogeneous carbonate systems show that bedrock elevation (i.e. paleoslope) is not a predictor of facies distribution (Rankey et al., 2006). The oolitic facies within the Westerville, however, are not unique in their distribution relative to depositional topography. Other ancient examples of field-area-scale, oolitic-rich deposits being preserved on the flanks of paleohighs include: the Drum Limestone in southeastern Kansas, where limited accommodation is thought to force oolitic deposits to prograde off the edge of a paleohigh (Gomez-Perez et al., 1997); the Bethany

Falls Limestone (Pennsylvanian) in the shallow subsurface, eastern Kansas, which has oolitic bodies that form on and are elongate perpendicular to paleoslope (French and Watney, 1993); and subsurface of western Kansas, where Mississippian elongate oolitic bodies form on and parallel to intermediate positions on the paleoslope (Handford, 1988). One way to explain the preservation of oolitic-rich facies on the margins of paleohighs is limited accommodation as sea level is falling at a rate that forces deposition down paleoslope (Fig. 39D).

On a scale encompassing the entire field area, the grainy deposits of Interval W2 fill regional paleorelief as they are thicker where the combined thickness of the underlying Wea Shale and Interval W1 deposits are thinner (Fig. 21–22). The relationship of carbonates forming in accommodation left vacant after siliciclastic deposition is well established in the Pennsylvanian Midcontinent (Gomez-Perez et al., 1997; McKirahan et al., 2003; Washburn, 2004; Emry, 2005). McKirahan et al. (2003) discussed two mechanisms for grainy sediment accumulation in lows. Grainy sediment accumulated in the lows after being shed from local highs by high energy shallow water or produced in lows in focused high energy currents. I argue that the grainy deposits of Interval W2 are an example of the latter. As evidenced at site 7 (Fig. 31), the onlapping relationships within the planar crossbedded oolitic grainstone shows that deposition occurred first within the local low and built positive relief out of the low. Later deposits lap out against the positive relief. If sediment was being shed from a local high, one would expect deposits to first fill the low and then be dispersed evenly. The lateral variation in thickness indicates that oolitic bars or lobes developed within the local low.

Surface D

After Interval W2, a relative fall in sea level of at least 9 m resulted in subaerial exposure of the entire field area (Surface D), and erosion in the subaerial environment modified paleotopography (Fig. 39E). The subaerial exposure surface overlies Interval W2, where preserved, and Interval W1 at sites 1, 5, 9, and 17 (Fig. 19, 21 and 22), and it is possible that Interval W2 oolitic grainstone facies preserved on the margins of a Westerville paleohigh were deposited at other sites, but were eroded during subaerial exposure. The subaerial erosion that occurred between Intervals W2 and W3 (Surface D) resulted in the greatest local relief (m-scale) preserved within the Westerville (Fig. 21, 22, and 34).

Interval W3

Local and regional paleorelief remaining after the erosion of Interval W2 was subdued during deposition of Interval W3, and oolitic grainstone was deposited at sites 1, 5, 7, 10, and 16. Interval W3 deposition initiated on local meter-scale relief (Surface D between sites 7 and 16, Fig. 21) proximal to the paleotopographically high area to the south where the underlying Wea Shale deposits were thickest (Fig. 25). Deposition occurred after a relative rise in sea level, and a period of non deposition (Fig. 39F), in water <2–5 m deep during a sea-level highstand where the local relief caused tidal currents to be funneled between local highs, creating an environment suitable for ooid formation (Fig. 35). Oolitic grainstone is preserved on top of local highs (site 16) and within local lows (site 10)(Fig. 22), indicating that initial sedimentation during Interval W3 was not limited by accommodation (Fig. 39G). Whereas the oolite in Interval W2 formed during a relative fall in sea level and was constrained to form in lows because of decreasing accommodation, oolites in Interval W3 formed during a highstand or sea-level turn-around point, where preexisting topography focused currents on and around small (meter-scale) bumps in low

areas. During the Pennsylvanian the area of study was in a middle ramp position (Fig. 6 and 7), so highstand deposits are uncommon and those found in Interval W3 most likely occurred after a smaller scale relative rise in sea level that interrupted an overall larger scale relative fall in sea level. If the relative rise in sea level was of small scale and short duration, then the unfilled accommodation could be due to the short duration of the highstand or a carbonate factory not producing at maximum rates.

Middle Interval W3 sedimentation occurred during an interpreted relative fall in sea level of at least 8.2 m (Fig. 38). As accommodation became limited, deposition of oolitic grainy sediment occurred on the flanks of paleohighs. Some of the oolitic material was shed into surrounding paleolows and incorporated within lower energy carbonate deposits (oncolitic packstone and microbial boundstone). Siliciclastic material (fossiliferous siliciclastic-mudstone) also accumulated in and filled paleolows (Fig. 39H). As discussed for Interval W2, the presence of high-energy grainy deposits in paleotopographically low areas can be a product of sediment transportation from a nearby topographic high or the generation of grainy sediment in low areas where current energy is focused (McKirahan et al., 2003; Franseen and Goldstein, 2004; Franseen et al., 2007). In middle Interval W3 deposits oolites are incorporated within both the microbial boundstone and oncolitic packstone, which are low energy facies that occur in local paleolows indicating shedding of ooids from surrounding highs.

During the latter stages of Interval W3 local paleolows were filled with oncolitic and fossiliferous siliciclastic sediment to the point where current energy was no longer focused and water depths became extremely shallow. Low energy peloidal sediment was then deposited in a supratidal environment (Fig 39I). The presence of peloidal packstone within Interval W3 is

interpreted to have occurred after a 8.2 m relative fall (#10–15 in Fig. 38), and during a 3 m relative rise in sea level (#15–16 in Fig. 38) to account for the relatively thick accumulation of supratidal deposits. The small scale (3 m) relative rise in sea level during the final stage of Interval W3 is the third relative rise in sea level recorded in the Westerville. Deposition initiated in regionally low areas and continued updip during the relative rise in sea level (transgression) (Fig. 39J). In the paleotopographic reconstruction these supratidal deposits are shown to accumulate in areas where the underlying sediments are thinner (Wea Shale, Intervals W1 and W2)(Fig. 21).

Surface E

After deposition of Interval W3 a relative fall in sea level of at least 2.4 m resulted in subaerial exposure of the entire field area (Fig. 39K). Only subtle (cm-scale) relief is preserved along Surface E on outcrop, indicating little erosion associated with subaerial exposure.

## Build-And-Fill Model

This section uses facies, stratal geometries, and the relative sea-level curve produced herein to evaluate the build-and-fill sequence concept (Fig. 40) for a mixed carbonate-siliciclastic system. Build-and-fill sequences are characterized by a building phase that predominates during rises, and a filling phase that predominates during falls. The result is an entire sequence that is of relatively equal thickness over a wide area. This area has been termed the *build-and-fill zone*, and was interpreted as the paleotopographic setting intermediate between highstand and lowstand positions, where rates of sea-level rise or fall are highest (Franseen and Goldstein, 2004; Franseen et al., 2007; and Franseen and Goldstein, 2012). The important

element for build-and-fill sequence development in this zone is less-than-optimal carbonate production, which leads to unfilled accommodation during rises. Franseen and Goldstein (2012) indicated that gentle substrate slopes result in broad build-and-fill zones that, when affected by fast rates of sea-level rise, promote broad areas of underfilled accommodation.

An important element in my study, which contributes to the build-and-fill concept, is that several minor fluctuations in sea level occurred during an overall fall. The highstand position was far upslope; lowstand position was far downslope; and field area was in an intermediate position (Fig. 7). Minor 3–11.5 m complete relative sea-level cycles were superimposed on the relative longer term relative fall in sea level in the field area. As discussed below, the deceleration of rates of change associated with turn-around positions of the minor fluctuations results in deposition of facies with complex geometries as a result of filling and constructional building of relief. These geometries and facies distributions associated with these minor fluctuations create additional heterogeneity during the overall relative fall in sea level.

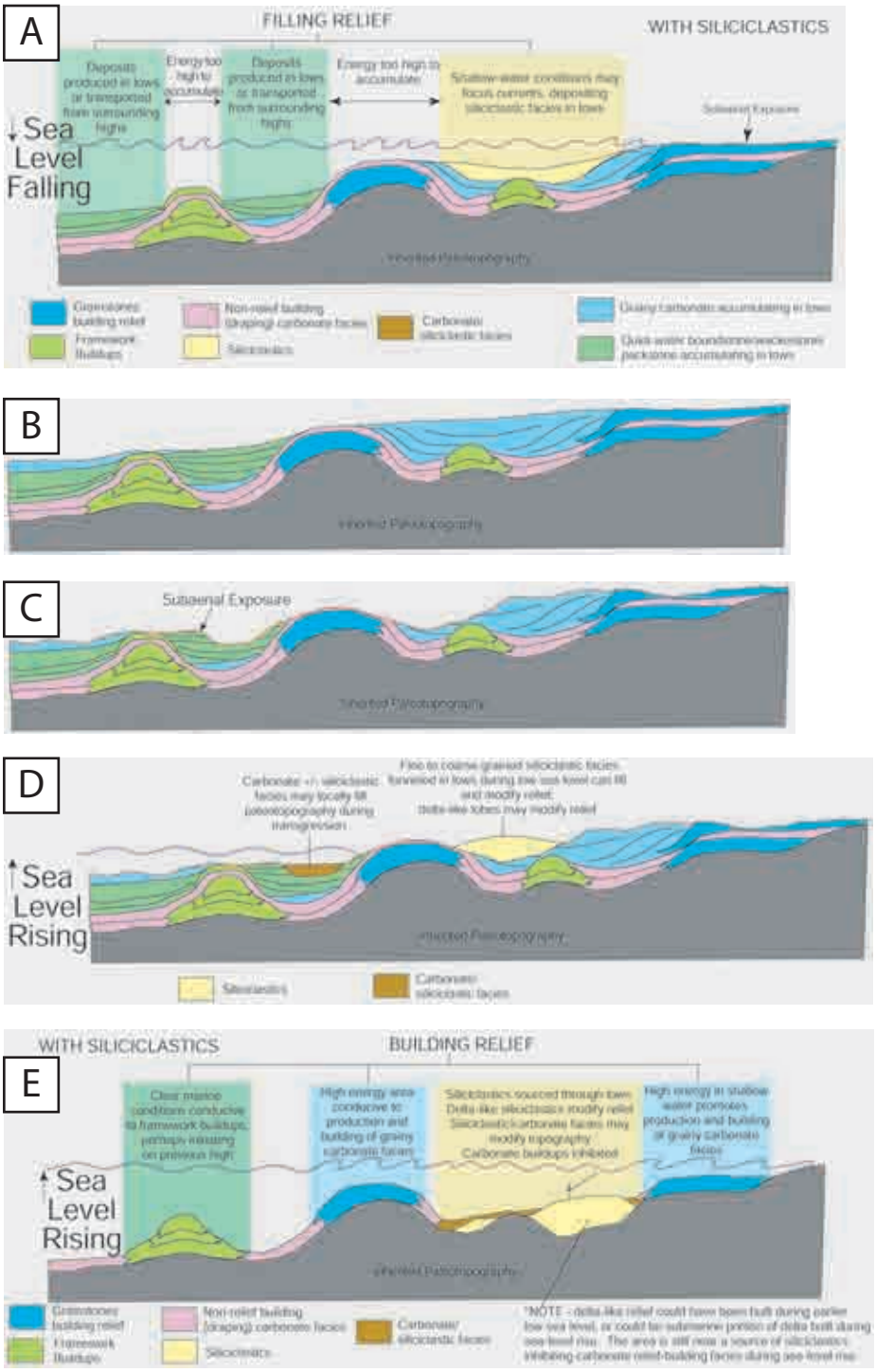


Figure 40. Schematic diagram of a typical build-and-fill sequence in a mixed siliciclastic and carbonate system. A) Relief filling during a fall in sea level as deposition is focused in lows due to limited accommodation. B) Relief filled creating a sequence of relatively uniform thickness. C) After sea level falls, a period of subaerial exposure and subaerial erosion modifies topography before the initiation of the next sequence. D) Initial stage of the next build-and-fill sequence. During the subsequent sea-level rise (transgression), mixed carbonate and siliciclastic deposits

can fill topographic lows and coarse-grained siliciclastic deposits can modify topographic relief E) Relief building and topography draping during sea-level rise. Carbonate production is not limited by accommodation, but can be hindered by siliciclastic input that is funneled through lows and modifies topography. Modified from Franseen and Goldstein (2004).

The Westerville and associated units were deposited in a mid-ramp position on a gently sloping ramp (Fig. 6) and, in general, show build-and-fill characteristics. The entire sequence, from the bottom of the Block Limestone to the top of the Westerville Limestone (Fig. 4) has a relatively uniform thickness, but internally is characterized by complex stratal geometries and facies distributions (Fig. 21). The overall thickness (~14 m) of the sequence (from the bottom of the Block Limestone to the top of the Westerville Limestone) is less than the interpreted minimum 80 m amplitudes of relative sea-level fluctuations estimated for Pennsylvanian cyclothems (Soreghan and Giles, 1999). Although the amplitude of sea-level fluctuation during the Lower Cherryvale Cycle is less than other Pennsylvanian fluctuations (Fig. 7), and may not have been 80 m, the cycle does include Westerville-equivalent marine deposits as far north as central Iowa (Bain, 1898). Marine deposition that far north would most likely provide more than 14 m of accommodation within the field area. Deposition of the Westerville and underlying Wea Shale is interpreted to have occurred in a mid ramp position during a 10's of meters-scale relative fall in sea level (Fig. 7)(Heckel, 1986). This study, however, shows that there are three minor (m-scale) relative rises in sea level, each of which interrupt the overall relative fall in sea level.

The interval of study starts with the Wea Shale and continues through the three intervals within the Westerville Limestone that were deposited during the overall large-scale relative sea-level fall for the entire sequence (Fig. 38). Deposition of the Wea Shale, during the fall, initially built regional relief, as an interpreted deltaic deposit, on a gently dipping substrate that lacked any regional relief (Fig. 39A). The interpreted minor relative rise associated with the overlying Interval W1 resulted in cessation of siliciclastic deposition and likely contributed to preservation of the constructional relief on the Wea Shale.

Deposition of Interval W1 during a relative rise in sea level resulted in deposition of mud-rich packstone (bioclastic packstone) that draped relief on the underlying Wea Shale throughout the field area. Interestingly, the highstand turn-around point of this minor sea-level rise occurred in the field area, but geometries such as aggradation (catch up) and progradation common in highstands are lacking. This suggests that either carbonate productivity was inhibited, depth was already too great to generate the catch up or progradation, or time available was not sufficient in relation to sedimentation rates to aggrade to base level (Fig. 39B). An interpreted abrupt relative fall in sea level marked the end of Interval W1 deposition (Fig. 38) and resulted in scouring of Interval W1 deposits to create erosional relief at decimeter scale (Fig. 39C). The high energy and erosion is a reasonable explanation for the lack of common highstand geometries.

During continued relative fall in sea level (Fig. 38) deposition resumed with Interval W2. This deposition was initiated in some of the more downslope areas of the field area because of the relative fall in sea level. As is common in the build-and-fill model, the high energy brought to intermediate ramp positions, associated with falling sea level, generated grainstone facies and focused deposition in lows (Fig 39D). The grainstone that filled the lows on regional and local scales, also created dm-scale constructional relief on a local scale (Fig 31).

The continued fall resulted in subaerial exposure and m-scale erosion of Interval W2 deposits across the entire field area (Fig. 39E). The erosion modified topography prior to the next phase of deposition. It is not known how far sea level fell, but the fall extended beyond the limits of the field area, indicating the lowstand turn-around point and beginning of subsequent rise occurred beyond the limits of the field area.

This subsequent rise reached its highstand turn-around point within the field area and the entirety of Interval W3 represents early-to-late highstand deposition and should not be expected to behave as a build-and-fill system. Therefore, Interval W3 strata provide an opportunity to examine a higher order highstand superimposed, at intermediate ramp position, on the build-and-fill zone of a lower order sea level cycle. The complex facies distributions and stratal geometries in Interval W3 appear to be a result of irregular topography on Surface D, lag time (non-deposition) during initial phase of rise, wave and current energy, and some interpreted minor sea-level fluctuations within this intermediate-elevation highstand. A main difference in Interval W3 deposits, compared to those deposited under the build-and-fill model, is that the facies in Interval W3 are all very shallow-water deposits with a wedge-shaped geometry. The deposits represent the following: (1) initial catch up (after lag time; Fig. 39F–G); (2) complex deposition during a minor relative fall in sea level (Fig. 39H; note that grainy sediment fills in local relief and may have been washed off of subtle highs); and (3) keep up phases during a minor relative sea-level rise which deposits a wedge of shallow-water sediment (Fig. 39I and J). The keep up phase illustrated in Figure 39 I and J resulted in supratidal deposits, initially deposited in a regional low and keeping up as sea level rose. The initiation of the relative fall in sea level resulted in subaerial exposure of Interval W3 and creation of Surface E (Fig. 39K).

Like build-and-fill systems, Interval W3 deposits have internal complexities associated with facies both building and filling relief. The Interval W3 system, however, is a higher order highstand deposit formed at an intermediate paleotopographic position in the build-and-fill zone of a lower order sea-level cycle. Overall, Interval W3 demonstrates how minor fluctuations in sea level can cause additional complexity within the build-and-fill pattern.

# CONCLUSIONS

A detailed study of the Pennsylvanian (Missourian) Westerville in a 510 $km^2$ area near Kansas City in northeastern Kansas and northwestern Missouri identified eight lithofacies: bioclastic packstone; bioclastic grainstone; oolitic grainstone; oncolitic packstone; fossiliferous siliciclastic-mudstone; peloidal packstone; microbial boundstone; and coarse-grained packstone. Deposition of the Westerville is divided into three depositional intervals (W1, W2, and W3), each separated by a marine or subaerial truncation surface. The interpreted depositional succession for the three intervals provides evidence for three smaller scale relative rises in sea level superimposed over a larger scale relative fall in sea level (Fig. 38). The relative sea-level curve shows a relative rise in sea level during deposition of Interval W1 followed by a relative fall in sea level of at least 15.5 m during Interval W2, leading to subaerial exposure across the field area (Surface D). Also shown, is a relative sea-level rise of at least 11.5 m during initiation of Interval W3, a relative fall in sea level of at least 8.2 m during the middle of Interval W3, a slight (3 m) relative rise in sea-level during final stage of Interval W3, and a period of subaerial exposure after a relative fall in sea level of at least 2.4 m. This detailed account of sea-level history had not been documented in the Westerville prior to this study.

Sequences in the Westerville interacted with paleotopography to create lateral facies and stratal geometry heterogeneity. Facies associations show consistent patterns in relation to paleorelief as deposition and erosion during the sequence of sea-level changes create and subdue paleotopography. Prior to deposition of the Westerville, local paleotopography consisted of a flat-topped siliciclastic lobe (Wea Shale) that thinned to the north and northwest in the field area.

Deposition of Interval W1 carbonate facies occurred in open-marine water below normal wave base and did not affect inherited paleotopography. Subtle, dm-scale, local paleorelief was created through marine erosion (Surface C) when shallow high-energy water encountered an erodible substrate. Tidal energy, possibly enhanced by dm-scale paleochannels, created an environment preferential for ooid production on the flanks of the regional paleohigh. Although typically thought to form constructional relief on high areas in shallow water, this study indicates that subtle paleorelief can be subdued through deposition of oolitic grainstone in low areas during falling stages of sea level (forced regression, e.g. Interval W2). Paleorelief can be significantly altered by subaerial erosion (e.g. Surface D). During highstand and sea-level turnaround, deposition of oolitic grainstone can alter paleorelief by building on local paleohighs in a regional paleolow. Deposition of mixed carbonate siliciclastic deposits (oncolitic packstone and fossiliferous siliciclastic-mudstone) in paleolows during a falling sea level can subdue paleorelief.

The Lower Cherryvale Cycle (Westerville and associated units) has characteristics of a build-and-fill sequence. The sediment package is of relatively uniform thickness, heterogeneous within, and the overall thickness is less than the amplitude of sea-level fluctuation. The mechanisms for deposition for a relative fall in sea level outlined by the build-and-fill model can be used to explain some of the heterogeneity found in the Westerville, including: oolitic grainstone deposited on the flanks of a regional high due to limited accommodation; regional paleotopography altered by a lobe of siliciclastic deposition (Wea Shale); and local relief was created by erosion during subaerial exposure (Surface D). Other facies geometries found within the Westerville (Interval W3) also build and fill constructional relief, but were deposited during

sea-level highstand at intermediate elevation on the ramp. These deposits do not show the typical build-and-fill pattern, but preserve a wedge of shallow-water sediment typical of highstand deposits.

The study of the Westerville can expand the build-and-fill model to include the possible effect of smaller scale fluctuations in sea level on sequence heterogeneity. Accelerations and decelerations in the rate (and direction changes) of the large scale fall in sea level that occurred during deposition of the Westerville had a significant effect on sequence heterogeneity. Although it is possible that these effects were more noticeable in the Westerville because the changes in the relative position of sea level created an exposure surface, the smaller scale fluctuations in sea level may also be able to explain heterogeneity within the build-and-fill zone.

# REFERENCES


ASHLEY, G.M., SOUTHARD, J.B., AND BOOTHROYD, J.C., 1982, Deposition of climbing-ripple beds: a flume simulation: Sedimentology, v. 29, p. 67–79

BAARS, D.L., AND TORRES, A.M., 1991, Late Paleozoic Phylloid Algae—A Pragmatic Review: Palaios, v. 6, p. 513-515.

BAIN, H.F., 1898, Geology of Decatur County: Iowa Geol. Survey Annual Report 1987, v. 8, pp. 276-277.

BAKER, J.A., 1995, Field guide to the quantitative assessment of borers and encrusters on Orthomyalina from an upper Paleozoic shell bed in the Stull Shale Member of the Kanawaka Shale (Upper Pennsylvanian, Virgilian of eastern Kansas): Kansas Geological Survey, Open File Report 95-3, p. 43.

BASSO, D., 1998, Deep rhodolith distribution in the Pontian Islands, Italy: a model for the paleoecology of a temperate sea: Palaeogeography, Palaeoclimatology, Palaeoecology, v. 137, p. 173–187.

BOGGS, S., 2001, Principles of Sedimentology and Stratigraphy: New Jersey, Prentice-Hall, Inc., p. 726.

BURCHETT, R.R., 1971, Stop 4: Richfield P.W.A. Quarry, in Burchett, R.R., Guidebook to the geology along portions of the lower Platte River Valley and Weeping Water Valley of eastern Nebraska: University of Nebraska Conservation and Survey Division, Lincoln, Nebraska Geological Survey, p. 23.

DENVER, L.E.II., AND KAESLER, R.L., 1992, Paleoenvironmental significance of stromatolites in the Americus Limestone Member (Lower Permian, Midcontinent, USA): University of Kansas Paleontological Contributions, v. 1–2, p. 1–11.

DOWNS, D.V., 1986, Diagenetic Patterns in Pennsylvanian Westerville Oolite, Kansas City, Missouri: Master's thesis, University of Missouri-Columbia, p. 43.

DUNHAM, R.J., 1962, Classification of carbonate rocks according to depositional texture in Classification of Carbonate Rocks—A Symposium: American Association of Petroleum Geologists, Memoir no. 1, p. 108-121.

DUNHAM, R.J., 1969, Early vadose silt in Townsend Mound (reef), New Mexico: Special publication Society of Economic Paleontologists and Mineralogists, v. 14, p. 139–181.

EMRY, J.R., 2005, Controls on build-and-fill architecture of the Argentine Limestone and associated strata in northeastern Kansas and development of a first-cut method for evaluating limestone aggregate durability: Master's thesis, University of Kansas, p. 268.

EROS, J.M., MONTAÑEZ, I.P., OSLEGER, D.A., DAVYDOV, V.I., NEMYROVSKA, T.I., POLETAEV, V.I., AND ZHYKALYAK, M.V., 2012, Sequence stratigraphy and onlap history of the Donets Basin, Ukraine: Insight into Carboniferous icehouse dynamics: Palaeogeography, Palaeoclimatology, Palaeoecology, v. 313–314, p. 1–25.

FELDMAN, H.R., FRANSEEN, E.K., MILLER, R.D., AND ANDERSON, N.L., 1993, A model of Missourian oolitic petroleum reservoirs based on the Drum Limestone in southeastern Kansas: Kansas Geological Survey Open-File Report 93-28.

FLÜGEL, E., 2004, Microfacies of Carbonate Rocks: Analysis, Interpretation and Application: Berlin, Springer, p. 976.

FORNOS, J.J, AND AHR, W.M., 1997, Temperate carbonates on a modern, low-energy, isolated ramp: the Balearic Platform, Spain: Journal of Sedimentary Research, v. 67, p. 364–373.

FRANSEEN, E.K., AND GOLDSTEIN, R.H., 2004, Build-and-Fill: A Stratigraphic Pattern Induced in Cyclic Sequences by Sea Level and Paleotopography: Geological Society of America Abstracts with Programs, v. 36, p. 377.

FRANSEEN, E.K., GOLDSTEIN, R.H., AND MINZONI, M., 2007, Build-and-fill sequences in carbonate systems; an emerging picture: American Association of Petroleum Geologists Annual Meeting Abstracts, v. 2007, p. 48.

FRANSEEN, E.K., AND GOLDSTEIN, R.H., 2012, Build-and-fill sequences in carbonate-dominated systems: Towards predictive models from global examples throughout the rock record: Kansas Interdisciplinary Carbonate Consortium Annual Review Meeting Extended Abstracts, v. 2012, p. 23–28.

FRENCH, J.A., AND WATNEY, W. L., 1993, Stratigraphy and depositional setting of the lower Missourian (Pennsylvanian) Bethany Falls and Mound Valley limestones, analogues for age-equivalent ooid-grainstone reservoirs, Kansas: Current Research on Kansas Geology, Bulletin 235, Kansas Geological Survey, Lawrence, p. 27–39.

GOMEZ-PEREZ, I., FELDMAN, H.R., FRANSEEN, E.K., AND SIMO, J.A., 1997, Evolution and diagenesis of an oolitic limestone (Drum Formation), Missourian, Kansas, USA: Kansas Geological Survey Open-File Report 97-74.

GONZALEZ, R., AND EBERLI, G.P., 1997, Sediment transport and bedforms in a carbonate tidal inlet; Lee Stoking Island, Exumas, Bahamas: Sedimentology, v. 44, p. 1015–1030.

GRAMMER, G.M., EBERLI, G.P., VAN BUCHEM, F.S.P., STEVENSON, R.M., AND HOMEWOOD, P., 1996, Application of high-resolution sequence stratigraphy to evaluate lateral variability in outcrop and subsurface–Desert Creek and Ismay intervals, Paradox Basin, in Longman, M.W., Sonnenfeld, M.D., eds., 1996, Paleozoic Systems of the Rocky Mountain Region. Rocky Mountain Section, Society for Sedimentary Geology (SEPM), p. 235–266.

HANDFORD, C.R., 1988, Review of carbonate sand-belt deposition of ooid grainstone and application to Mississippian reservoir, Damme Field, southwestern Kansas: The American Association of Petroleum Geologists Bulletin, v. 72, p. 1184–1199.

HANDFORD, C.R., AND LOUCKS, R.G., 1993, Carbonate depositional sequences and systems tracts; responses of carbonate platforms to relative sea-level changes, in Loucks, R.G., and Sarg, J.F., eds., Carbonate sequence stratigraphy; recent developments and application: AAPG Memoir 57, p. 3-41.

HARRIS P.M., 1984, Cores from a modern Carbonate Sand Body: The Joulters ooid shoal, Great Bahama Bank in Harris, P.M., ed., Carbonate Sands—A Core Workshop: Society of Economic Paleontologists and Mineralogists Core Workshop, No. 5, p. 429-464.

HECKEL, P.H., 1972, Recognition of ancient shallow marine environments in Rigby, J.K., and Hamblin, W.K., eds., Recognition of Ancient Sedimentary Environments: Society of Economic Paleontologists and Mineralogists, Special Publication No. 16, p. 226-286.

HECKEL, P.H., 1977, Origin of phosphatic black shale facies in Pennsylvanian cyclothems of mid-continent North America: AAPG Bulletin, v. 61, no. 7, p. 1045-1068.

HECKEL, P.H., 1986, Sea-level curve for Pennsylvanian eustatic marine transgressive-regressive depositional cycles along Midcontinent outcrop belt, North America: Geology (Boulder), v. 14, no. 4, p. 330-334.

HECKEL, P.H., 1999, Overview of Pennsylvanian (Upper Carboniferous) stratigraphy in midcontinent region of North America in Heckel, P.H. eds., Field trip #8: Middle and Upper Pennsylvanian (Upper Carboniferous) cyclothem succession in midcontinent basin, U.S.A.: Kansas Geological Survey Open File Report 99-27, p. 68–102.

HECKEL, P.H., AND BAESEMANN, J.F, 1975, Environmental Interpretation of Conodont Distribution in Upper Pennsylvanian (Missourian) Megacyclothems in Eastern Kansas: American Association of Petroleum Geologists Bulletin 59, p. 486-508.

HECKEL, P.H., AND WATNEY, W.L., 2002, Revision of Stratigraphic Nomenclature and Classification of the Pleasanton, Kansas City, Lansing, and Lower Part of the Douglas Groups (Lower Upper Pennsylvanian, Missourian) in Kansas: Kansas Geological Survey Bulletin 246, p. 68.

INDEN, R.F., AND MOORE, C.H., 1983, Beach environment, in Scholle, P.A., Bebout, D.G., and Moore, C.H., eds., Carbonate Depositional Systems: AAPG Memoir 33, p. 212–265.

JONES, B., AND GOODBODY, Q.H., 1985, Oncolites from a shallow lagoon, Grand Cayman Island: Bulletin of Canadian Petroleum Geology, v. 32, no. 2, p. 254–260.

KIRKLAND B.L., MOORE, C.H., AND DICKSON, J.A.D., 1993, Well-preserved aragonitic phylloid algae (Eugonophyllum, Udoteacea) from the Pennsylvanian Holder Formation, Sacremento Mountains, New Mexico: Palaios, v. 8, no.1, p. 111-120.

KRAINER, K., AND LUCAS, S.G., 2004, The Upper Pennsylvanian Red Tanks Member of the Bursum Formation at Carrizo Arroyo, central New Mexico: Transition from shallow marine to nonmarine facies in Lucas, S.G. and Zeigler, K.E., eds., 2004, Carboniferous-Permian transition, New Mexico Museum of Natural History and Science Bulletin No. 25, p. 53–69.

MARTIN, L.G., MONTAÑEZ, I.P., AND BISHOP, J.W., 2012, A paleotropical carbonate-dominated archive of carboniferous icehouse dynamics, Bird Spring Fm., Southern Great Basin, USA: Palaeogeography, Palaeoclimatology, Palaeoecology, v. 329–330, p. 64–82.

MCKIRAHAN, J.R, GOLDSTEIN, R.H., AND FRANSEEN, E.K, 2003, Build-and-fill sequences: how subtle paleotopography affects 3_D heterogeneity of potential reservoir facies, in Ahr, W.M., Harris, P.M., Morgan, W.A., and Somerville, I.D., eds., Special Publication - Society for Sedimentary Geology, v. 78; p. 97-116.

MOORE, R.C., 1936, Stratigraphic classification of the Pennsylvanian rocks of Kansas: Kansas Geological Survey, Bulletin, v. 22, p. 256.

MOORE, R.C., 1949, Divisions of the Pennsylvanian system in Kansas: Kansas Geological Survey, Bulletin, v. 83, p. 203.

NICHOLS, G., 1999, Sedimentology and Stratigraphy: Malden, Blackwell Science Ltd., p. 355.

PEMBERTON, S.G., MACEACHERN, J.A., AND FREY, R.W., 1992, Trace fossil models: environmental and allostratigraphic significance in Walker, R.G., and James, N.P., eds., Facies Models, Geological Association of Canada Publications, p. 47–72.

POMAR, L., 2001, Types of carbonate platforms: a genetic approach: Basin Research, v. 13, p. 313–334.

QING, H., AND NIMEGEERS, A.R., 2008, Lithofacies and depositional history of Midale carbonate-evaporite cycles in a Mississippian ramp setting, Steelman-Bienfait area, southeastern Saskatchewan, Canada: Bulletin of Canadian Petroleum Geology, v. 56, no. 3, p. 209–234.

RAEF, A.E., MILLER, R.D., FRANSEEN, E.K., BYRNES, A.P., WATNEY, W.L., AND HARRISON, W.E., 2005, 4D seismic to image a thin carbonate reservoir during a miscible CO2 flood: Hall-Gurney Field, Kansas, USA: Leading Edge, v. 24, no. 5, p. 521–526.

RANKEY, E.C., AND REEDER, S.L., 2011, HOlocene oolitic marine sand complexes of the Bahamas: Journal of Sedimentary Research, v. 81, p. 97–117.

RANKEY, E.C., RIEGL, B., AND STEFFEN, K., 2006, Form, function and feedbacks in a tidally dominated ooid shoal, Bahamas: Sedimentology, v. 53, p. 1191–1210.

RASBURY, E.T., HANSON, G.N., MEYERS, W.J., HOLT, W.E., GOLDSTEIN, R.H., AND SALLER, A.H., 1998, U-Pb dates of paleosols: Constraints on late Paleozoic cycle durations and boundary ages: Geology, v. 26, no. 5, p. 403–406.

REEDER, S.L., AND RANKEY, E.C., 2008, Interactions between tidal flows and ooid shoals, northern Bahamas: Journal of Sedimentary Research, v. 78, p. 175–186.

RUF, M., AND AIGNER, T., 2004, Facies and poroperm characteristics of a carbonate shoal (Muschelkalk, South German Basin): a reservoir analogue investigation: Journal of Petroleum Geology, v. 27, no. 3, p. 215–239.

SAMANKASSOU, E., AND WEST, R.R., 2002, Construction versus accumulation in phylloid algal mounds: an example of a small constructed mound in the Pennsylvanian of Kansas, USA: Palaeogeography, Palaeoclimatology, Palaeoecology, v. 185, p. 379–389.

SHAPIRO, R.S., AND WEST, R.R., 1999, Late Paleozoic stromatolites: new insights from the Lower Permian of Kansas: Lethaia, v. 32, p. 131–139.

SHINN, E.A., 1983, Tidal flat environment, in Scholle, P.A., Bebout, D.G., and Moore, C.H., eds., Carbonate Depositional Systems: AAPG Memoir 33, p. 171–210.

SOREGHAN, G.S., GILES, K.A., 1999. Amplitudes of Late Pennsylvanian glacioeustasy, Geology, v. 27, p. 255–258.

STONE, W.P.JR., 1984, Origin and Evolution of Oolite in the Drum Limestone (Pennsylvanian, Missourian), Montgomery County, Kansas: Tulsa Geological Society Special Publication, v. 2, p. 51–85.

SULLIVAN, J.S., 1969, Sedimentation and carbonate petrology of the Westerville Limestone Member (Pennsylvanian), Raytown, Missouri: Master's thesis, University of Missouri-Columbia, p. 102.

TESSIER, B., ARCHER, A.W., LANIER, W.P., AND FELDMAN, H.R., 1995, Comparison of ancient tidal rhythmites (Carboniferous of Kansas and Indiana, USA) with modern analogues (the Bay of Mont-Saint-Michel, France): Special Publication of the International Association of Sedimentologists, v. 24, p. 259–271.

TUCKER, M.E., 2001, Sedimentary Petrology: An Introduction to the Origin of Sedimentary Rocks: Oxford, Blackwell Scientific Publications, p. 262.

TUCKER, M.E., AND WRIGHT, V.P., 1990, Carbonate Sedimentology: Oxford, Blackwell Scientific Publications, p. 482.

WASHBURN, E.L., 2004, Paleotopography and sea-level controls on facies distribution and stratal architecture in the Plattsburg Limestone (Upper Pennsylvanian), NE Kansas: Master's thesis, University of Kansas, p. 364.

WATNEY, W.L., 1999, Stratigraphic analysis of Pennsylvanian in the subsurface of Kansas in Heckel, P.H., eds., Field trip #8: Middle and Upper Pennsylvanian (Upper Carboniferous) cyclothem succession in midcontinent basin, U.S.A., Kansas Geological Survey Open File Report 99-27, p. 119–146.

WATNEY, W. L., FRENCH, J.A., AND FRANSEEN, E.K., 1989, Sequence stratigraphic interpretations and modeling of cyclothems in the Upper Pennsylvanian (Missourian), Lansing and Kansas City groups in eastern Kansas: Guidebook of the Kansas Geological Survey, 41st Annual Fieldtrip, p. 211.

WEBER, J.L., WRIGHT, F.M., SARG, J.F., SHAW, ED, HARMAN, L.P., VANDERHILL, J.B., AND BEST, D.A., 1995, Reservoir delineation and performance--Application of sequence stratigraphy and integration of petrophysics and engineering data, Aneth field, southeast Utah, U.S.A.; in, E.L. Stoudt and P.M. Harris, eds., Hydrocarbon Reservoir Characterization, Geologic Framework and Flow Unit modeling. SEPM (Society for Sedimentary Geology) Short Course 34, p. 1-29.

WELLER, J.M., 1958, Cyclothems and larger sedimentary cycles of the Pennsylvanian: The Journal of Geology, v. 66, no. 2, p. 195–207.

WELLS, M.R., ALLISON, P.A., PIGGOTT, M.D., GORMAN, G.J., HAMPSON, G.J., PAIN, C.C., AND FANG, F., 2007, Numerical modeling of tides in the late Pennsylvanian midcontinent seaway of North America with implications for hydrography and sedimentation: Journal of Sedimentary Research, v. 77, p. 843–865.

WILSON, J.L, AND JORDAN, C., 1983, Middle shelf environment, in Scholle, P.A., Bebout, D.G., and Moore, C.H., eds., Carbonate Depositional Systems: AAPG Memoir 33, p. 297–343.

WRAY, J.L., 1964, Archaeolithophyllum, an abundant calcareous alga in limestone of the Lansing Group (Pennsylvanian), southeastern Kansas: Kansas Geological Survey Bulletin 170, pt. 1, p. 13.

WRIGHT, V.P., 1983 Morphogenesis of oncoids in the Lower Carboniferous Lanelly Formation of South Wales, in Peryt, T.M., ed., Coated Grains: New York, Springer-Verlag, p. 424–434.

# APPENDIX 1

Isopach maps of individual facies (Fig. 41–46) were created by dividing the total Westerville stratigraphic unit thickness into individual facies according to relationships at outcrop. The confidence in these maps is therefore greatest proximal to the dense outcrop area near Raytown, Missouri and decreases to the south and west, away from the surface exposures.

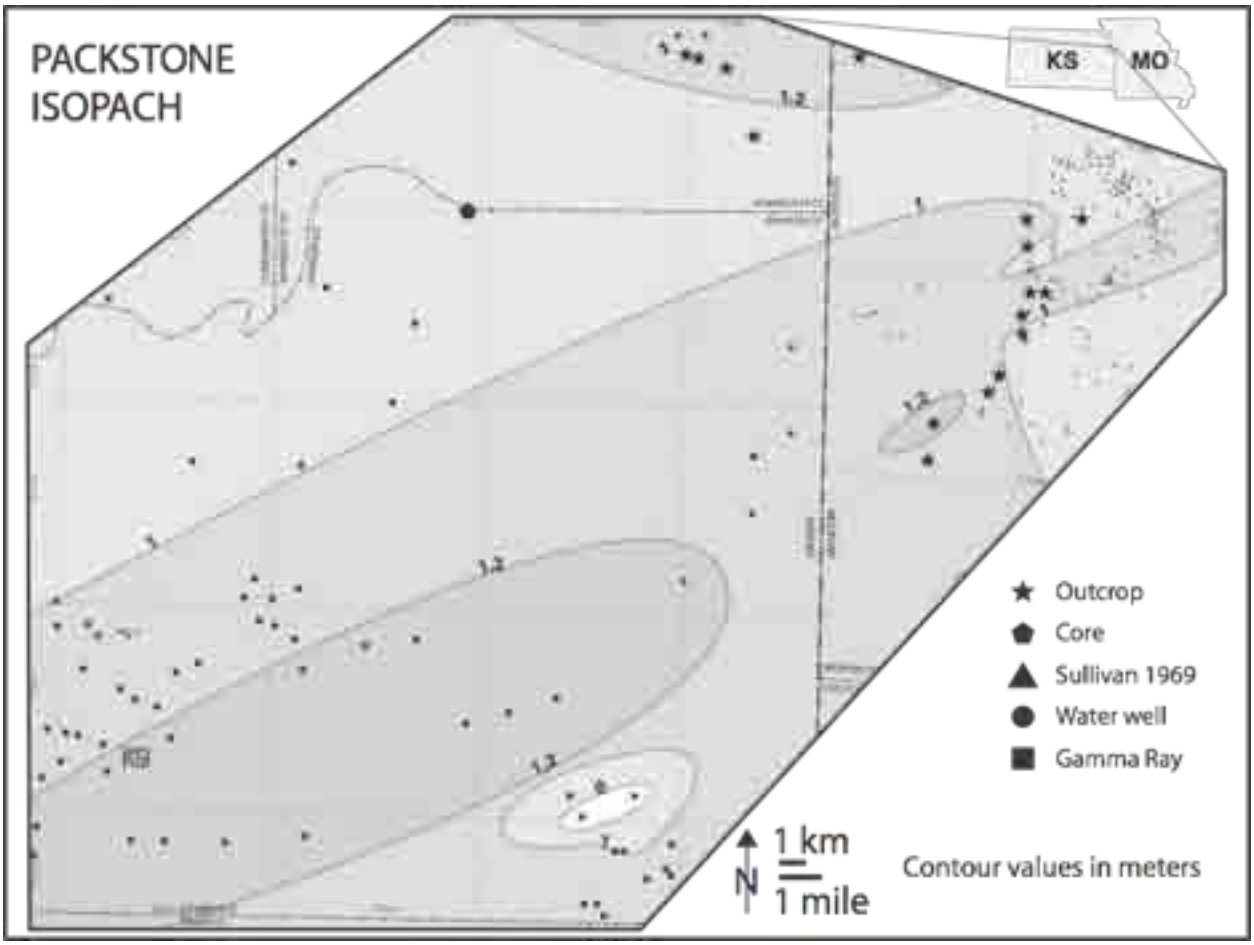


Figure 41. Isopach of the bioclastic packstone facies of unit W1. Notice relative thickness consistency throughout field area.

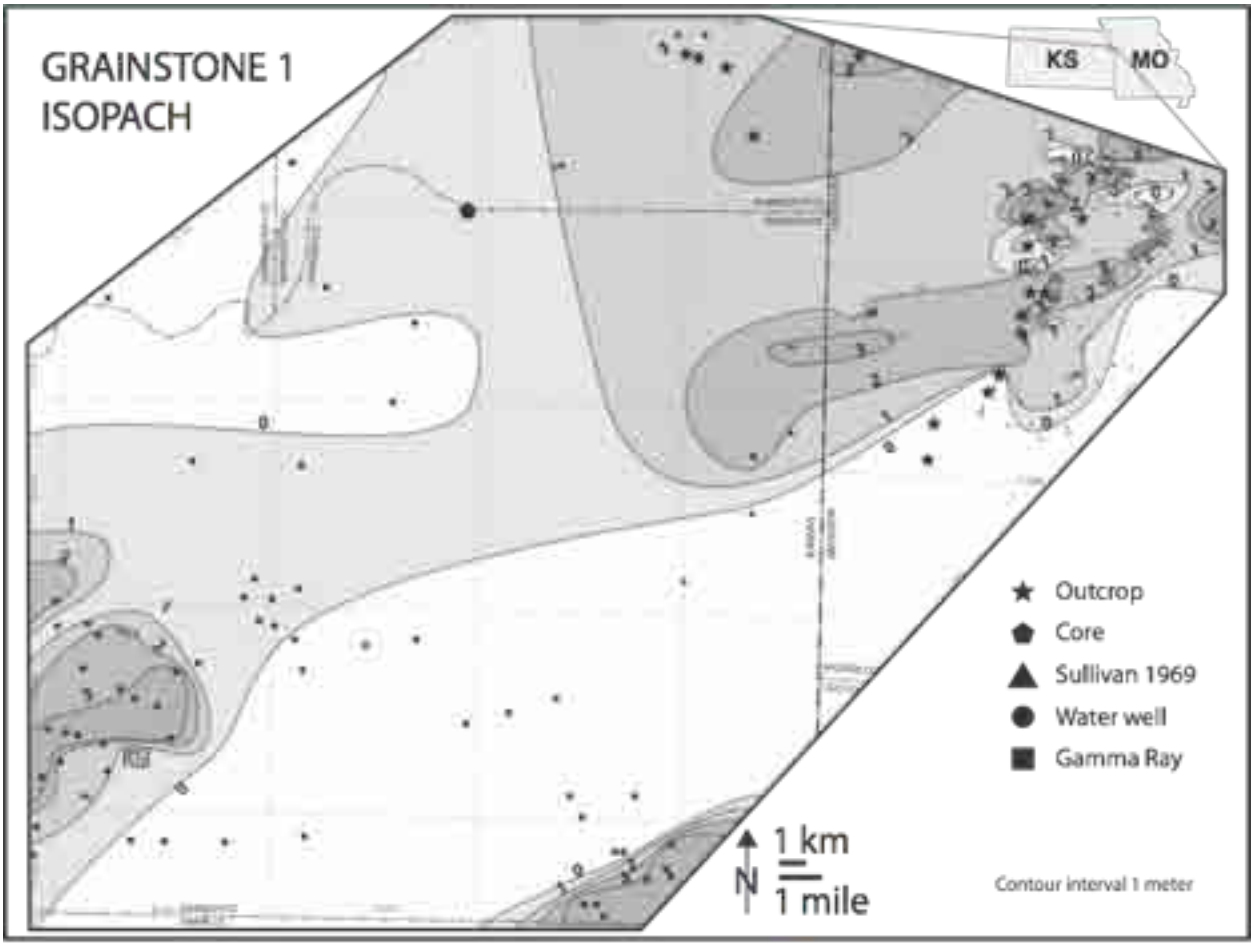


Figure 42. Isopach of oolitic and bioclastic grainstone deposited during Interval W2. Thick portions concentrated at break in slope of underlying Wea Shale. Thickness variation highly variable at outcrop scale.

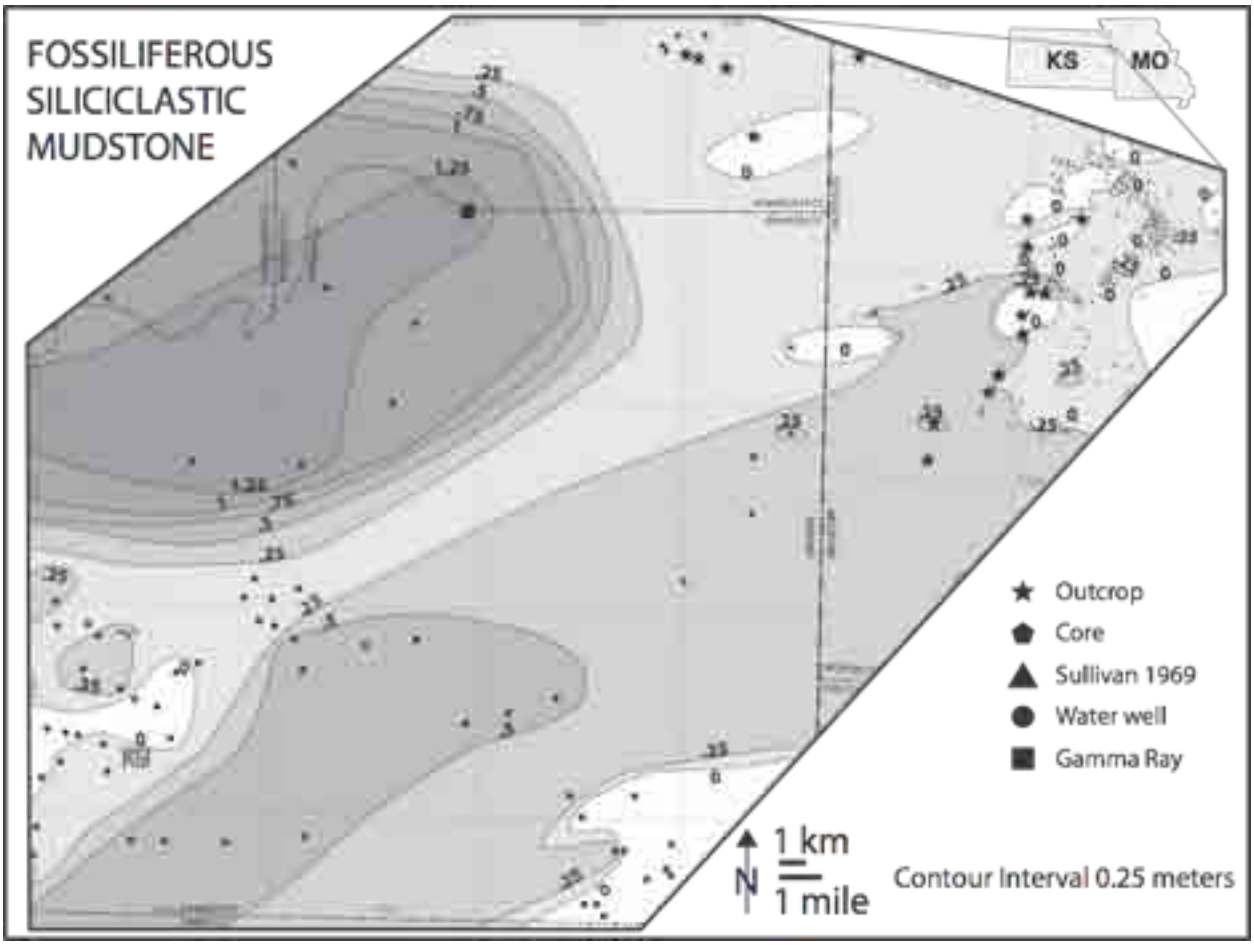


Figure 43. Isopach of fossiliferous siliciclastic-mudstone deposited during Interval W3.

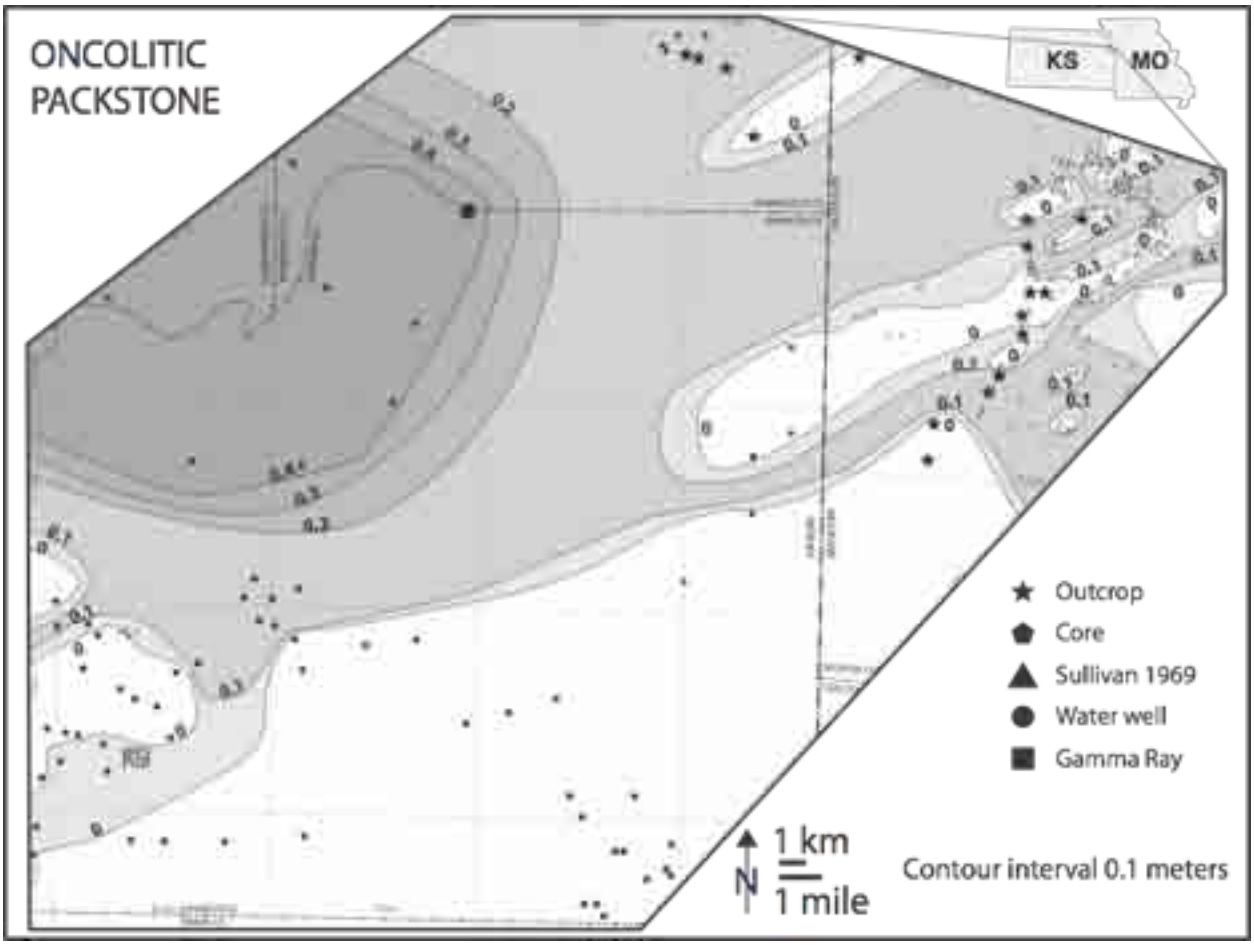


Figure 44. Isopach of oncolitic packstone deposited during Interval W3.

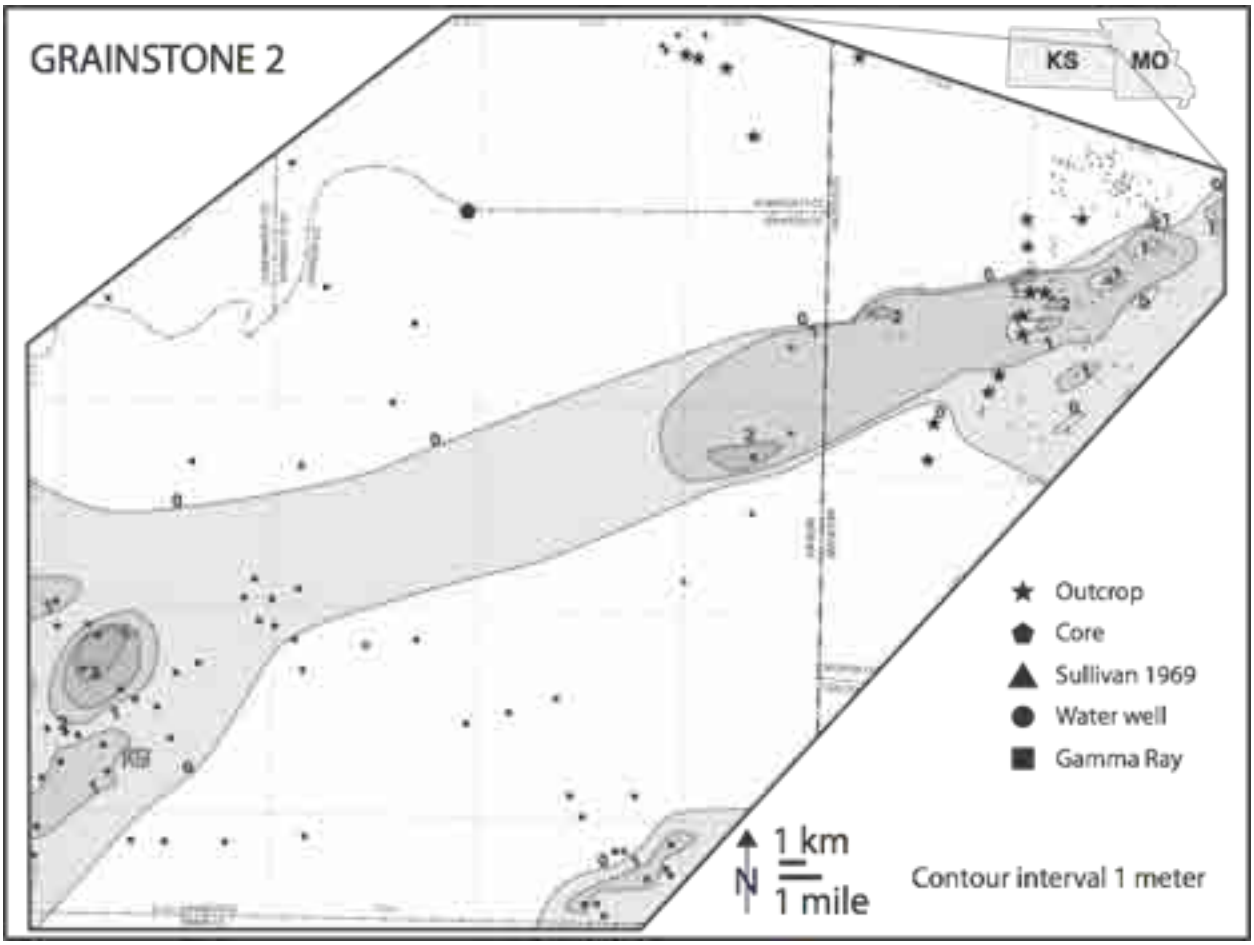


Figure 45. Isopach of oolitic grainstone deposited during Interval W3.

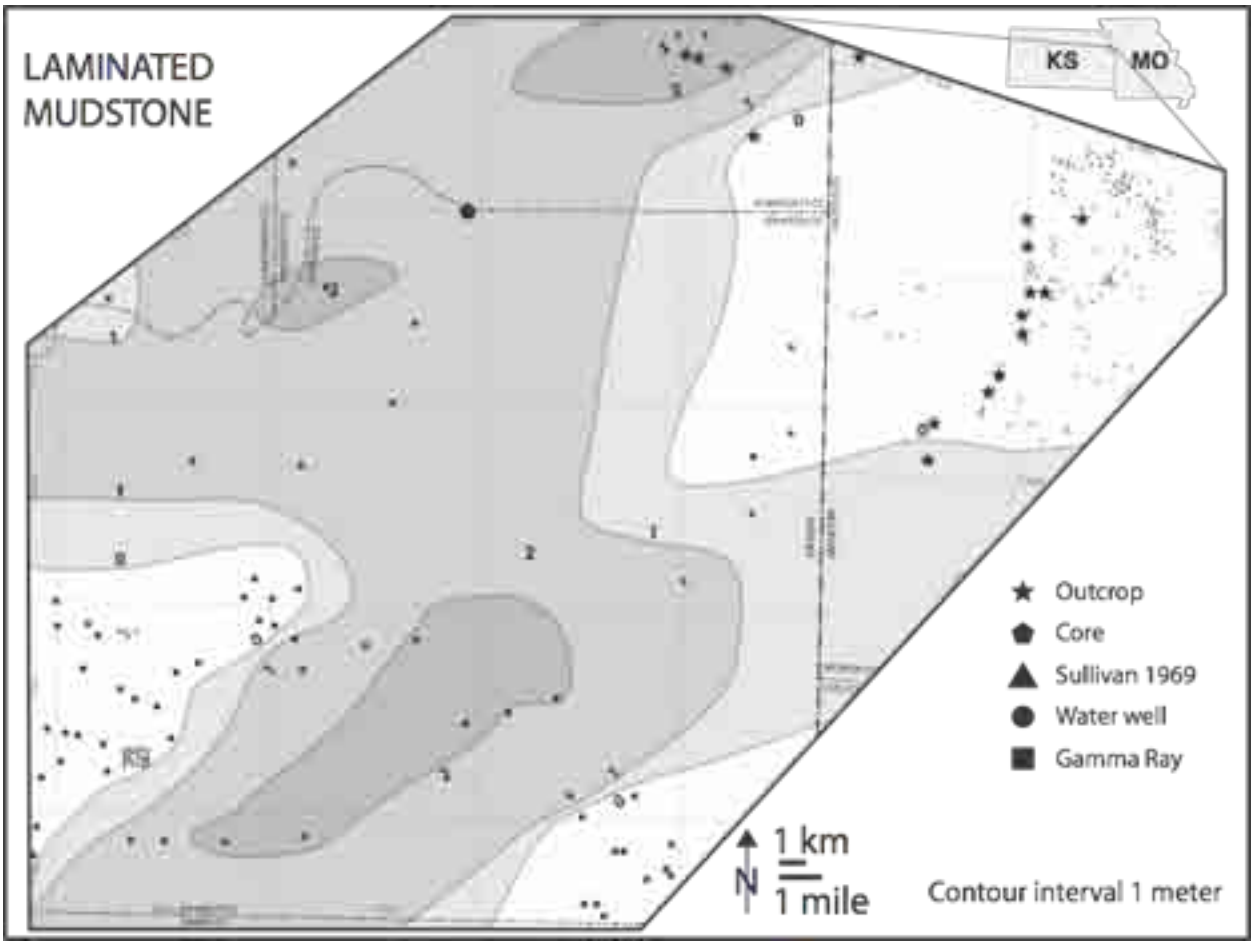


Figure 46. Isopach of peloidal packstone deposited during Interval W3.